

CRWMS/M&O

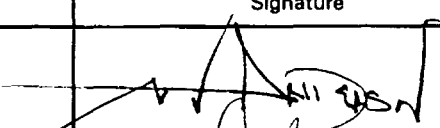
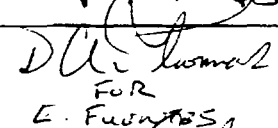
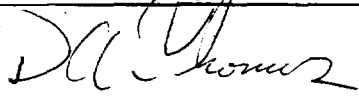
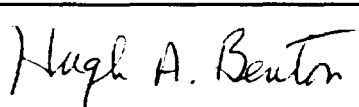
Design Analysis Cover Sheet

Complete only applicable items.

1.

QA: L

Page: 1 Of: 120

2. DESIGN ANALYSIS TITLE			
MCNP Evaluation of Laboratory Critical Experiments: Lattice Criticals			
3. DOCUMENT IDENTIFIER (Including Rev. No.)			4. TOTAL PAGES
BBA000000-01717-0200-00009 REV 00			120
5. TOTAL ATTACHMENTS		6. ATTACHMENT NUMBERS - NO. OF PAGES IN EACH	
1		I-1	
	Printed Name	Signature	Date
7. Originator	M. J. Anderson		9/12/97
8. Checker	E. Fuentes <i>D.A. THOMAS FOR</i>	 <i>D.A. Thomas FOR E. Fuentes</i>	09/12/97
9. Lead Design Engineer	D. A. Thomas		09/12/97
10. Department Manager	H. A. Benton		9/12/97
11. REMARKS			

Design Analysis Revision Record

Complete only applicable items.

1.

2. DESIGN ANALYSIS TITLE	
MCNP Evaluation of Laboratory Critical Experiments: Lattice Criticals	
3. DOCUMENT IDENTIFIER (Including Rev. No.)	
BBA000000-01717-0200-00009 REV 00	
4. Revision No.	5. Description of Revision
00	Initial Issuance

Table of Contents

<u>Item</u>	<u>Page</u>
1. Purpose	4
2. Quality Assurance	4
3. Method	5
4. Design Inputs	5
4.1 Design Parameters	5
4.2 Criteria	5
4.3 Assumptions	6
4.4 Codes and Standards	6
5. References	7
6. Use of Computer Software	9
7. Design Analysis	10
7.1 The MCNP Code System	10
7.2 Laboratory Critical Experiment Descriptions	13
7.3 Laboratory Critical Experiment k_{eff} Results	103
7.4 MCNP Results	117
8. Conclusions	119
9. Attachments	120

1. Purpose

The purpose of this analysis is to document the MCNP evaluations of benchmark lattice Laboratory Critical Experiments (LCE's). The objective of this analysis is to quantify the MCNP 4A (Reference 5.4) code system's ability to accurately calculate the effective neutron multiplication factor (k_{eff}) for various measured critical (i.e., $k_{eff} = 1.0$) configurations. This analysis quantifies the effectiveness of the MCNP criticality calculation for lattice configurations containing UO_2 and PuO_2 fissile oxide fuel using two different cross section data libraries. The two cross section libraries utilized in this analysis include the following:

- 1) ENDF/B-V libraries generated by Los Alamos National Laboratory (LANL); and
- 2) ENDF/B-VI libraries generated by LANL.

The results of this analysis will be used to support the development of the disposal criticality analysis methodology.

2. Quality Assurance

The Quality Assurance (QA) program applies to this analysis. The work reported in this document is part of the Waste Package Design analysis that will eventually support the License Application Design phase. This activity, when appropriately confirmed, can impact the proper functioning of the Mined Geologic Disposal System (MGDS) waste package; the waste package has been identified as an MGDS Q-List item important to safety and waste isolation (pp. 4, 15, Reference 5.1). The waste package is on the Q-List by direct inclusion by the Department of Energy (DOE), without conducting a QAP-2-3 evaluation. The Waste Package Development Department (WPDD) responsible manager has evaluated this activity in accordance with QAP-2-0, *Conduct of Activities. The Perform Criticality, Thermal, Structural, and Shielding Analyses* (Reference 5.3) evaluation has determined the preparation and review of this design analysis is subject to *Quality Assurance Requirements and Description* (Reference 5.2) requirements. As specified in NLP-3-18, this activity is subject to QA controls.

The analysis described in this document supports development of the disposal criticality analysis methodology. No designs were analyzed in this document. This document will not directly support any construction, fabrication, or procurement activity and therefore is not required to be procedurally controlled as TBV (to be verified). The calculation design inputs or information used in this document come from data accepted by the Nuclear Regulatory Commission and by the scientific and engineering community as established fact. The specific references are listed in Section 5 and identified in Section 7. The information is therefore not treated as unqualified data.

3. Method

The analytical model employed in this analysis consisted of using the MCNP computer program (Reference 5.4) to determine the effective neutron multiplication factor (k_{eff}) for LCE's. The results reported for the MCNP calculations are the combined average values of k_{eff} from the three estimates (collision, absorption, and track length) listed in the final generation summary in the MCNP output. The calculation of acceptable bias values and subcritical margins are based on the results of numerous LCE evaluations performed using the MCNP code system. The LCE's documented in this analysis may be used to determine appropriate bias values for use in subsequent criticality evaluations performed with MCNP.

4. Design Inputs

No repository-related designs were analyzed and no design inputs were used in this document. The systems analyzed in this document are both LCE's used in prior licensing activities approved by the Nuclear Regulatory Commission and LCE's accepted by the scientific and engineering community. The input information is, therefore, not treated as unqualified data. Thus the results of the analysis described in this document can be used to support construction, fabrication, or procurement activities in accordance with the appropriate procedures. The dimensions listed throughout this analysis are in the metric units used directly in the codes to facilitate checking and minimize the potential for errors in input.

4.1 Design Parameters

The section is not applicable. This analysis does not evaluate designs or components for designs. Therefore, no design parameters are used. The experimental parameters used in MCNP are described for each experiment in Section 7.2.

4.2 Criteria

The design of the waste package will depend on waste package configuration criticality analyses performed using an acceptable disposal criticality analysis methodology. Criteria that relate to the development and design of repository and engineered barrier components are derived from the applicable requirements and planning documents. The Engineered Barrier Design Requirements Document (EBDRD, Reference 5.17) provides requirements for engineered barrier segment design. The Repository Design Requirements Document (RDRD, Reference 5.18) provides requirements for repository design. The Controlled Design Assumptions Document (Reference 5.19) provides guidance for requirements listed in the EBDRD and RDRD which have unqualified or unconfirmed data associated with the requirement.

This analysis supports the disposal criticality analysis methodology by providing input in the form of methods benchmarking. These benchmark calculations will help determine the bias values to be applied for criticality analytic tools used in disposal criticality analyses. The requirements for utilizing the bias in the method of calculation of the critical multiplication factor for disposal configurations containing spent nuclear fuel are located in Section 3.2.2.5 of the RDRD and Section 3.2.2.6 of the EBDRD. This analysis does not satisfy these requirements, but the results from this analysis will be used as input to subsequent analyses which will satisfy these requirements.

4.3 Assumptions

This section is not used. No assumptions affecting repository design elements are made in this analysis.

4.4 Codes and Standards

This section is not applicable.

5. References

- 5.1 Q-List. YMP/90-55Q, REV 4, Yucca Mountain Site Characterization Project.
- 5.2 Quality Assurance Requirements and Description (QARD), DOE/RW-0333P REV 7, US Department of Energy (DOE) Office of Civilian Radioactive Waste Management (OCRWM).
- 5.3 QAP-2-0 Activity Evaluations: ID #WP-20, *Perform Criticality, Thermal, Structural, and Shielding Analyses*, Civilian Radioactive Waste Management System (CRWMS), Management and Operating Contractor (M&O), August 3, 1997.
- 5.4 J. F. Briesmeister, Ed., *MCNP--A General Monte Carlo N-Particle Transport Code, Version 4A*, LA-12625-M, Los Alamos National Laboratory (LANL), November 1993.
- 5.5 S. R. Bierman, E. D. Clayton, and B. M. Durst. *Critical Separation Between Subcritical Clusters of 2.35 Wt% ^{235}U Enriched UO_2 Rods in Water with Fixed Neutron Poisons*, PNL-2438, Battelle Pacific Northwest Laboratories (PNL), October 1977.
- 5.6 S. R. Bierman, B. M. Durst, and E. D. Clayton. *Criticality Experiments with Subcritical Clusters of 2.35 Wt% and 4.31 Wt% ^{235}U Enriched UO_2 Rods in Water with Uranium or Lead Reflecting Walls*, PNL-3926, PNL, December 1981.
- 5.7 S. R. Bierman and E. D. Clayton. *Criticality Experiments with Subcritical Clusters of 2.35 Wt% and 4.31 Wt% ^{235}U Enriched UO_2 Rods in Water with Steel Reflecting Walls*, PNL-3602, PNL, April 1981.
- 5.8 B. M. Durst, S. R. Bierman, and E. D. Clayton. *Critical Experiments with 4.31 Wt% ^{235}U Enriched UO_2 Rods in Highly Borated Water Lattices*, PNL-4267, PNL, May 1982.
- 5.9 S. R. Bierman. *Criticality Experiments with Neutron Flux Traps Containing Voids*, PNL-7167, PNL, April 1990.
- 5.10 S. M. Bowman and O. W. Hermann. *Reference Problem Set to Benchmark Analysis Methods for Burnup Credit Applications (DRAFT)*, ORNL/TM-12295, Computing Applications Division ORNL, Manuscript Date: November 19, 1993.
- 5.11 R. I. Smith and G. J. Konzek. *Clean Critical Experiment Benchmarks for Plutonium Recycle in LWR's*, EPRINP-196, Volumes 1 and 2, Electric Power Research Institute, April 1976 and September 1978.

- 5.12 L. W. Newman. *Urania-Gadolinia: Nuclear Model Development and Critical Experiment Benchmark*, BAW-1810, April 1984.
- 5.13 E. G. Taylor et al. *Saxton Plutonium Critical Experiments for the Saxton Partial Plutonium Core*, WCAP-3385-54, Westinghouse Electric Corporation, December 1965.
- 5.14 M. N. Baldwin, G. S. Hoovler, R. L. Eng, and F. G. Welfare. *Critical Experiments Supporting Close Proximity Water Storage of Power Reactor Fuel*, BAW-1484-7, July 1979.
- 5.15 S. R. Bierman, E. S. Murphy, E. D. Clayton, and R. T. Keay. *Criticality Experiments with Low Enriched UO_2 Fuel Rods in Water Containing Dissolved Gadolinium*, PNL-4976, PNL, February 1984.
- 5.16 S. M. Bowman, O. W. Hermann, and M. C. Brady. *Scale-4 Analysis of Pressurized Water Reactor Critical Configurations: Volume 2 -- Sequoyah Unit 2 Cycle 3*, Oak Ridge National Laboratory, Document Number: ORNL/TM-12294/V2.
- 5.17 *Engineered Barrier Design Requirements Document*, YMP/CM-0024, REV 00, ICN 01, DOE OCRWM.
- 5.18 *Respository Design Requirements Document*, YMP/CM-0023, REV 00, ICN 01, DOE OCRWM.
- 5.19 *Controlled Design Assumptions Document*, Document Identifier: B000000000-01717-4600-00032, REV 04, ICN 02, CRWMS M&O.
- 5.20 *Software Qualification Report for MNCP 4A, A General Monte Carlo N-Particle Transport Code*, CSCI: 30006 V4A, Document Identifier: 30006-2003 REV 02, CRWMS M&O.
- 5.21 NEA/NSC/DOC(95)03/J, *International Handbook of Evaluated Criticality Safety Benchmark Experiments*, Nuclear Energy Agency, Organization for Economic Cooperation and Development, Paris, 1995.
- 5.22 Attachment for BBA000000-01717-0200-00009 REV 00 -- MCNP Evaluation of Laboratory Critical Experiments: Lattice Criticals. Batch Number: MOY-970904-16.

6. Use of Computer Software -

- 6.1 MCNP 4A HP 9000 Version, CSCI: 30006 VER. 4A (Reference 5.20), installed on a Hewlett Packard 9000 Workstation. The neutron interaction libraries used in this analysis are those documented in the Software Qualification Report. Both the ENDF/B-V and ENDF/B-VI libraries were qualified for use in Reference 5.20.

The input files used are reiterated in the output files and those output files are contained on a magnetic tape (Reference 5.22). The contents of this tape are given in Attachment I.

- a) The MCNP 4A computer code (Reference 5.4) is an appropriate tool to determine the criticality potential, k_{eff} , of fresh and spent lattices of light water reactor fuel assemblies.
 - b) This software has been validated over the range it was used.
 - c) It was previously obtained from the Software Control Management (SCM) in accordance with appropriate procedures.
- 6.2 EXCEL, Version 7.0a, loaded on a Gateway 2000 PC.

This software was used to prepare tables and plots of the results. The only computations were to compute averages and uncertainties, which are merely averages computed in a quadratic sense.

7. Design Analysis

As previously stated, this analysis involves the use of the MCNP code system (Reference 5.4) to perform criticality analyses on various LCE configurations to determine the neutron multiplication factors (k_{eff} values). Each analyzed critical configuration represents an actual eigenvalue experiment. The k_{eff} result obtained from the MCNP computer simulation of each critical experiment using each of the two cross-section libraries is compared to unity -- since each experiment is critical -- to quantify the effectiveness of the MCNP criticality calculation and the respective cross section library.

The specific objectives of this analysis include the following:

- 1) provide a general description of the MCNP code system including an identification of the utilized cross-section indices; and
- 2) provide descriptions of the MCNP simulation k_{eff} results for each LCE documented in this analysis.

These analyses verify the applicability of the MCNP code system to the calculation of k_{eff} values for configurations relevant to development and licensing calculations.

7.1 The MCNP Code System

MCNP is a general-purpose particle transport code that can simulate neutron, photon, and electron transport or coupled systems of such particles. This capability extends to the modeling of neutron-multiplying systems. Geometrical representations of actual structures is accomplished by creating arbitrary three-dimensional configurations bounded by first-degree and second-degree surfaces and fourth-degree elliptical tori. Verification of the appropriateness of these geometrical representations is obtained through a powerful plotting package incorporated into MCNP.

These configurations are filled with material definitions representing the isotopic constituents of the volumes. The particle-transport characteristics of these materials are obtained from pointwise cross section data. For neutrons, all the reactions given in a particular cross section evaluation (e.g., ENDF/B-V) are included. The data includes very little "thinning," resulting in good reconstruction of resonance integrals. The transport of thermal neutrons may be approximated as a free gas. Alternatively, the more sophisticated $S(\alpha,\beta)$ model that accurately represents scattering from molecules and crystalline solids is used in the current evaluations.

While MCNP incorporates a wide variety of variance reduction techniques, computational efficiency and variance reduction in the present evaluations are achieved through implicit neutron capture and neutron weight variations that depend of the reaction experienced during the transport simulation. (Reference 5.4)

7.1.1 The Monte Carlo Method

The Monte Carlo method is a technique for simulating and recording the behavior of individual particles within a system. The behavior of the simulated particles is extrapolated to describe the average behavior of all of the particles within the system. In the abstract, the Monte Carlo method, as applied to neutrons in an MCNP criticality calculation, is based upon following many individual neutrons through their various transport experiences such as scattering, fission, absorption, or leakage. The fission process is regarded as the birth event that separates generations of neutrons. A generation is the lifetime of a neutron from birth by fission to death by either escape, parasitic capture, or absorption leading to fission. The average behavior of the sample set of neutrons is used to describe the average behavior of the system (i.e., neutron multiplication factor, k_{eff}).

7.1.2 MCNP Critical Multiplication Factor (k_{eff}) Results

MCNP Version 4A calculates three k_{eff} estimates for each neutron cycle in a given problem:

1. the collision estimate,
2. the absorption estimate, and
3. the track length estimate.

A detailed description of the three k_{eff} estimates may be found in Chapter 2, Section VIII, Part B, of Reference 5.4. The k_{eff} estimate used in the criticality analyses related to waste package development and in the bias value determination of this analysis is the statistical combination of all three k_{eff} estimates. For most systems involving neutron multiplication, the combined k_{eff} estimator is the best estimate of the neutron multiplication from MCNP (Reference 5.4).

7.1.3 Assessing the Validity of a Criticality Calculation

While MCNP is a powerful tool for analyzing neutron-multiplying systems, the results must be scrutinized to ensure that the simulation results are consistent with physical expectations. Two minimum requirements for assessing the validity of an MCNP criticality calculation are:

1. all cells containing fissionable material should be adequately sampled; and
2. the fundamental spatial mode should be achieved before commencing the accumulation of data for calculation of the mean k_{eff} .

MCNP also provides several features that assist in assessing the validity of a k_{eff} calculation. To satisfy the first requirement, MCNP verifies that at least one fission source point was generated in each cell containing fissionable material.

To satisfy the second requirement, MCNP provides several edits to determine if the fundamental spatial mode was achieved before the completion of the source cycles, I_c (I_c is the number of cycles skipped before fission simulation begins). One check is the comparison of the combined k_{eff} estimates and their standard deviations for the first and second half of the active k_{eff} cycles. If the difference between the average k_{eff} values for the two halves does not appear to be zero, or if the ratio of the two standard deviations is larger than expected, a "WARNING" message is provided in the output. MCNP determines the number of cycles which must be skipped to produce the minimum standard deviation for the combined three-eigenvalue estimate. If this result is larger than I_c , it may indicate that more cycles should be skipped before accumulating k_{eff} data. MCNP checks the k_{eff} estimate from each cycle to assure normality at the 95% and 99% confidence levels. If a k_{eff} estimate is not normally distributed with respect to the mean k_{eff} at the 99% confidence level, a "WARNING" message is provided in the output. "Unless there is a high positive correlation among the three estimates, it is expected to be rare that all three k_{eff} estimates will not appear normally distributed at the 99% confidence level when the normal spatial mode has been achieved and maintained (Reference 5.4)." Finally, MCNP tests for a monotonic trend of the combined three-eigenvalue estimate's results over the last ten active cycles. If the spatial mode is well converged and maintained, there should not be a monotonic trend within the last ten active cycles. Again, a "WARNING" message is provided in the output if a monotonic trend is detected.

Compliance with the two minimum requirements addressed above should be verified for each criticality calculation using the checks provided by the MCNP code. If either of the two requirements appear to be violated, the k_{eff} results for the calculation should be evaluated further.

7.1.4 Cross Sections

Using the appropriate material cross sections in an MCNP criticality calculation is essential to obtaining credible results.

The MCNP neutron interaction tables provide the following data:

1. all available cross section data;
2. angular distribution data for scattered neutrons;
3. energy distribution data for inelastically scattered neutrons;
4. data about secondary photon production;
5. Q-value data for each reaction; and
6. the average number of neutrons per fission data for fissionable isotopes.

For these calculations, the ENDF/B-V and ENDF/B-VI cross sections compiled by Los Alamos National Laboratory (LANL) were used (see Appendix G of Reference 5.4). While "thinned" cross section sets are available for some nuclides to increase computational speed, the most complete cross

section tables were used for the present work. These tables are sufficiently dense to permit linear interpolation and reportedly reproduce the basis data to within one percent or less.

Neutron interaction table designations are included as part of the material composition input to MCNP. Each material composition is composed of one or more elements or isotopes designated by a ZAID identifier. The ZAID identifier takes the form "ZZZAAA.nnC" where "ZZZ" represents the atomic number of the element ("ZZZ" may be one or two digits), "AAA" represents the elemental isotope ("AAA" must be three digits incorporating leading zeros), and "nn" represents the neutron interaction table designation. The ENDF/B-V neutron interaction tables generated by LANL use the ".50C" or ".55C" suffix. The ENDF/B-VI neutron interaction tables use the ".60C" suffix.

7.1.6 $S(\alpha,\beta)$ Thermal Treatment

The $S(\alpha,\beta)$ thermal treatment accounts for binding effects in molecules and crystalline solids. The $S(\alpha,\beta)$ thermal scattering treatment is necessary in a highly moderating medium where low-energy scattering may be dominant. $S(\alpha,\beta)$ thermal treatment tables are available for a limited number of materials. In this analysis the thermal treatment is consistently applied to the materials having available data. The $S(\alpha,\beta)$ treatment is consistently applied to water in the LCE's of this analysis.

7.2 Laboratory Critical Experiment Descriptions

The fresh fuel LCE's presented in this section represent moderated lattice configurations containing fissile oxide fuel. Each of the LCE configurations described in this section have been analyzed with the MCNP code system using both of the cross section libraries previously described. The MCNP input decks for each of the benchmark calculations are included in the output files which are contained on the accompanying magnetic tape. An experiment identifier for each configuration is provided for subsequent reference in this document.

7.2.1 Critical Configurations of Subcritical Clusters of 2.35 wt% Enriched UO_2 Rods in Water with Fixed Neutron Absorber Plates

Experiments with subcritical clusters of low-enrichment UO_2 fuel rods were performed at the Pacific Northwest Laboratory and originally documented by Bierman (Reference 5.5). The subsequent evaluation of the experiment by Bowman (Reference 5.10) was used in the formulation of the present MCNP model. A sample schematic illustrating the experimental assembly is shown in Figure 7.2.1-1. The four experiments modeled with MCNP consisted of three rectangular arrays of aluminum-clad fuel rods on a fuel rod pitch of 2.032 cm. The fuel rods comprising the arrays had a uniform enrichment of 2.35 wt% U-235. The three arrays of fuel were arranged in a row and, in three of the experiments, sheets of neutron poison were interposed between adjacent arrays. The structure of the experimental assembly was provided by aluminum structural members on the margins of the fuel arrays. Axial support for the fuel rods was provided by an acrylic base plate and lateral alignment

of the fuel rods was provided by another acrylic plate. The experimental apparatus was closely reflected by 30 cm of full-density water.

The pertinent differences among these four experiments are shown in Table 7.2.1-1. The height and width of the Boral™ absorber plate are 36.5 cm and 91.5 cm, respectively. For aluminum and stainless steel absorber plates, the height was 35.6 cm. These critical experiments help demonstrate the ability of MCNP accurately to predict the critical multiplication factor for configurations containing light-water reactor fuel separated by absorber plates as is often found in fuel storage rack, transportation cask, and storage cask designs.

The fuel rod description is shown in Figure 7.2.1-2. The UO₂ composition used in the MCNP models is shown in Table 7.2.1-2. The Type 1100, 5052-H32, and 6061 aluminum compositions used in the MCNP models are shown in Table 7.2.1-3. The acrylic spacer grids and base plate shown in Figure 7.2.1-1 were modeled as plexiglass. Substituting plexiglass for acrylic in the models will have an insignificant effect on the critical multiplication factor of these configurations due the minimal neutron absorptive properties of the constituent isotopes and scattering characteristics similar to the water that it is displacing. The plexiglass composition used in the models is shown in Table 7.2.1-4.

Table 7.2.1-1. Differences in Experimental Configurations for Clusters of 2.35 wt% UO₂ Fuel Rods

Case	Interposed Plate	Assembly Spacing (cm) [e]	Interposed Plate Thickness (cm)
exp1	none	8.39	n/a
exp2	Boral [a]	5.05	0.713 [b]
exp3	Type 6061 Aluminum [c]	8.67	0.625
exp4	Type 304 Stainless Steel [d]	6.88	0.485

[a]. The composition of Boral™ used in the problem is shown in Table 7.2.1-5.

[b]. The total thickness included a 0.102 cm thick cladding on each side of the absorber material.

[c]. The composition of Type 6061 aluminum is shown in Table 7.2.1-3.

[d]. The composition of Type 304 stainless steel is shown in Table 7.2.1-6.

[e]. This is the value measured from rod surface to rod surface in accordance with Reference 5.10.

Table 7.2.1-2. 2.35 wt% U-235 Enriched UO₂ Composition (9.20 g/cc)

Element/Isotope	Weight Percent [a]
U-234	0.0049
U-235	2.0715
U-238	86.0741
Oxygen	11.8495

[a]. These were computed assuming only U-235, U-238 and Oxygen as constituents. U-234 weight percentage was subsequently computed assuming a natural relative abundance to the computed uranium weight percentage. Result was balanced to obtain a consistent result (i.e., weight percentages sum to 100%).

Table 7.2.1-3. Aluminum Compositions

Element/Isotope [a]	Weight Percent		
	Type 6061 Aluminum (2.6989 g/cc)	Type 1100 Aluminum (2.71 g/cc)	Type 5052-H32 Aluminum (2.70 g/cc)
Aluminum	97.15	99.88	96.4
Carbon	---	---	2.5
Sulfur	0.06	---	---
Silicon	0.82	---	0.25
Titanium	0.61	---	---
Chromium	0.21	---	0.25
Manganese	0.21	---	0.1
Iron	0.82	---	0.4
Copper	0.12	0.12	0.1

[a]. For the ENDF/B-VI analyses here and in subsequent analyses, it was necessary to isotopically expand the chromium, iron, and copper material definitions.

Table 7.2.1-4. Plexiglass Composition (1.18 g/cc)

Element/Isotope	Atom Density (atoms/b-cm)
Hydrogen	0.05678
Carbon	0.03549
Oxygen	0.01420

Table 7.2.1-5. Boral™ Absorber Plate Composition (2.49 g/cc)

Element/Isotope	Weight Percent
Boron-10	5.28
Boron-11	23.42
Carbon	7.97
Sodium	0.02
Magnesium	0.05
Aluminum	62.39
Silicon	0.2
Sulfur	0.03
Chromium	0.05
Iron	0.33
Nickel	0.02
Copper	0.09

Table 7.2.1-6. Type 304 Stainless Steel Composition (7.93 g/cc)

Element/Isotope	Weight Percent
Chromium	18.56
Manganese	1.58
Iron	68.24
Nickel	11.09
Copper	0.27
Molybdenum	0.26

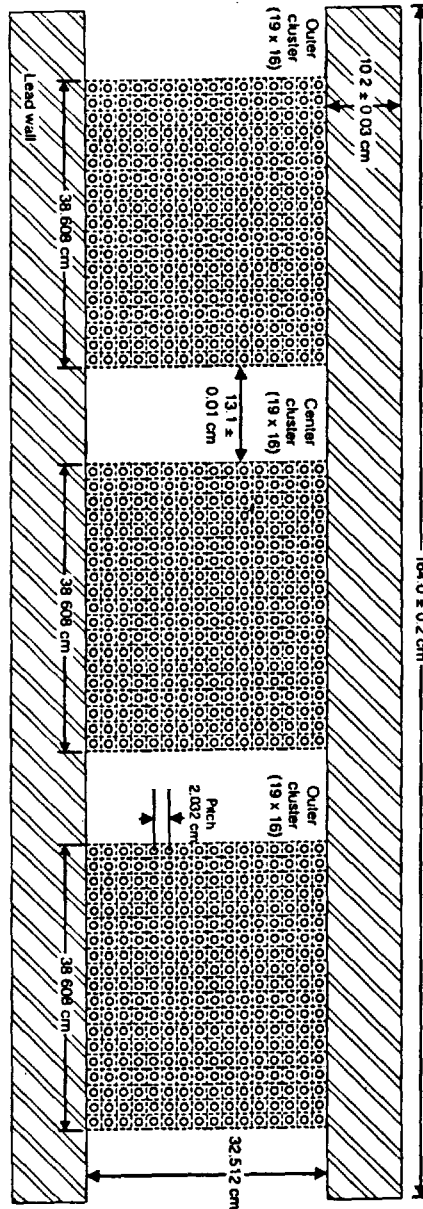
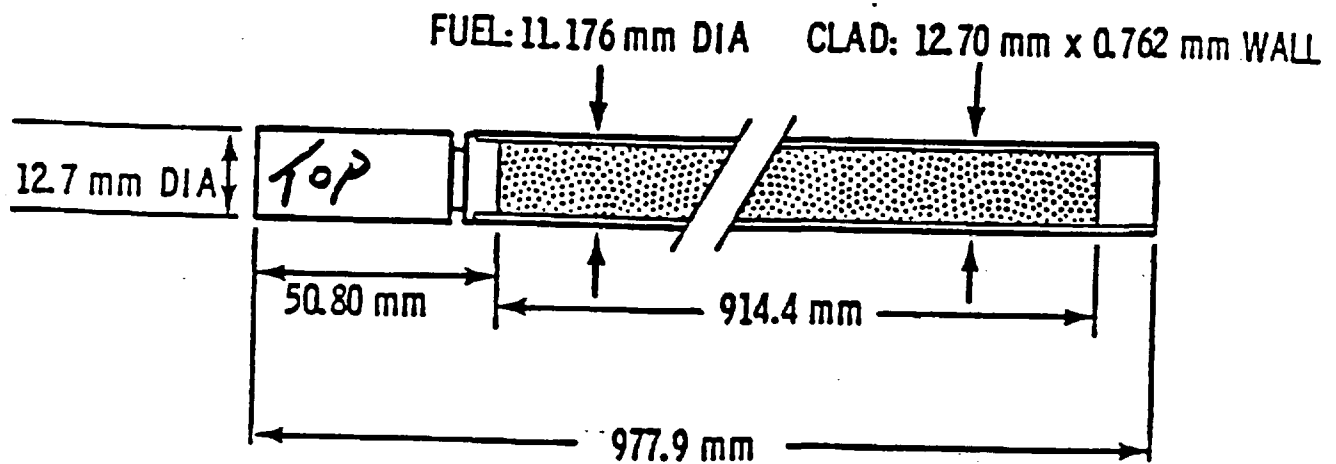


Figure 7.2.1-1.

Experimental Setup for Critical Configurations of Subcritical Clusters of 2.35 wt% Enriched UO_2 Rods in Water with Fixed Neutron Absorber Plates

DESCRIPTION OF 2.35 wt% ^{235}U ENRICHED UO_2 RODS

CLADDING: 6061 ALUMINUM TUBING SEAL WELDED WITH A LOWER END PLUG OF 5052-H32 ALUMINUM AND A TOP PLUG OF 1100 ALUMINUM

TOTAL WEIGHT OF LOADED FUEL RODS: 917 gm (AVERAGE)

LOADING:

825 gm OF UO_2 POWDER / ROD, 726 gm OF U/ROD, 17.08 gm OF U-235/ROD
ENRICHMENT - 2.35 \pm 0.05 w/o U-235

FUEL DENSITY - 9.20 mg/mm³ (84% THEORETICAL DENSITY)

Figure 7.2.1-2. Fuel Rod Description for Critical Configurations of Subcritical Clusters of 2.35 wt% Enriched UO_2 Rods in Water with Fixed Neutron Absorber Plates

7.2.2 Critical Configurations with Subcritical Clusters of 4.31 wt% Enriched UO₂ Rods in Water with Reflecting Walls

As was true for the previously described set of four experiments, these experiments were also performed at the Pacific Northwest Laboratory and were again documented by Bierman (References 5.6 and 5.7). In these experiments three similar fuel assemblies were laterally surrounded by reflectors of different compositions. The fuel lattices in each critical experiment contained 4.31 wt% U-235 enriched UO₂ fuel rods on a square pitch of 1.892 cm. The distinguishing characteristics of each experiment are given in Table 7.2.2-1. These critical experiments demonstrate the ability of MCNP accurately to predict the critical multiplication factor for configurations with different shielding materials used for reflectors. The apparatus for the three experiments is the same as that shown in Figure 7.2.1-1.

Table 7.2.2-1. Differences in Experimental Configurations for Clusters of 4.31 wt% UO₂ Fuel Rods

Case	Reference	Reflector	Assembly Spacing (cm)
exp5	5.6	uranium [a]	19.24
exp6	5.6	lead [b]	17.43
exp7	5.7	stainless steel [c]	15.84

[a]. This component is illustrated in Figure 7.2.2-2.

[b]. This component is illustrated in Figure 7.2.2-3 (note that the trace copper and antimony was neglected in the analysis).

[c]. This component is illustrated in Figure 7.2.2-4.

The fuel rod description is shown in Figure 7.2.2-1 (note that the cladding outer diameter was used to model the rubber end-cap radius rather than the value shown in the drawing). The UO₂ composition used in the MCNP models is shown in Table 7.2.2-2. The Type 6061 aluminum composition used in the MCNP models is shown in Table 7.2.1-3. The acrylic or polypropylene spacer grids and base plate shown in Figure 7.2.1-1 were modeled as plexiglass. Substituting plexiglass for acrylic or polypropylene in the models will have an insignificant effect on the critical multiplication factor of the configurations due the minimal neutron absorptive properties of the constituent isotopes and scattering characteristics similar to water that it is displacing. The plexiglass composition used in the models is shown in Table 7.2.1-4. The fuel rod rubber end-cap composition is shown in Table 7.2.2-3. The 0.952 cm thick carbon steel tank bottom was included in the MCNP models. The carbon steel tank composition is shown in Table 7.2.2-4.

The weight percentages of fuel constituents were computed in accordance with the following equations (Reference 5.16):

(7.2.2-1)

$$f_{U-234}(\%) = 0.007731 \cdot [f_{U-235}(\%)]^{1.0038}$$

(7.2.2-2)

$$f_{U-236}(\%) = 0.0046 \cdot f_{U-235}(\%)$$

(7.2.2-3)

$$f_{U-238}(\%) = 100.0 - f_{U-234}(\%) - f_{U-235}(\%) - f_{U-236}(\%)$$

Table 7.2.2-2. 4.31 wt% U-235 Enriched UO₂ Composition (9.2 g/cc)

Element/Isotope	Weight Percent
U-234	0.03319
U-235	3.79926
U-236	0.01748
U-238	84.29988
Oxygen	11.85019

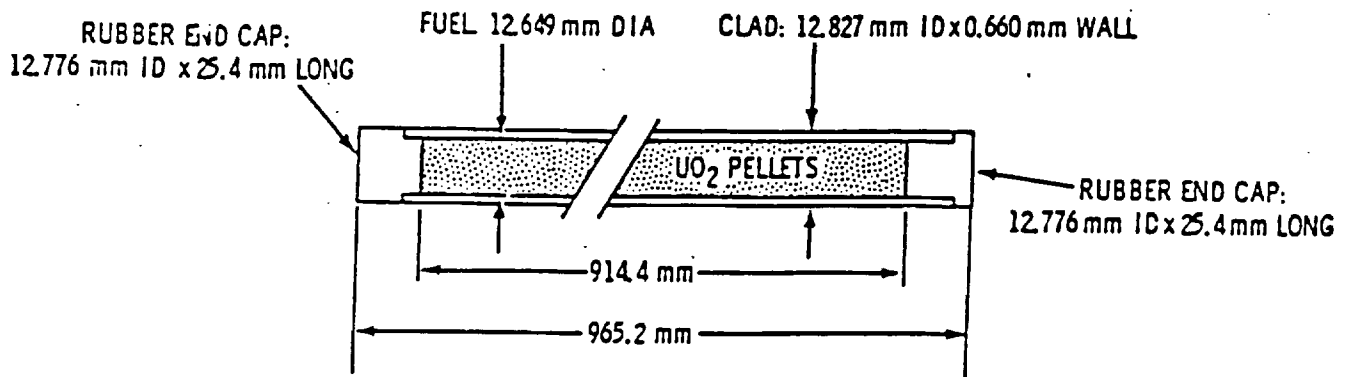
Table 7.2.2-3. Fuel Rod Rubber End-Cap Composition (1.321 g/cc)

Element/Isotope	Weight Percent
Hydrogen	6.5
Carbon	58.0
Calcium	11.4
Sulfur	1.7
Oxygen	22.1
Silicon	0.30

Table 7.2.2-4. Carbon Steel Composition

Element/Isotope	Weight Percent
Iron	98.535
Carbon	0.22
Manganese	0.90
Silicon	0.275
Phosphorus	0.035
Sulfer	0.035

4.31 wt% ²³⁵U ENRICHED UO₂ RODS



CLADDING: 6061 ALUMINUM TUBING

LOADING:

ENRICHMENT - 4.31 ± 0.01 wt% ²³⁵U

FUEL DENSITY - 94.9 ± 0.55% OF THEORETICAL DENSITY

URANIUM ASSAY - 88.055 ± 0.261 wt% OF TOTAL FUEL COMPOSITION

UO₂ - 1203.38 ± 4.12 g/ROD

END CAP:

DENSITY - 1.321 g/cm³

COMPOSITION- C - 58 ± 1 wt%

H - 6.5 ± 0.3 wt%

Ca - 11.4 ± 1.8 wt%

S - 1.7 ± 0.2 wt%

O - 22.1 wt% (BALANCE)

SI - 0.3 ± 0.1 wt%

Figure 7.2.2-1.

Fuel Rod Description for Critical Configurations with Subcritical Clusters of 4.31 wt% Enriched UO₂ Rods in Water with Reflecting Walls

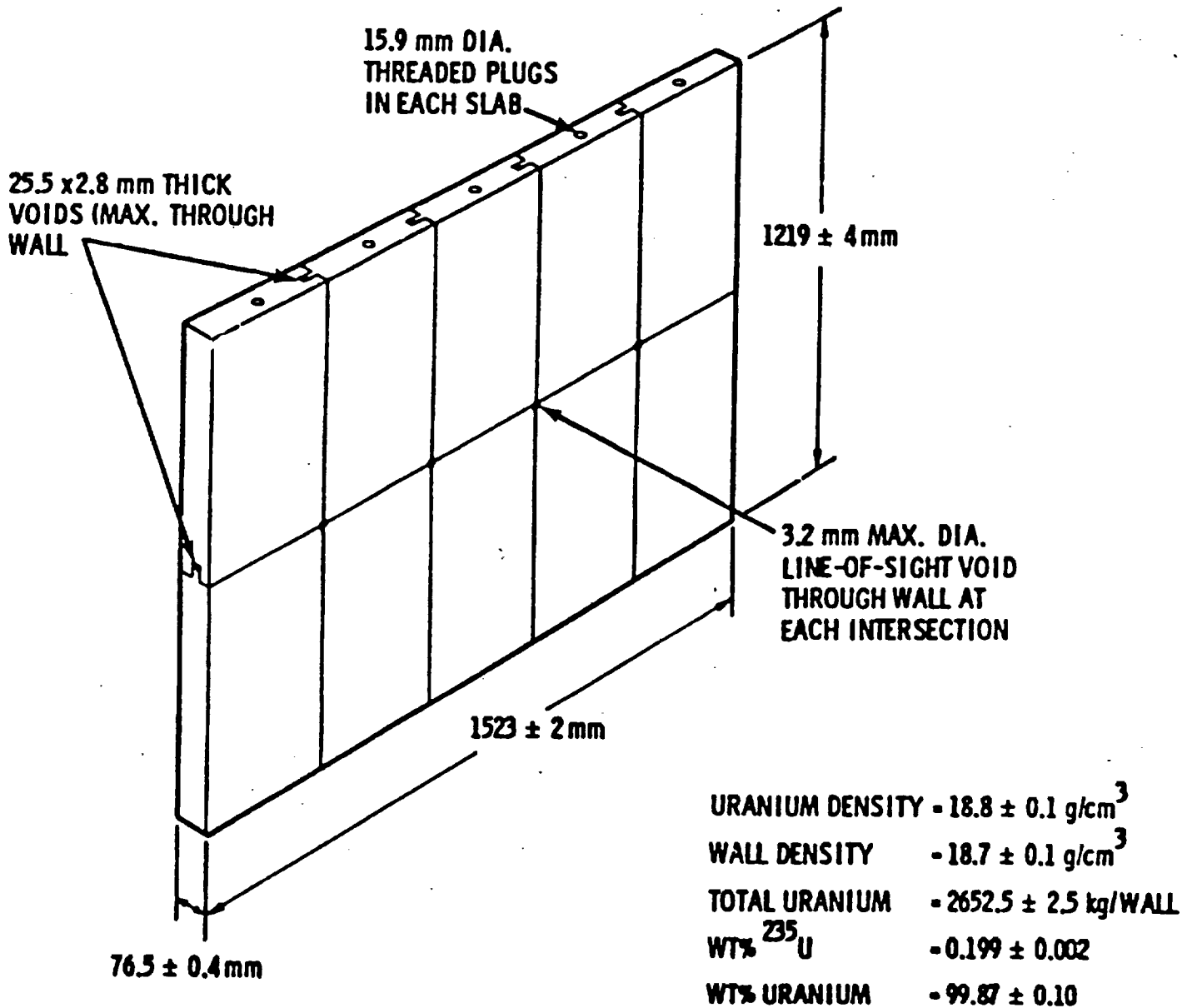


Figure 7.2.2-2.

Uranium Reflecting Wall Description for Critical Configurations with Subcritical Clusters of 4.31 wt% Enriched UO₂ Rods in Water with Reflecting Walls

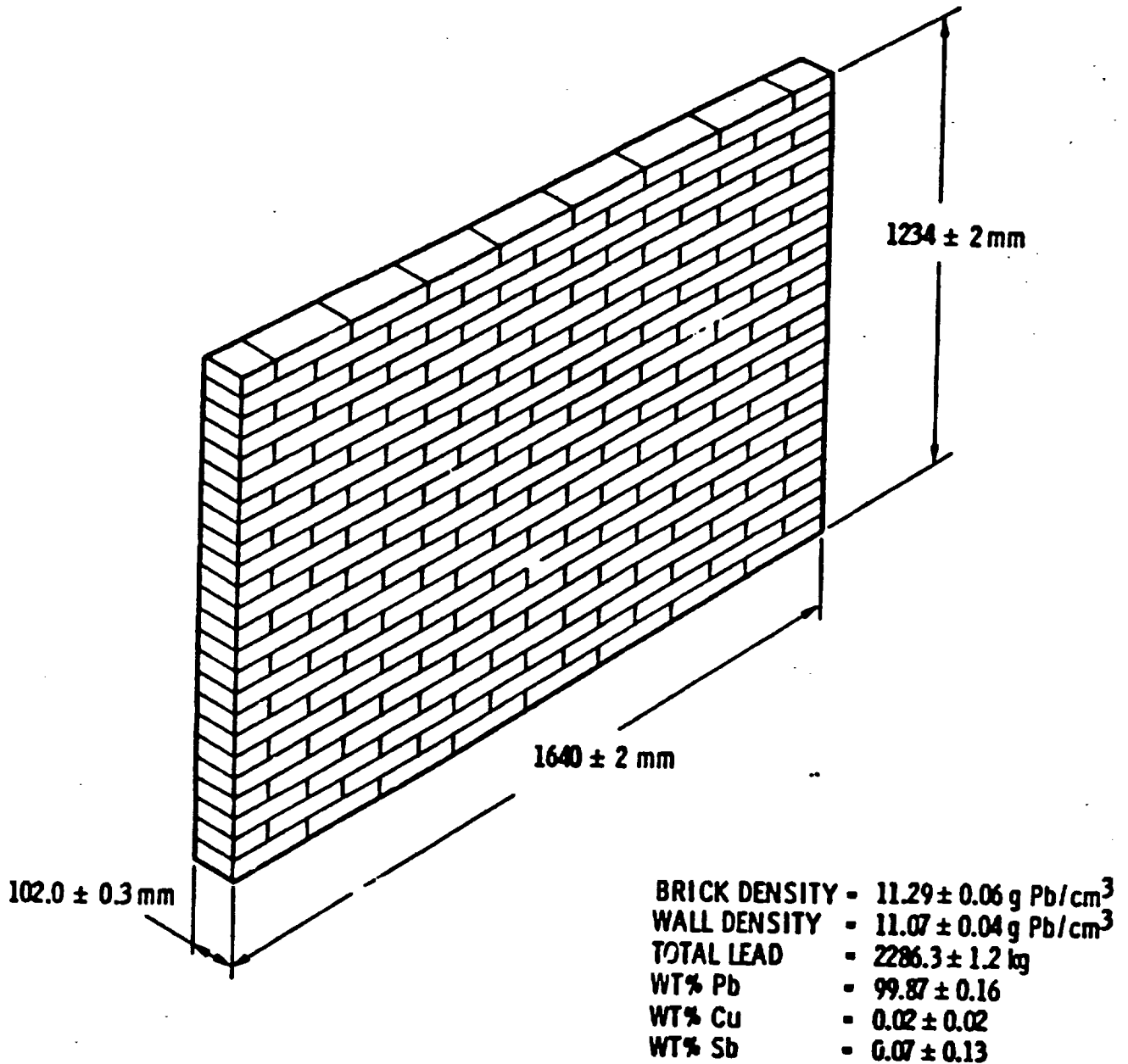


Figure 7.2.2-3.

Lead Reflecting Wall Description for Critical Configurations with Subcritical Clusters of 4.31 wt% Enriched UO₂ Rods in Water with Reflecting Walls

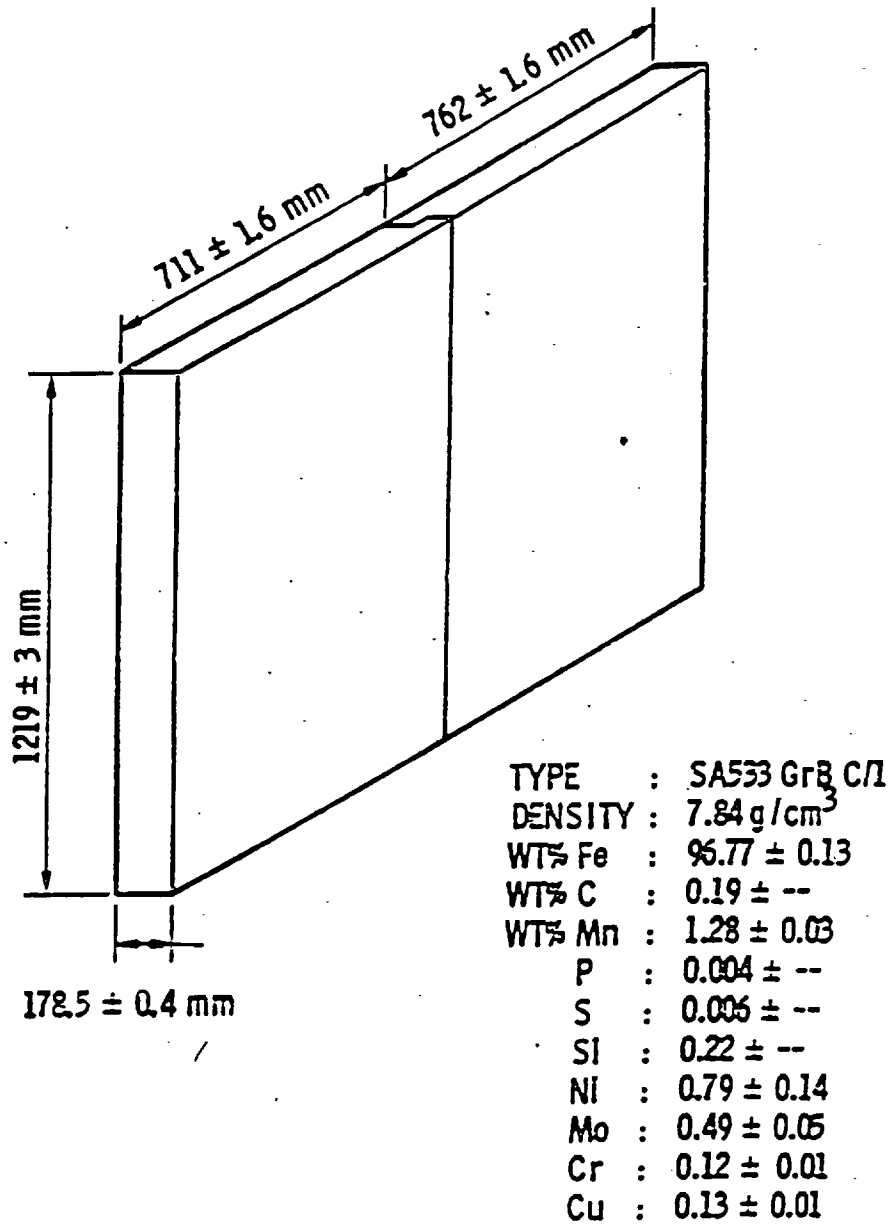


Figure 7.2.2-4. Stainless Steel Reflecting Wall Description for Critical Configurations with Subcritical Clusters of 4.31 wt% Enriched UO₂ Rods in Water with Reflecting Walls

7.2.3 Critical Configurations with 4.31 wt% U-235 Enriched UO_2 Rods in Highly Borated Water Lattices

This is a set of four experiments performed at the Pacific Northwest Laboratory and documented by Durst (Reference 5.8). These experiments used 4.31 wt% U-235 uniformly enriched UO_2 fuel rods arranged in square-pitched water-moderated lattices of different size with various amounts of boric acid in the moderator. The fuel rods were loaded into polypropylene lattice templates fastened inside a plexiglass tank. The fuel rod description is shown in Figure 7.2.3-1. The plexiglass tank was surrounded on all four sides by an unborated water reflector. The plexiglass tank was positioned atop a 15.2 cm thick plexiglass slab. The borated water was restricted to the water volume inside the plexiglass tank. The general experimental configuration is shown in Figure 7.2.3-2.

Rectangular critical arrays were constructed by sequentially filling rows of the lattice template starting at the plexiglass tank wall. The water level in the tank was held constant by removing an appropriate volume of water as each fuel rod is loaded. The critical array width remained constant at either 40 or 44 rods depending on the lattice pitch.

The UO_2 fuel isotopic composition used in the MCNP model is shown in Table 7.2.3-1. The Type 6061 aluminum composition used for the fuel rod cladding in the MCNP model for "exp8" is shown in Table 7.2.1-3. The fuel rod rubber end-cap composition used in the MCNP model is shown in Table 7.2.2-3. The plexiglas material composition used in the model is shown in Table 7.2.1-4, while that for polypropylene is shown in Table 7.2.3-2.

Table 7.2.3-1. 4.31 wt% U-235 Enriched UO_2 Fuel Composition (10.4 g/cc)

Element/Isotope	Weight Percent [a]
U-234	0.03319
U-235	3.79926
U-236	0.01748
U-238	84.29988
Oxygen	11.85019

[a]. These values were computed according to the equations shown in §7.2.2.

Table 7.2.3-2. Polypropylene Composition

Element/Isotope	Polypropylene Weight Percent (0.90 g/cc)
Hydrogen	14.372
Carbon	85.628

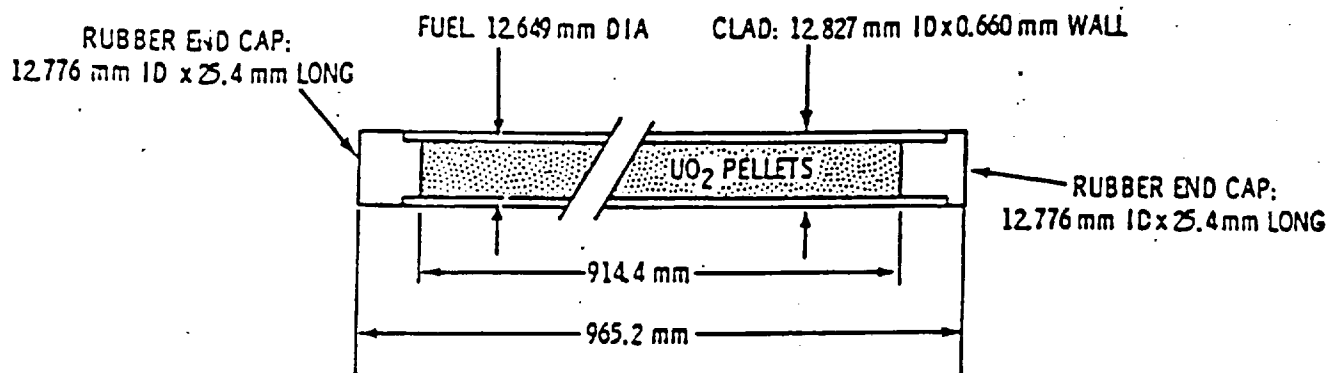
The first experiment, designated "exp8," is a 1.89 cm square pitch array of 357 fuel rods immersed in a non-borated water moderator. The critical array width is 40 rods. The last row of the critical array contains 37 rods.

The second experiment, designated "exp9," is a 1.89 cm square pitch array of 1237 fuel rods immersed in a water moderator containing 2.55 g/liter of boron. The critical array width is 40 rods. The last row of the critical array contains 37 rods.

The third experiment, designated "exp10," is a 1.715 cm square pitch array of 509 fuel rods immersed in a non-borated water moderator. The critical array width is 44 rods. The last row of the critical array contains 25 rods.

The fourth experiment, designated "exp11," is a 1.715 cm square pitch array of 1192 fuel rods immersed in a non-borated water moderator. The critical array width is 44 rods. The last row of the critical array contains 4 rods.

4.31 wt% ²³⁵U ENRICHED UO₂ RODS



CLADDING: 6061 ALUMINUM TUBING

LOADING:

ENRICHMENT - 4.31 ± 0.01 wt% ²³⁵U

FUEL DENSITY - 94.9 ± 0.55% OF THEORETICAL DENSITY

URANIUM ASSAY - 88.055 ± 0.261 wt% OF TOTAL FUEL COMPOSITION

UO₂ - 1203.38 ± 4.12 g/ROD

END CAP:

DENSITY - 1.321 g/cm³

COMPOSITION- C-58 ± 1 wt%

H-6.5 ± 0.3 wt%

Ca-11.4 ± 1.8 wt%

S-1.7 ± 0.2 wt%

O-22.1 wt% (BALANCE)

SI-0.3 ± 0.1 wt%

Figure 7.2.3-1.

Fuel Rod Description for Critical Configurations with 4.31 wt% Enriched UO₂ Rods in Highly Borated Water Lattices

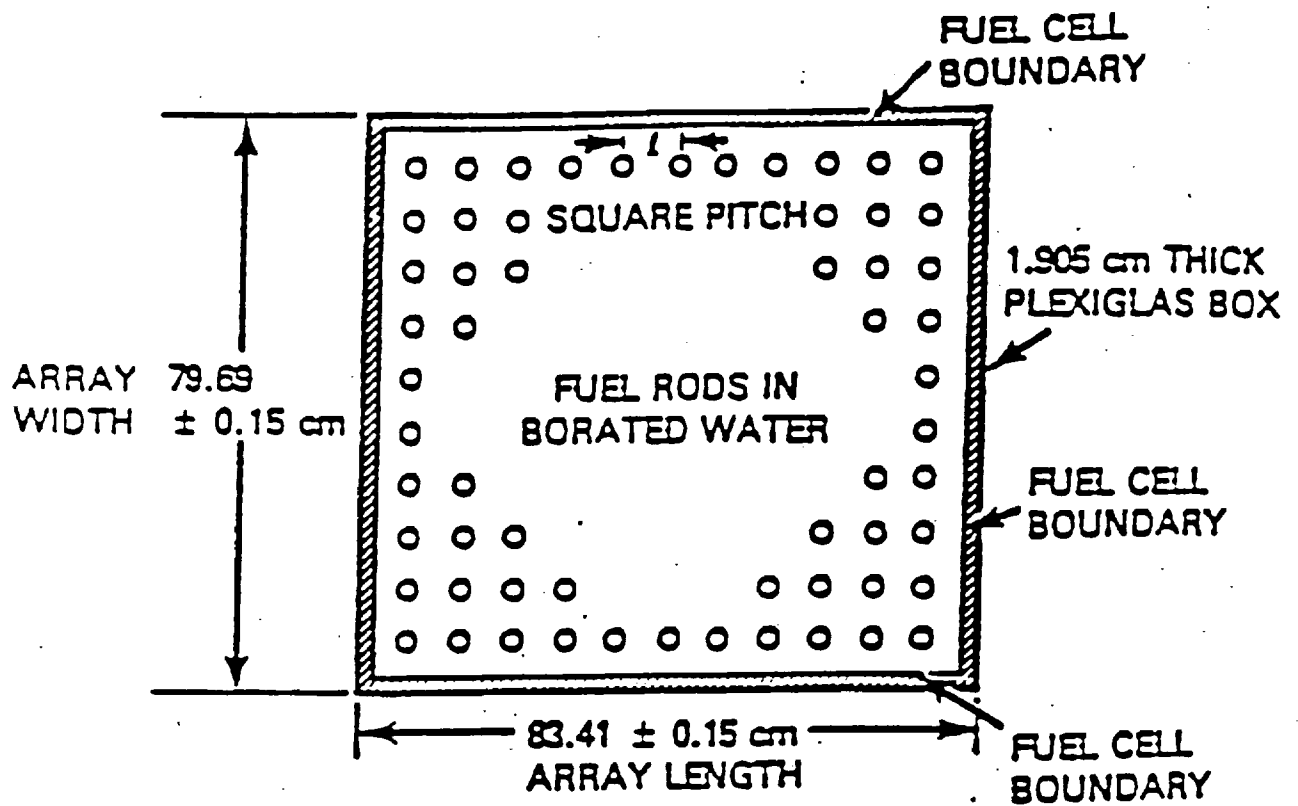


Figure 7.2.3-2. General Experimental Setup for Critical Configurations with 4.31 wt% Enriched UO_2 Rods in Highly Borated Water Lattices

7.2.4 Critical Configurations with Neutron Flux Traps

Pacific Northwest Laboratories performed experiments studying the effect of neutron flux traps on criticality. These experiments were documented by Bierman (Reference 5.9) and served as the source for two such configurations modeled with MCNP. These two critical experiments were each composed of four fuel rod arrays arranged in a square and separated by a neutron flux trap region. Each fuel lattice in a given configuration is nearly equal in size. Two polypropylene lattice templates were used to position the fuel rods with a 1.891 cm square pitch. The axial profile of the general experimental configuration is shown in Figure 7.2.4-1. The fuel rods are composed of aluminum-clad 4.31 wt% U-235 enriched UO₂ fuel. The 4.31 wt% U-235 enriched UO₂ fuel rods are described in Figure 7.2.4-2. The UO₂ fuel isotopic composition used in the MCNP models is shown in Table 7.2.4-1. The Type 6061 aluminum cladding composition is shown in Table 7.2.4-2. The fuel rod rubber end-cap composition is shown in Table 7.2.2-3. The polypropylene lattice plates are 1.23 cm thick with a density of 0.90 g/cc. The polypropylene composition (C₃H₆) used in the MCNP models is shown in Table 7.2.3-2. The neutron flux traps are created by positioning two plates of Boral™ between interacting faces of each fuel lattice. The Boral™ plates are separated by 3.73 cm of water. The Boral™ plates are composed of a homogeneous mixture of aluminum and boron-carbide particles sandwiched between two 0.102 cm thick plates of aluminum alloy. The material composition and physical description of the neutron absorber plates are shown in Table 7.2.4-3. The experimental configurations are moderated and closely reflected by full-density water.

Table 7.2.4-1. 4.31 wt% U-235 Enriched UO₂ Fuel Composition (10.47 g/cc)

Element/Isotope	Weight Percent
U-234	0.01937
U-235	3.79166
U-236	0.01937
U-238	84.22490
Oxygen	11.94469

Table 7.2.4-2. Aluminum Composition for "exp12" and "exp13"

Element/Isotope	Weight Percent
Aluminum	96.93
Magnesium	1.0
Silicon	0.6
Titanium	0.15
Chromium	0.195
Manganese	0.15
Iron	0.7
Copper	0.275

Table 7.2.4-3. Neutron Absorber Plate Description

Material	Weight Percent
Aluminum	62.54
Boron	29.22
Carbon	8.16
Oxygen	0.06
Iron	0.02
Core Density: 2.64 g/cc Core Thickness: 0.470 cm Length: 96 cm Width: 45 cm	

The first critical configuration, designated "exp12," contains a total of 952 fuel rods. The fuel rods are arranged into three 15 x 16 arrays and one 15 x 15 array with a partial sixteenth row of seven fuel rods. Each fuel array is positioned in one of the four quadrants delineated by the flux

trap region. A planar view of the general configuration is shown in Figure 7.2.4-3. The experiment identifier number corresponding to "exp12" in Reference 5.9 is 214R.

The second critical configuration, designated "exp13," contains a total of 862 fuel rods. The fuel rods are arranged into two 14 x 15 arrays, one 15 x 15 array, and one 14 x 15 array with a partial fifteenth row of seven fuel rods. Each fuel array is positioned in one of the four quadrants delineated by the flux trap region. Each segment of the flux trap region contains three equally spaced, 0.63 cm thick, Type 6061 aluminum plates. The aluminum plates are used to simulate voiding in the flux trap region. A planar view of the general configuration is shown in Figure 7.2.4-4. The experiment identifier number corresponding to "exp13" in Reference 5.9 is 214V3.

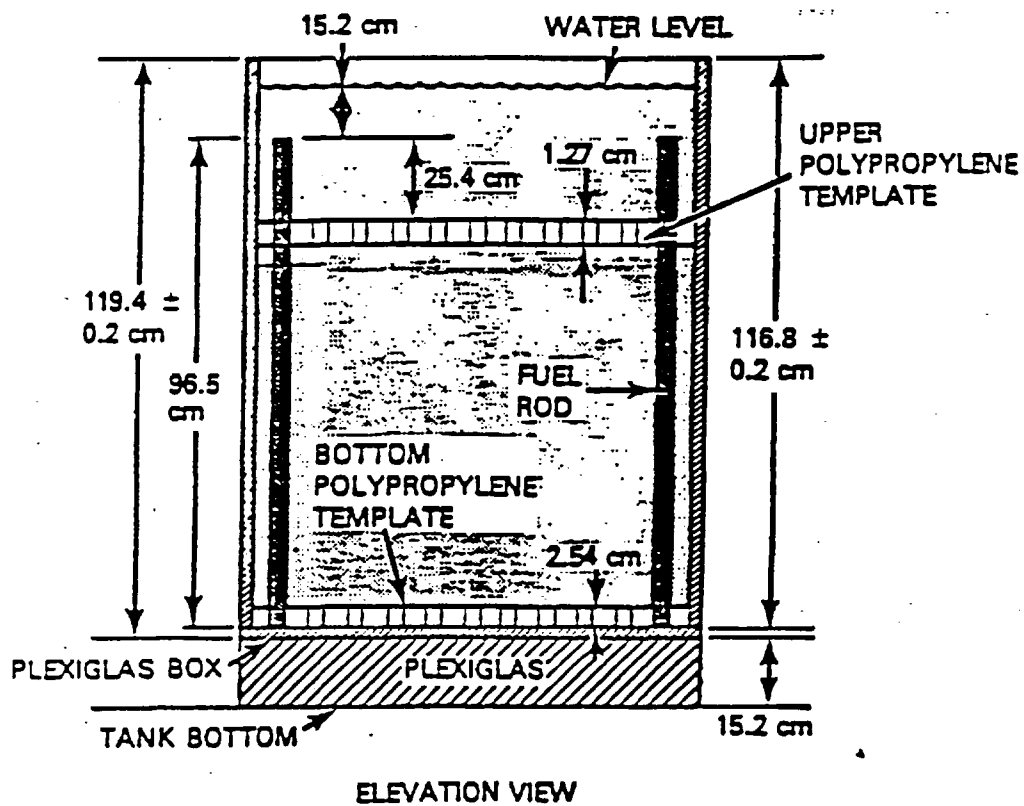
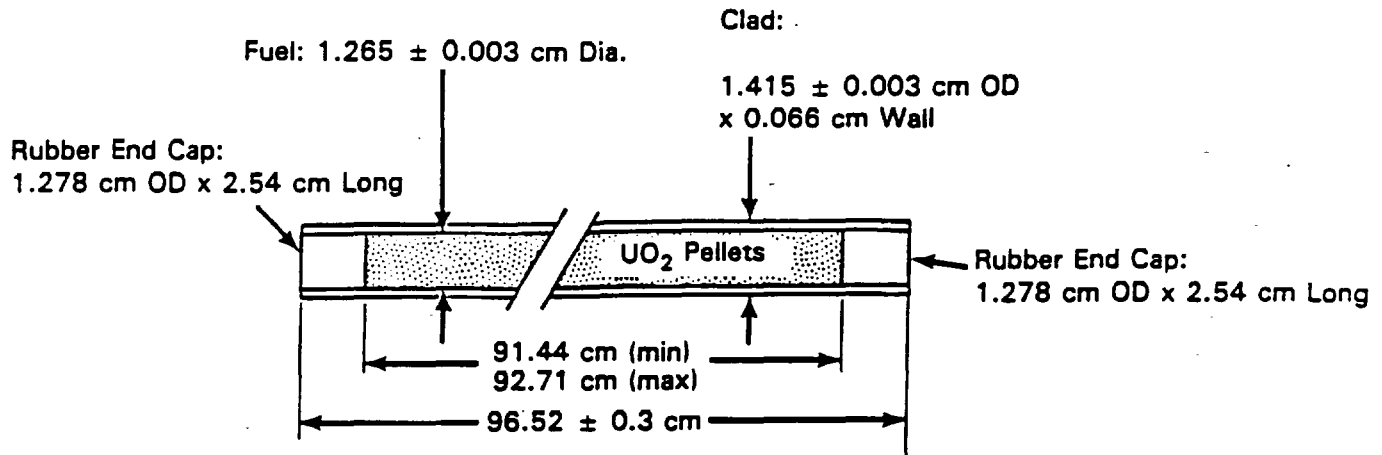


Figure 7.2.4-1. Axial Profile of General Configuration for Experiments Containing Neutron Flux Trap Regions



Cladding: 6061 Aluminum Tubing

Loading

Enrichment - 4.306 ± 0.013 wt% ^{235}U
 Oxide Density - 10.40 ± 0.06 g/cm³
 UO₂ - 1203.38 ± 4.12 g/Rod
 U - 1059.64 ± 4.80 g/Rod

Uranium Composition:

^{234}U - 0.022 ± 0.002 wt%
 ^{235}U - 4.306 ± 0.013 wt%
 ^{236}U - 0.022 ± 0.002 wt%
 ^{238}U - 95.650 ± 0.017 wt%

End Cap:

C- 58 ± 1 wt% S- 1.7 ± 0.2 wt%
 H- 6.5 ± 0.3 wt% O- 22.1 wt% (Balance)
 Ca- 11.4 ± 1.8 wt% Si- 0.3 ± 0.1 wt%

Notes:

1. Error limits are one standard deviation
2. End Cap Density is 1.321 g/cm³

Figure 7.2.4-2. Fuel Rod Description for Critical Configurations Using 4.31 wt% Enriched UO₂ Rods and Neutron Flux Trap Regions

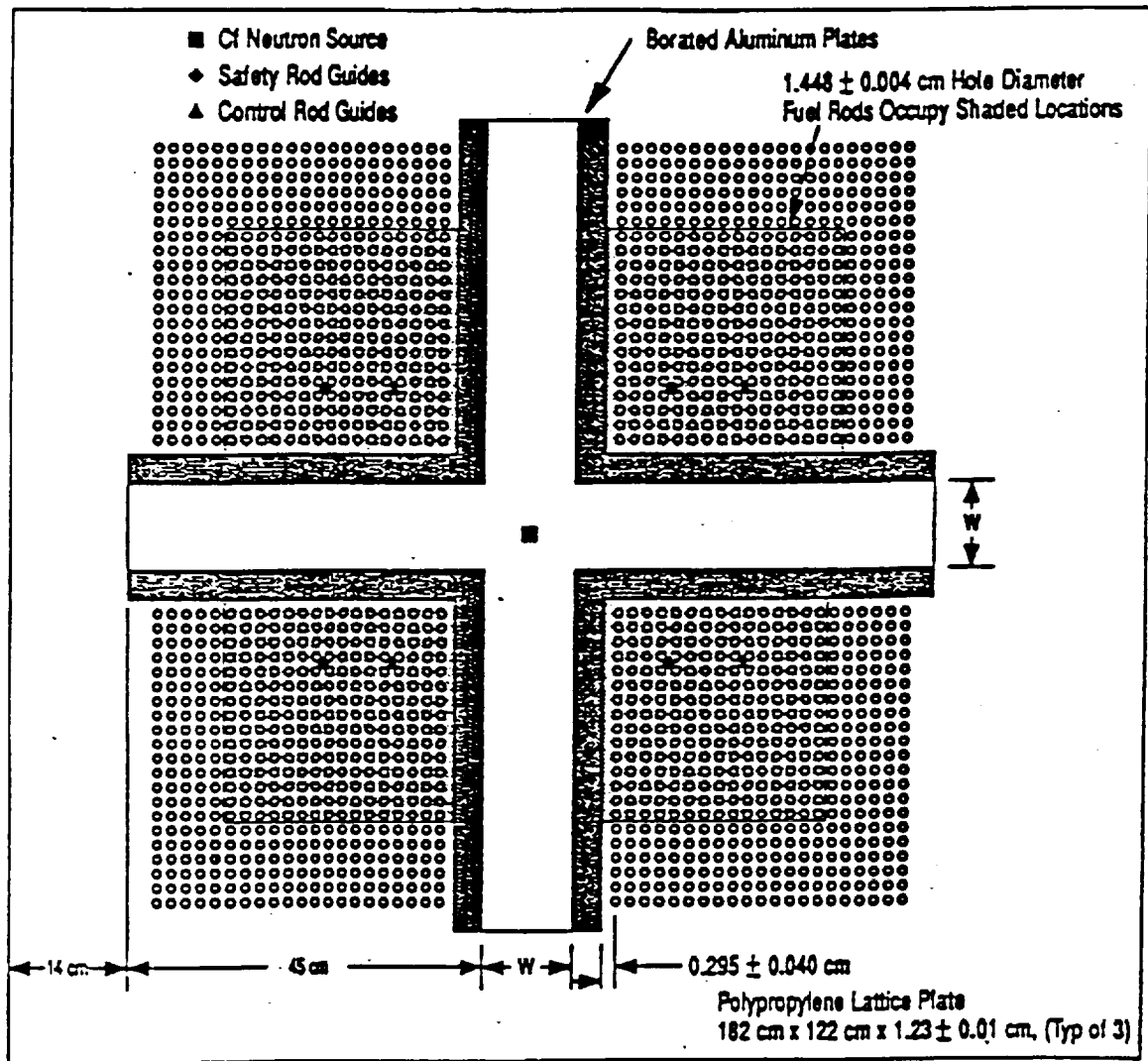


Figure 7.2.4-3. Planar View of "exp12" in the Set of Critical Configurations Containing Neutron Flux Trap Regions

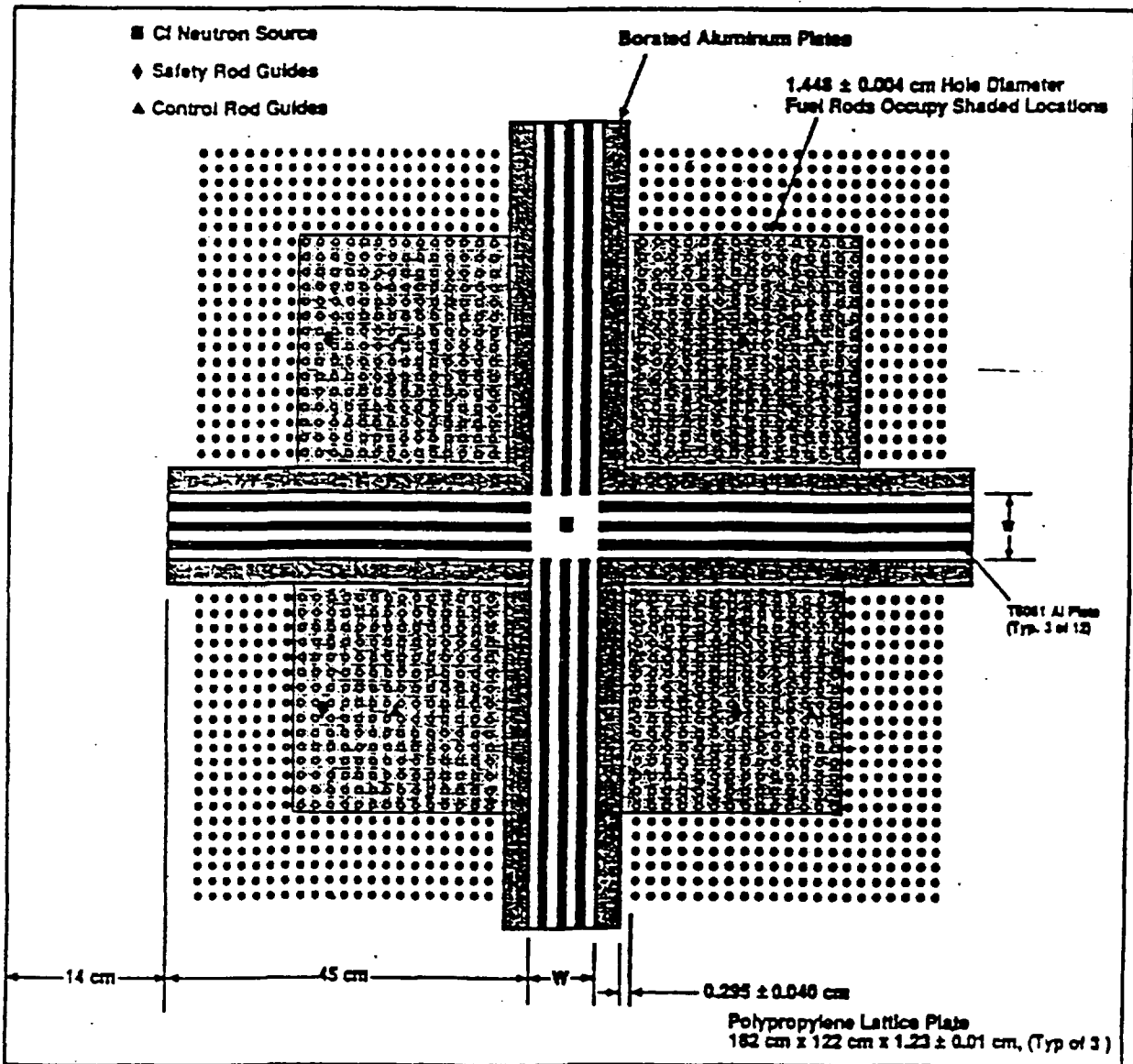


Figure 7.2.4-4. Planar View of "exp13" in the Set of Critical Configurations Containing Neutron Flux Trap Regions

7.2.5 Electric Power Research Institute 2.35 wt% U-235 Enriched Light Water Reactor Fuel Critical Configurations

Under the aegis of the Electric Power Research Institute, criticality experiments were performed for light water reactor fuel configurations. These were documented by Smith (Reference 5.11) and subsequently described by Bowman (Reference 5.10). Two critical experiment configurations composed of water-moderated lattices of 2.35 wt% enriched UO_2 fuel rods were modeled with MCNP. The UO_2 fuel rod description is shown in Figure 7.2.5-1. The UO_2 composition used in the MCNP models is shown in Table 7.2.5-1. The fuel rods were supported in a core structure composed of "eggcrate" type lattice plates with an upper lead shield. The axial view of the general core configuration is shown in Figure 7.2.5-2. The eggcrate lattice description is shown in Figure 7.2.5-3. The aluminum compositions used in the MCNP models are comprised of 99.88 wt% aluminum and 0.12 wt% copper. The configuration was closely reflected by at least 30 cm of water laterally and below the aluminum base plate.

Table 7.2.5-1. 2.35 wt% U-235 Enriched UO_2 Fuel Composition (9.20 g/cc)

Element/Isotope	Atom Density (atom/b·cm)
U-234	$3.2442 \cdot 10^{-6}$
U-235	$5.5412 \cdot 10^{-4}$
U-236	$4.0150 \cdot 10^{-6}$
U-238	$2.2728 \cdot 10^{-2}$
Oxygen	$4.1559 \cdot 10^{-2}$

The first experiment, designated "exp14," is a square lattice on a 1.526 cm pitch and contains 708 fuel rods (the MCNP model has 709 fuel rods due to the symmetrical modeling used). The core loading diagram is shown in Figure 7.2.5-4. The water-to-fuel volume ratio is 1.196 and the water moderator is unborated.

The second experiment, designated "exp15," is a square lattice on a 2.210 cm pitch and contains 342 fuel rods (the MCNP model has 341 fuel rods, again to obtain a symmetrical problem). The core loading diagram is shown in Figure 7.2.5-5. The same eggcrate lattice plate used in the "exp14" (1.526 cm) core was used in this experiment. The fuel rods are loaded into every other lattice location to obtain the 2.210 cm pitch. The water-to-fuel volume ratio is 3.687 and the water moderator is unborated.

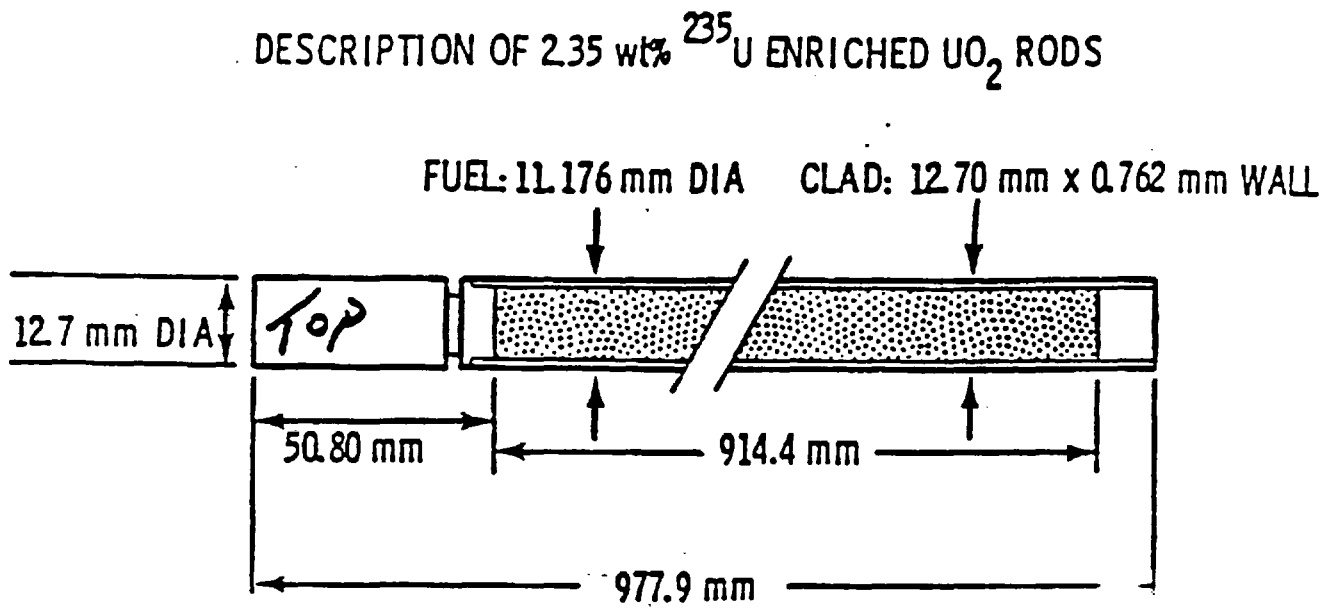


Figure 7.2.5-1. Fuel Rod Description for the EPRI 2.35 wt% Enriched Light Water Reactor Fuel Critical Configurations

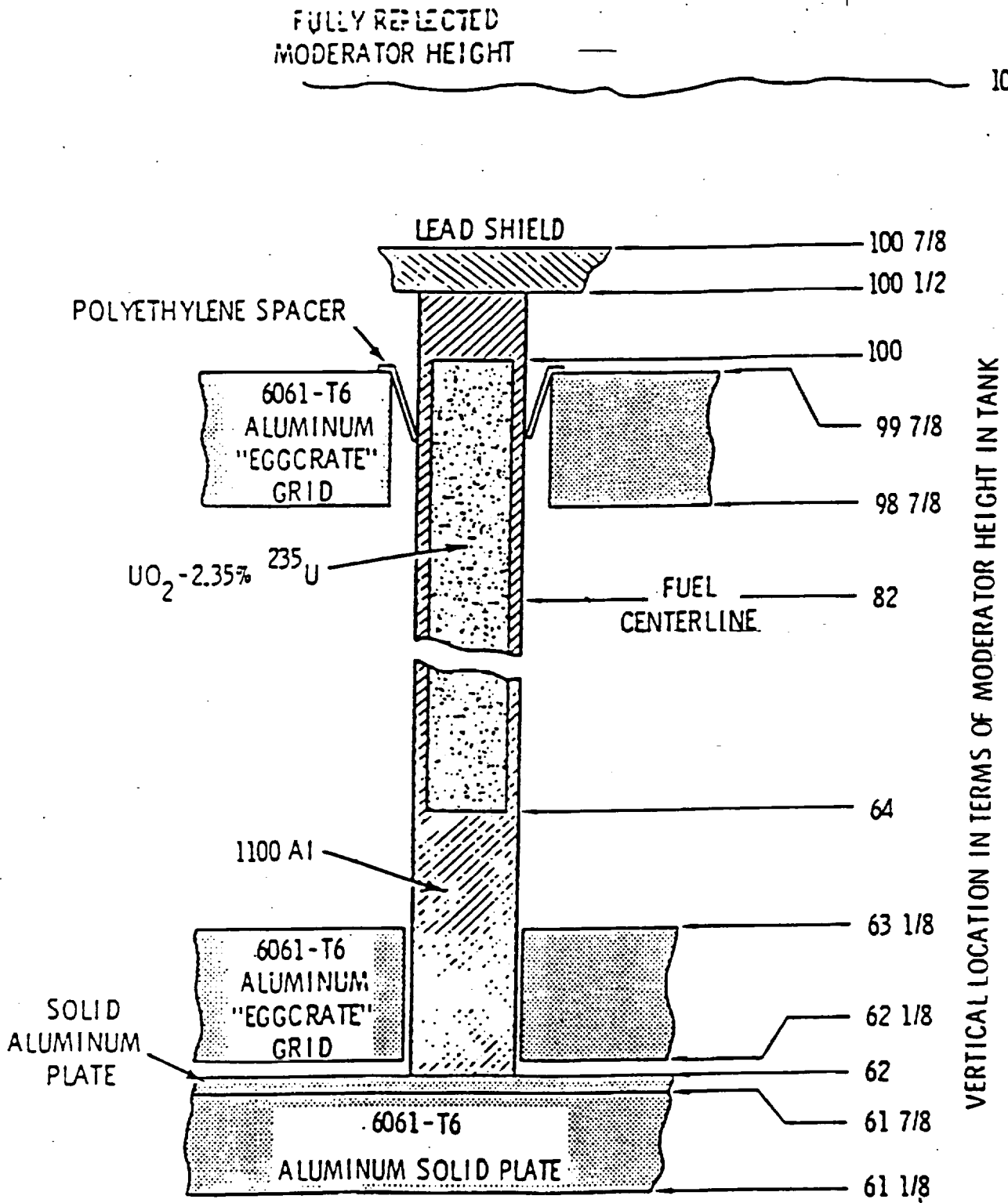
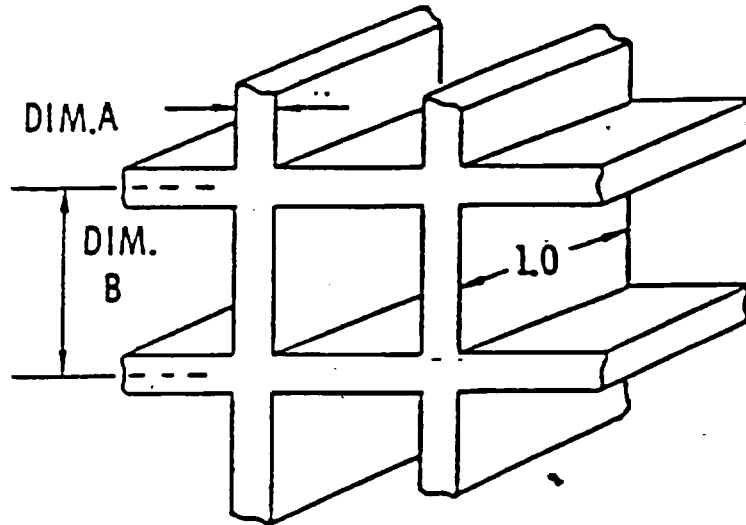


Figure 7.2.5-2. Axial View of the EPRI 2.35 wt% Enriched Light Water Reactor Fuel Critical Configurations



FUEL TYPE	PITCH	GRID	DIM.A	DIM B
UO ₂ -2.35% ²³⁵ U	0.615 0.87	UPPER LOWER	0.032 0.090	0.615
UO ₂ -2 WT% PuO ₂ (8% ²⁴⁰ Pu)	0.87	UPPER LOWER	0.032 0.032	0.615
UO ₂ -2 WT% PuO ₂ (8% ²⁴⁰ Pu)	0.70 0.99	UPPER LOWER	0.125 0.125	0.70

Figure 7.2.5-3. Egg-Crate Lattice Description for the EPRI 2.35 wt% Enriched Light Water Reactor Fuel Critical Configurations

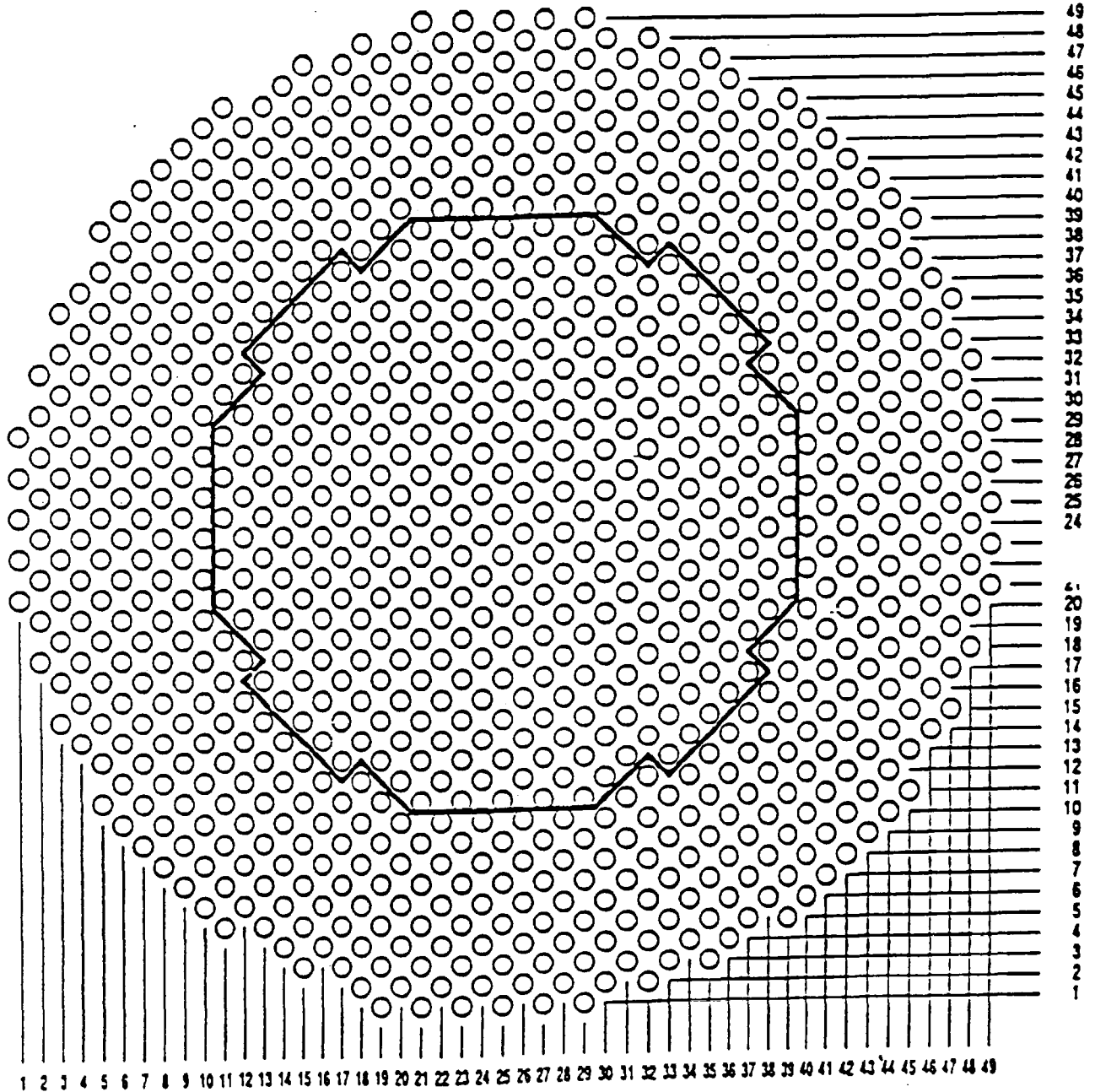


Figure 7.2.5-5. Core Loading Description for "exp15" of the EPRI 2.35 wt% Enriched Light Water Reactor Fuel Critical Configurations

7.2.6 Laboratory Critical Experiments from the Urania-Gadolinia: Nuclear Model Development and Critical Experiment Benchmark Report

Babcock and Wilcox performed a number of critical experiments for urania fuel incorporating gadolinia as an integral burnable absorber. These experiments were documented by Newman (Reference 5.12). The configurations modeled with MCNP include critical configurations containing arrangements of 2.46 wt% U-235 enriched UO_2 fuel rods, 4.02 wt% U-235 enriched UO_2 fuel rods, combination 4 wt% Gd_2O_3 and 96 wt% (1.944 wt% U-235 enriched) UO_2 fuel rods, Ag-In-Cd absorber rods, and B_4C absorber rods. Each critical configuration contains an array of fuel rods on a square pitch of 1.636 cm. The fuel rods are supported by a top and bottom aluminum "eggcrate" type grid plate. The eggcrate grid plate is composed of 2.54 cm wide by 0.4064 cm thick slotted aluminum strips interlocked to form a square matrix. The fuel rods rest on a 5.08 cm thick aluminum base plate. The central 45 x 45 array of rod lattice cells is separated into nine 15 x 15 arrays of rod lattice cells. The 15 x 15 arrays simulate Pressurized Water Reactor fuel assembly lattices. The fuel loading in the core configuration is altered to produce the various critical configurations examined in this analysis. Tables 7.2.6-1, 7.2.6-2, 7.2.6-3, and 7.2.6-4 contain the descriptions for the 2.46 wt% UO_2 , 4.02 wt% UO_2 , UO_2/Gd_2O_3 fuel rods, and Ag-In-Cd pins, respectively. All of the configurations are modeled assuming one-eighth symmetry.

Table 7.2.6-1. 2.46 wt% U-235 Enriched UO_2 Fuel Rod Description

Parameter	Value
Outside Diameter	1.206 cm
Wall Thickness	0.081 cm
Wall Material	Aluminum
Pellet Diameter	1.030 cm
Total Length	156.44 cm
Active Fuel Length	153.34 cm
Enrichment	2.459 wt% U-235 in U
Density	9.46 g/cc

Table 7.2.6-2. 4.02 wt% U-235 Enriched UO₂ Fuel Rod Description

Parameter	Value
Outside Diameter	1.2078 cm
Wall Thickness	0.0406 cm
Wall Material	Type 304 Stainless Steel
Fuel Diameter	1.1278 cm
Total Length	181.6 cm
Active Fuel Length	169.4 cm
Enrichment	4.020 wt% U-235 in U
Fuel Density	9.46 g/cc

**Table 7.2.6-3
4 wt% Gd₂O₃, 96 wt% (1.944 wt% U-235 Enriched) UO₂ Fuel Rod Description**

Parameter	Value
Outside Diameter	1.2065 cm
Inner Diameter (Annular Pellets)	0.3302 cm
Wall Thickness	0.0813 cm
Wall Material	Type 6063 Aluminum [a]
Fuel Diameter	1.030 cm
Total Length	160.0 cm [b]
Active Fuel Length	153.4 cm
Weight Percent of UO ₂	96 wt%
Weight Percent of Gd ₂ O ₃	4 wt%
Enrichment	1.944 wt% U-235 in U
Fuel Density	10.11 g/cc

[a] The composition for Type 6063 aluminum is given in Table 7.2.6-6.

[b] Includes 0.3175 cm thick aluminum plug at top and bottom.

Table 7.2.6-4. Physical Properties of Ag-In-Cd Rods

Parameter	Value
Length	157.556 cm (62.03 inches)
Diameter	1.016 cm (0.400 inches)
Composition	
Material	Weight Percent
Silver	79.70
Indium	15.09
Cadmium	5.2
Copper	0.05

The Ag-In-Cd absorber rods are clad with 1.2065 cm outer diameter (OD) by 0.0813 cm thick Type 6063 aluminum. The aluminum is sealed at the bottom by a 1/8 inch thick aluminum plug welded in place. The aluminum is sealed at the top by a removable cork.

The B₄C absorber rods are composed of 1.1125 cm OD by 0.0889 cm thick aluminum tubes filled with B₄C powder. As with the Ag-In-Cd rods, the bottom ends are sealed with welded aluminum plugs, and the top ends are sealed with a removable cork. Each rod contains 156 grams of B₄C which equates to a column height ranging over the full core height. The space within the rod above the B₄C is void. The B₄C powder is compacted to a linear density of 0.8791 ± 0.001 grams per centimeter in all rods. The results of a certified B₄C chemical analysis are shown in Table 7.2.6-5.

Table 7.2.6-5. B₄C Composition used in Analyses

Element/Isotope	Weight Percent
B-10	14.44957
B-11	63.94897
Carbon	21.23300
Oxygen	0.36747

Table 7.2.6-6 Type 6063 Aluminum Composition

Element/Isotope	Weight Percent
Magnesium	0.675
Aluminum	98.175
Silicon	0.400
Titanium	0.100
Chromium	0.100
Manganese	0.100
Iron	0.350
Copper	0.100

Descriptions of the experimental configurations are shown in Table 7.2.6-7. The core loading diagrams for experimental configurations are shown in Figures 7.2.6-1 through 7.2.6-19.

Table 7.2.6-7 Urania-Gadolinia Critical Experiment Descriptions

Exp. Ident.	Number of 2.46 wt% U-235 Fuel Rods	Number of 4.02 wt% U-235 Fuel Rods	Number of Gd ₂ O ₃ Fuel Rods	Number of B ₄ C Rods	Number of Ag-In-Cd Rods	Number of Void Rods	Number of Water Holes	Mod. Boron Conc. (ppm)
ugd1	4808	0	0	0	0	0	153	1337.9 ± 0.4
ugd2	4808	0	0	0	16	0	137	1250.0 ± 1.0
ugd3	4788	0	20	0	0	0	153	1239.3 ± 0.7
ugd4	4788	0	20	0	16	0	137	1171.7 ± 1.0
ugd5	4780	0	28	0	0	0	153	1208.0 ± 0.4
ugd6	4780	0	28	0	16	0	137	1155.8 ± 1.5
ugd7	4780	0	28 (Annular)	0	0	0	153	1208.8 ± 0.5
ugd8	4772	0	36	0	0	0	153	1170.7 ± 0.5
ugd9	4772	0	36	0	16	0	137	1130.5 ± 0.6
ugd10	4772	0	36	0	0	16	137	1177.1 ± 0.6
ugd12	3920	888	0	0	0	0	153	1899.3 ± 0.9
ugd13	3920	888	0	16	0	0	137	1635.4 ± 0.7
ugd14	3920	860	28	0	0	0	153	1653.8 ± 0.7

Title: MCNP Evaluation of Laboratory Critical Experiments: Lattice Criticals

Document Identifier: BBA000000-01717-0200-00009 REV 00

Page 50 of 120

Exp. Ident.	Number of 2.46 wt% U-235 Fuel Rods	Number of 4.02 wt% U-235 Fuel Rods	Number of Gd ₂ O ₃ Fuel Rods	Number of B ₄ C Rods	Number of Ag-In-Cd Rods	Number of Void Rods	Number of Water Holes	Mod. Boron Conc. (ppm)
ugd15	3920	860	28	16	0	0	137	1479.7 ± 0.6
ugd16	3920	852	36	0	0	0	153	1579.4 ± 0.9
ugd17	3920	852	36	16	0	0	137	1432.1 ± 1.5
ugd18	3676	944	0	0	0	0	180	1776.8 ± 1.0
ugd19	3676	928	16	0	0	0	180	1628.3 ± 0.8
ugd20	3676	912	32	0	0	0	180	1499.0 ± 0.6

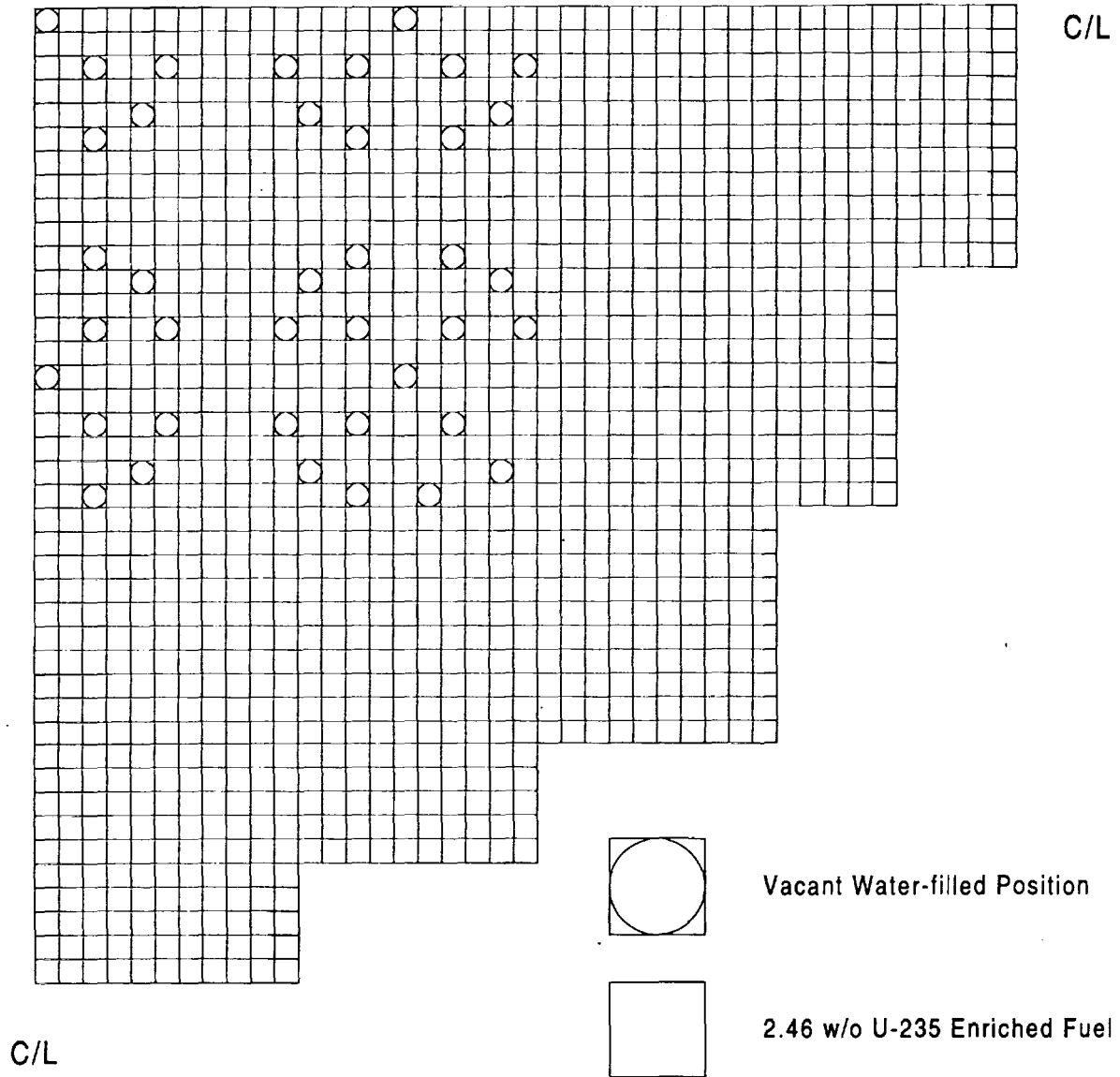


Figure 7.2.6-1. Core Loading Description for "ugd1" Experiment of the Urania-Gadolinia Critical Benchmark Set

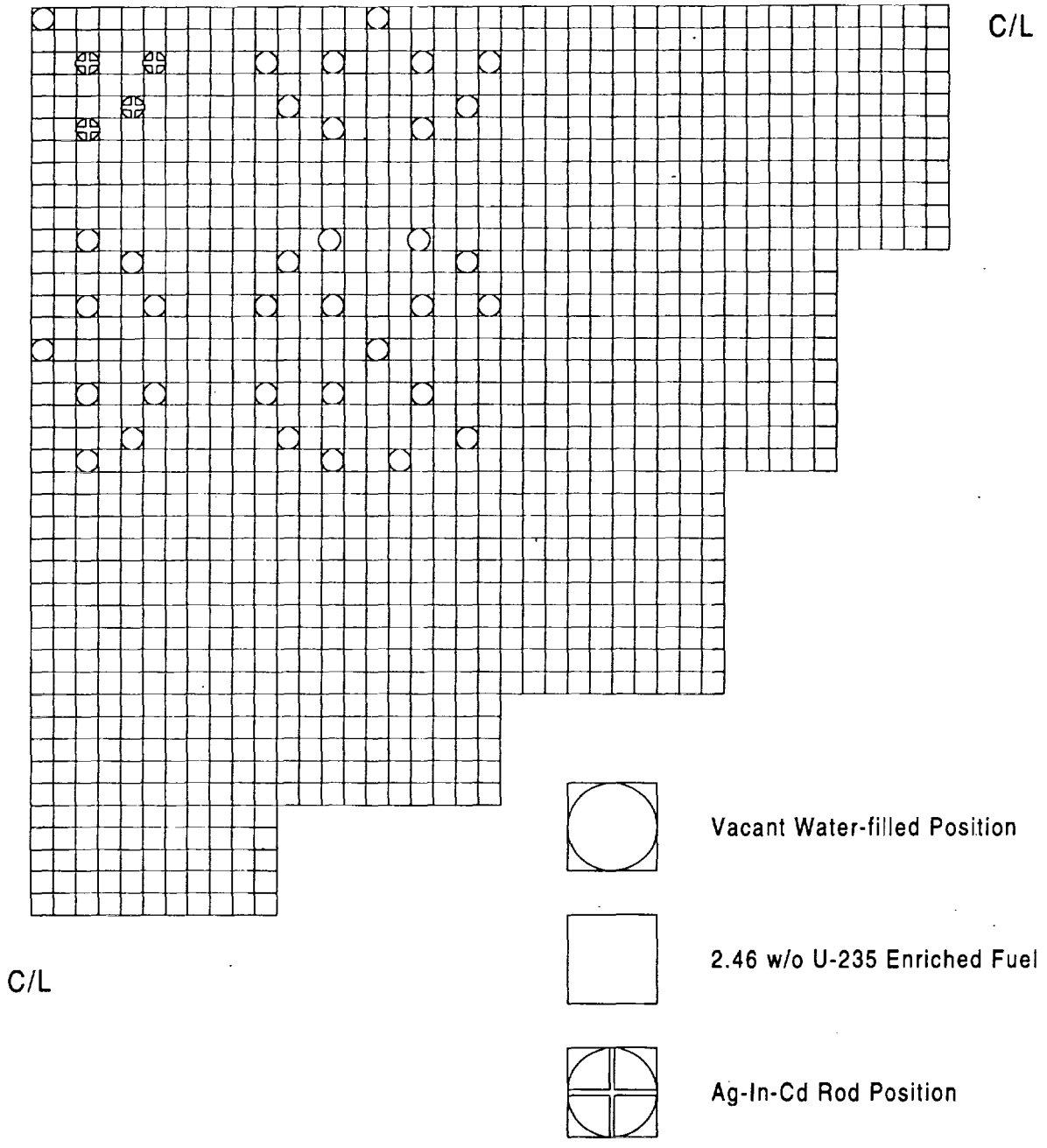


Figure 7.2.6-2. Core Loading Description for "ugd2" Experiment of the Urania-Gadolinia Critical Benchmark Set

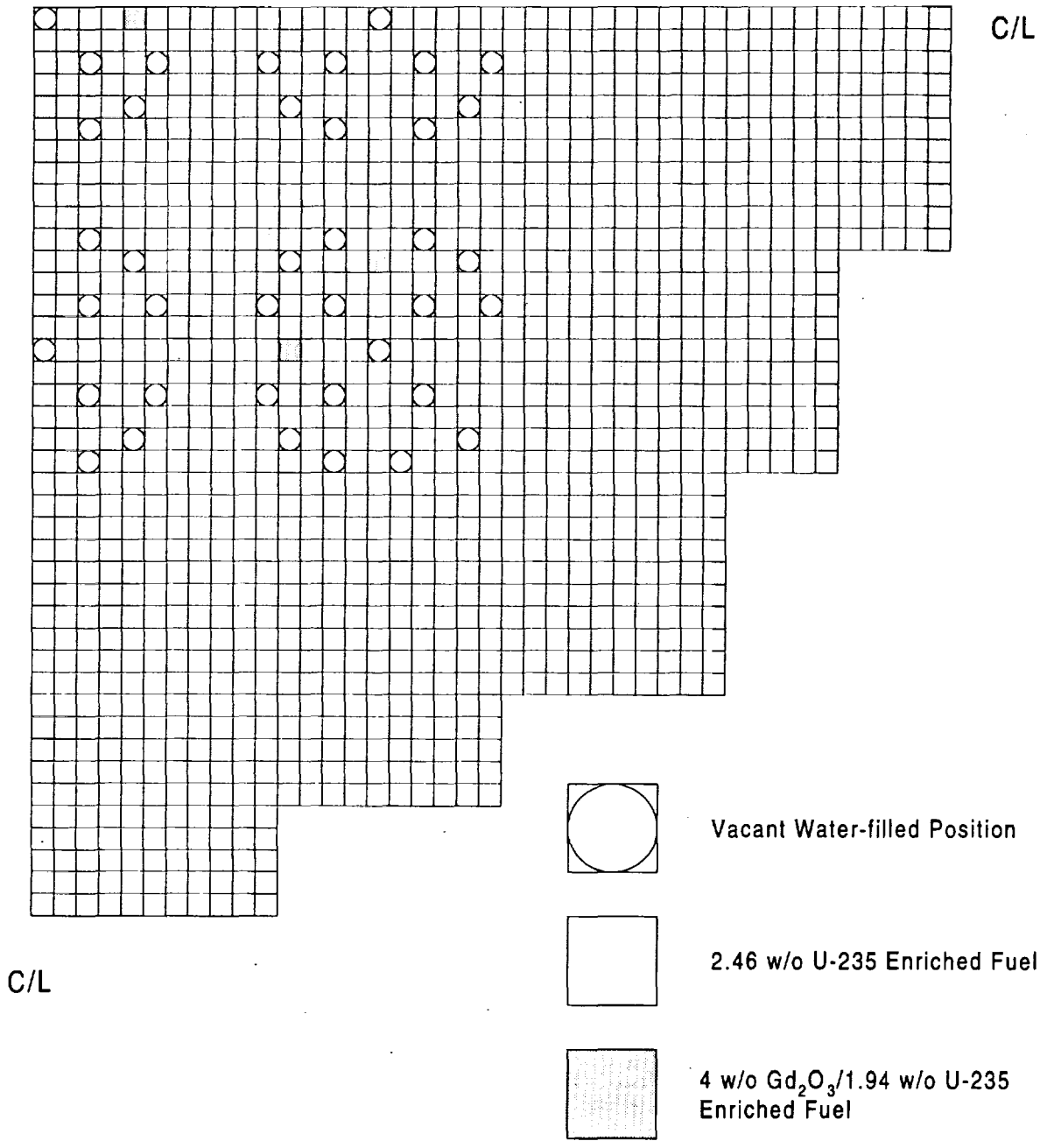


Figure 7.2.6-3.

Core Loading Description for "ugd3" Experiment of the Urania-Gadolinia Critical Benchmark Set

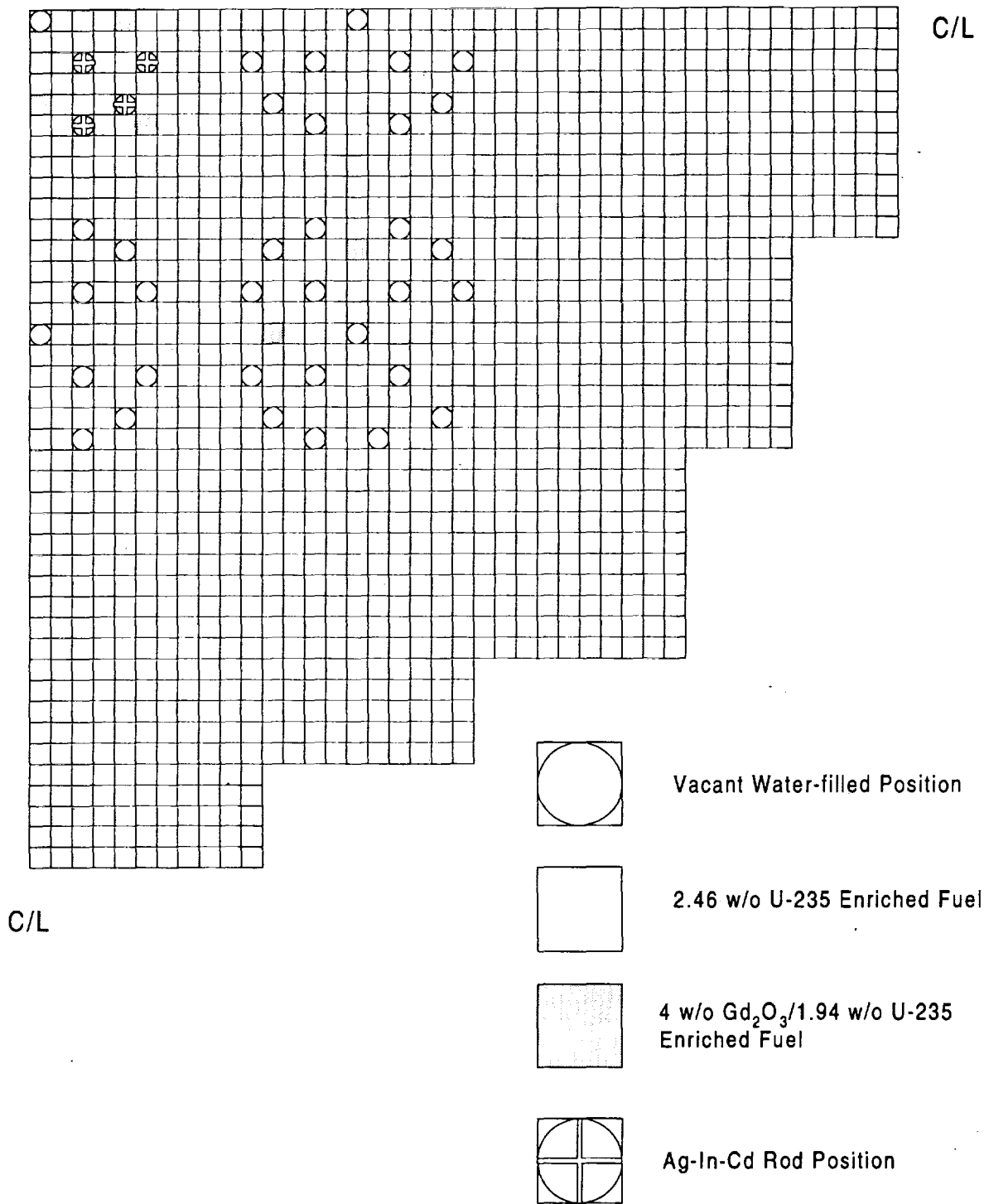


Figure 7.2.6-4. Core Loading Description for "ugd4" Experiment of the Urania-Gadolinia Critical Benchmark Set

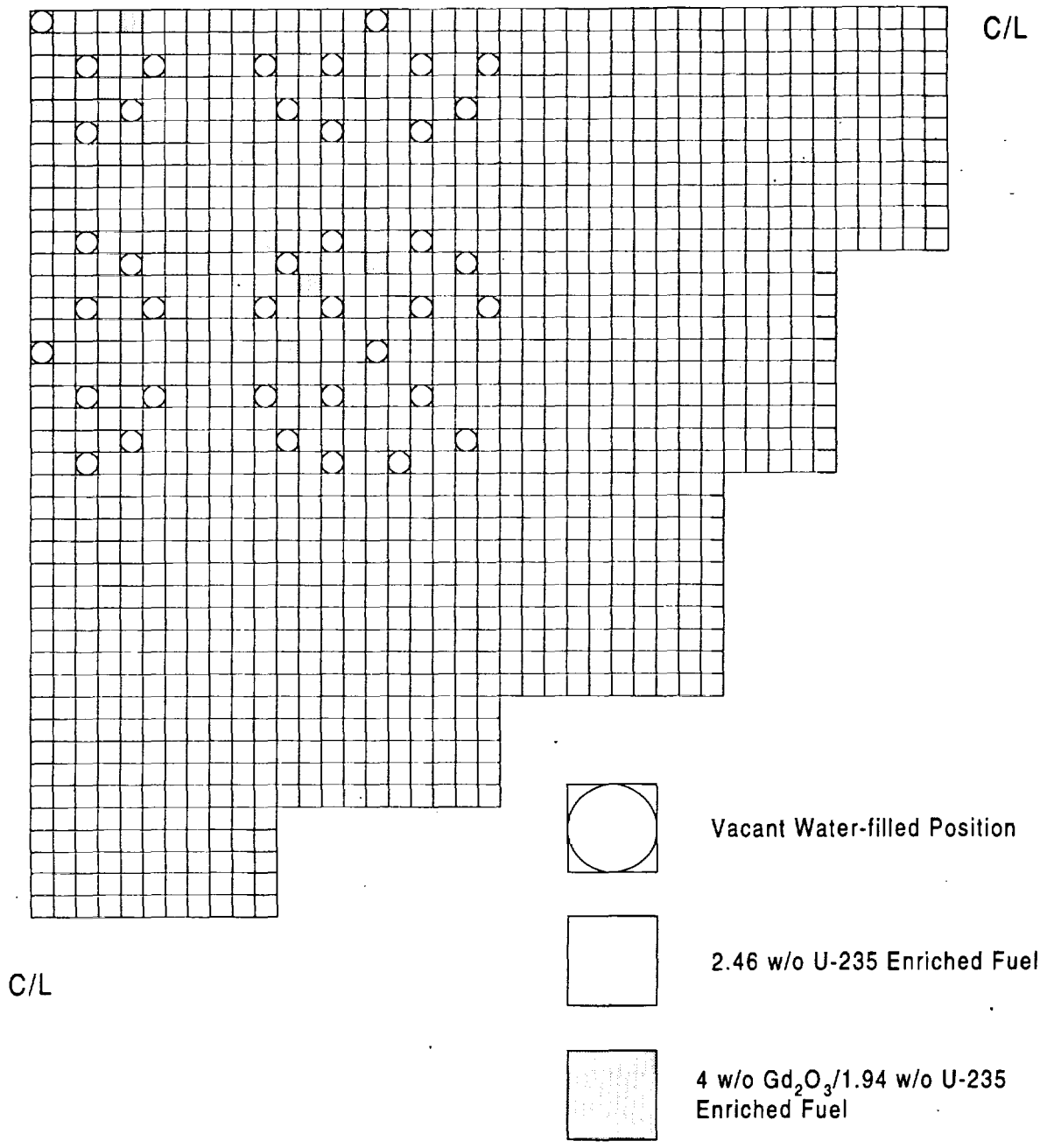


Figure 7.2.6-5. Core Loading Description for "ugd5" Experiment of the Urania-Gadolinia Critical Benchmark Set

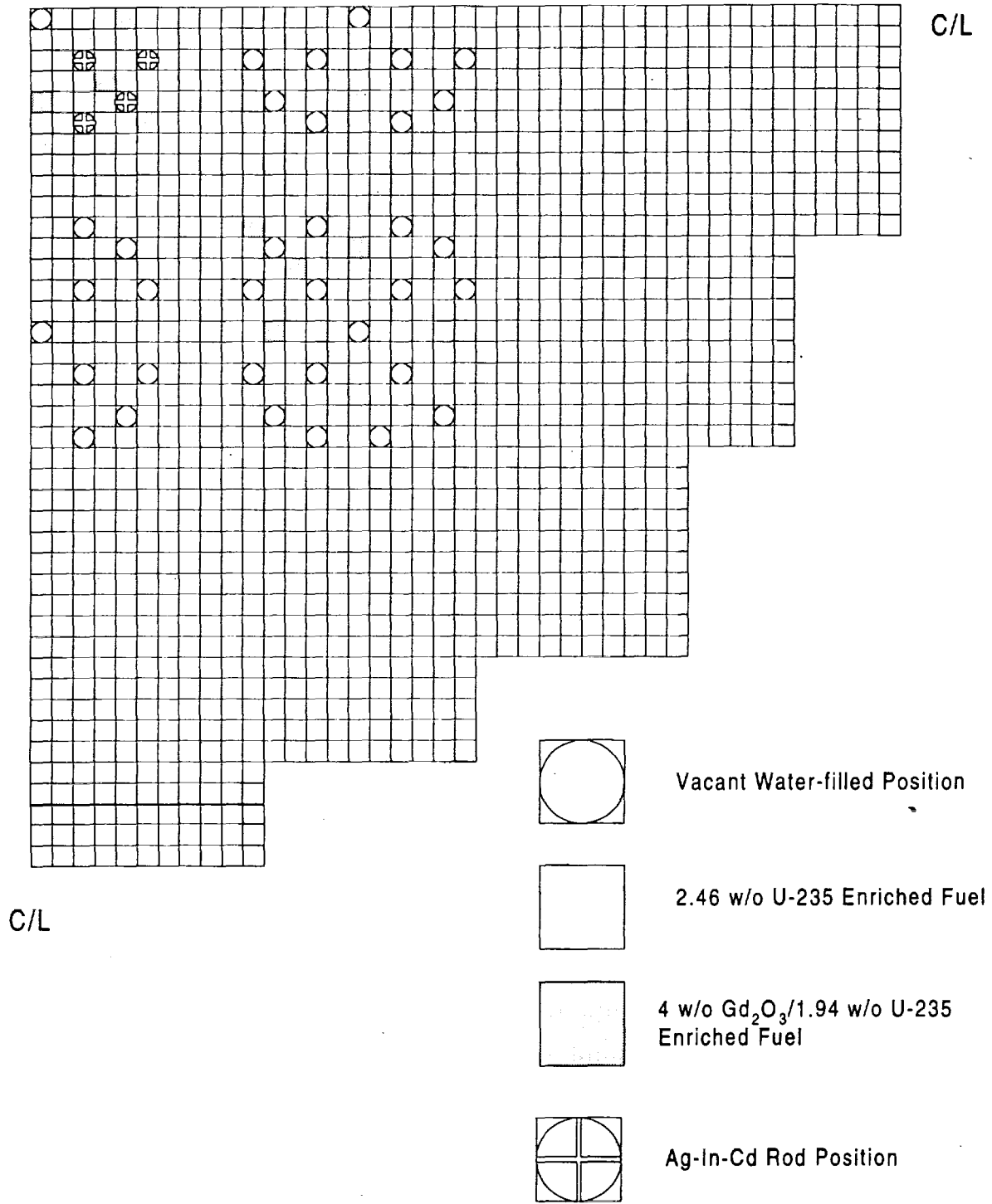


Figure 7.2.6-6. Core Loading Description for "ugd6" Experiment of the Urania-Gadolinia Critical Benchmark Set

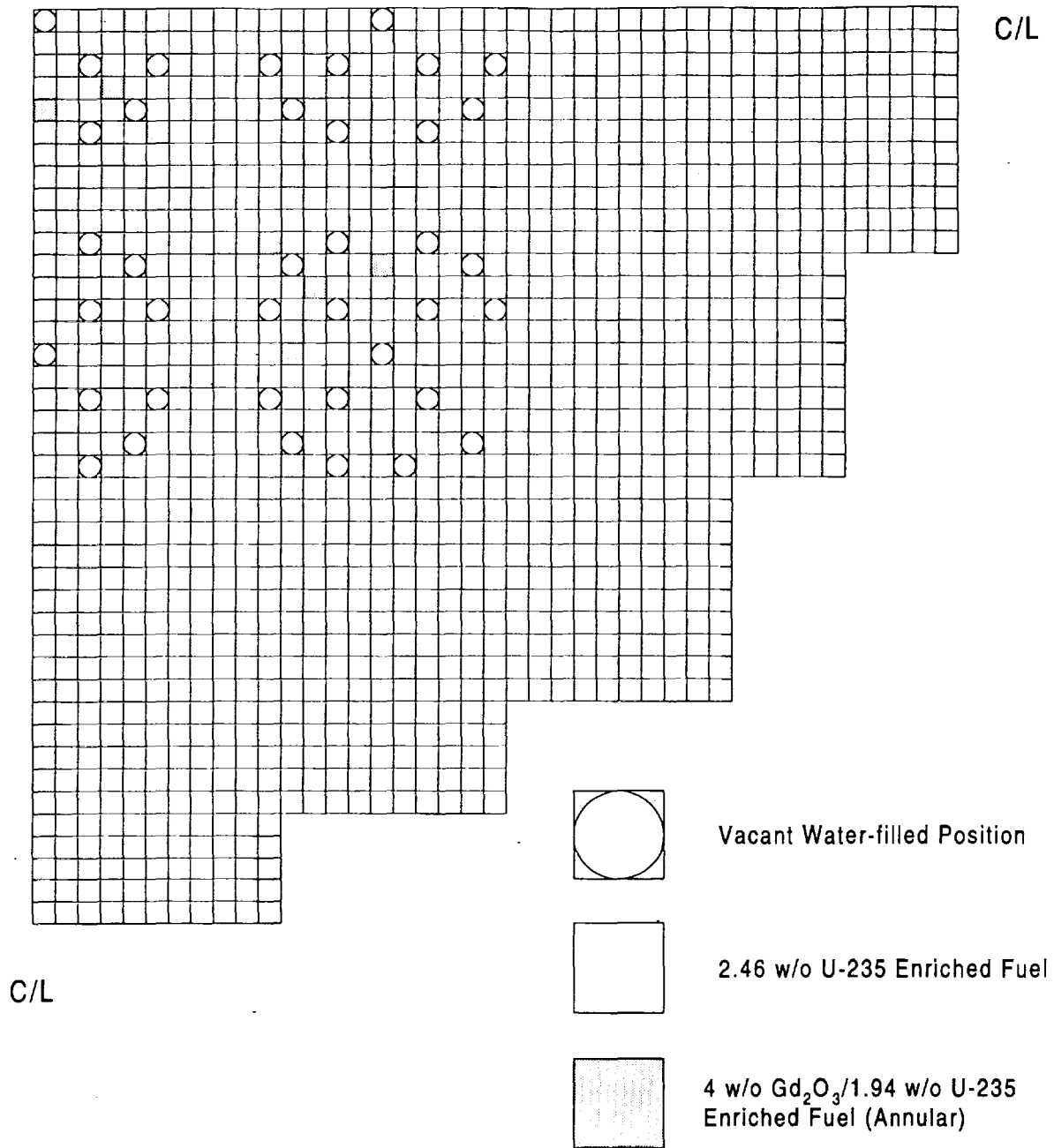


Figure 7.2.6-7.

Core Loading Description for "ugd7" Experiment of the Urania-Gadolinia Critical Benchmark Set

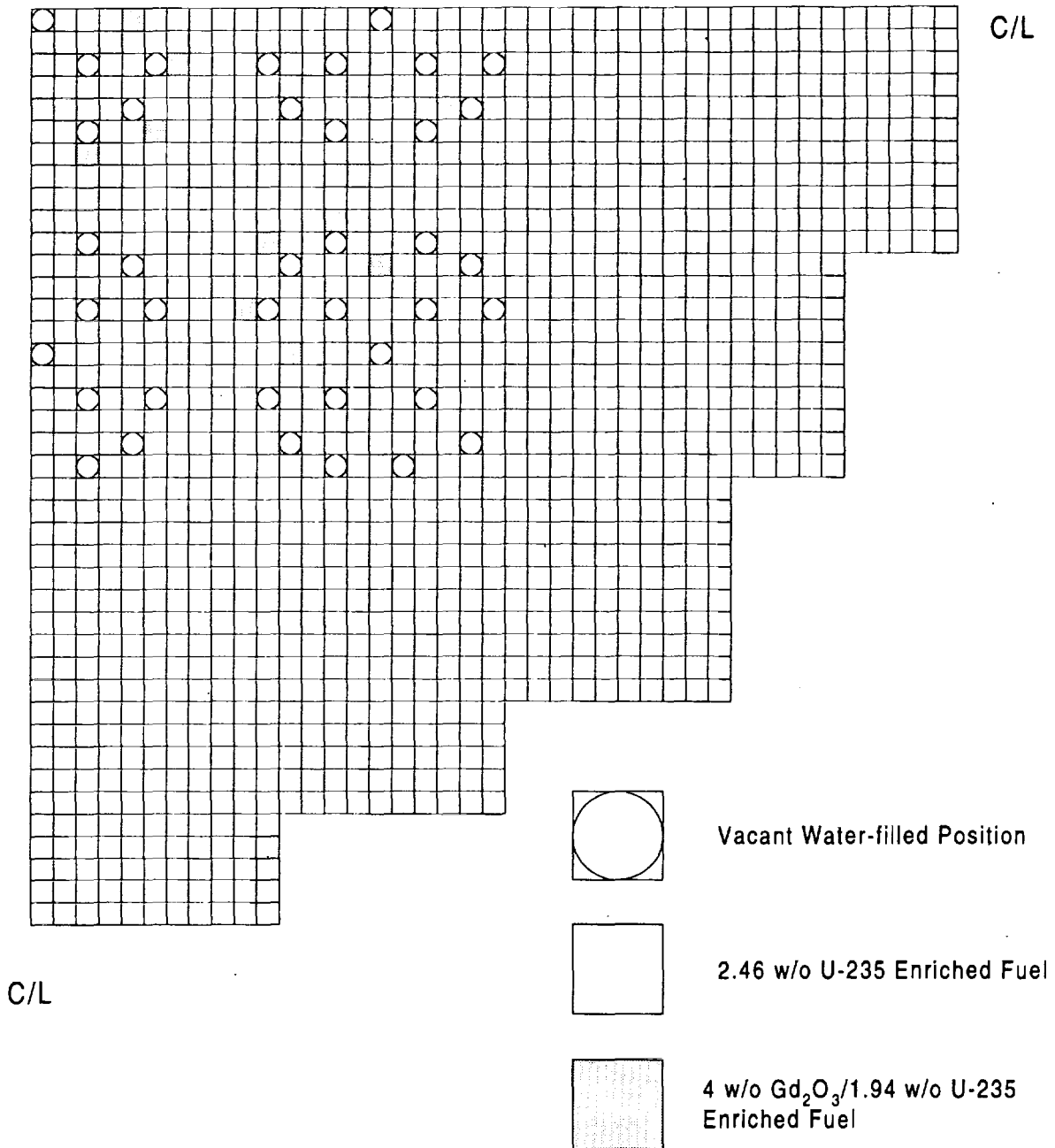


Figure 7.2.6-8.

Core Loading Description for "ugd8" Experiment of the Urania-Gadolinia Critical Benchmark Set

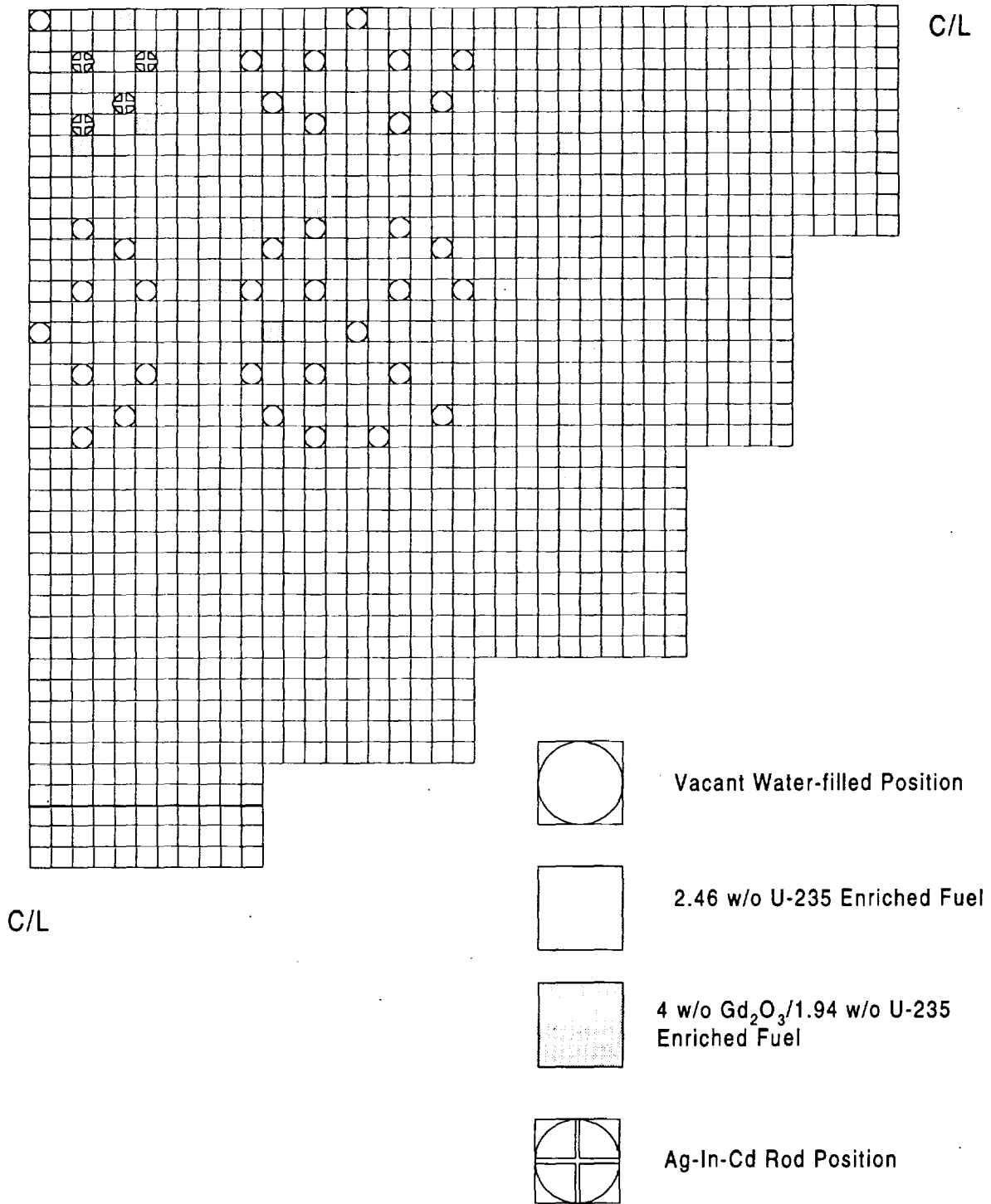


Figure 7.2.6-9. Core Loading Description for "ugd9" Experiment of the Urania-Gadolinia Critical Benchmark Set

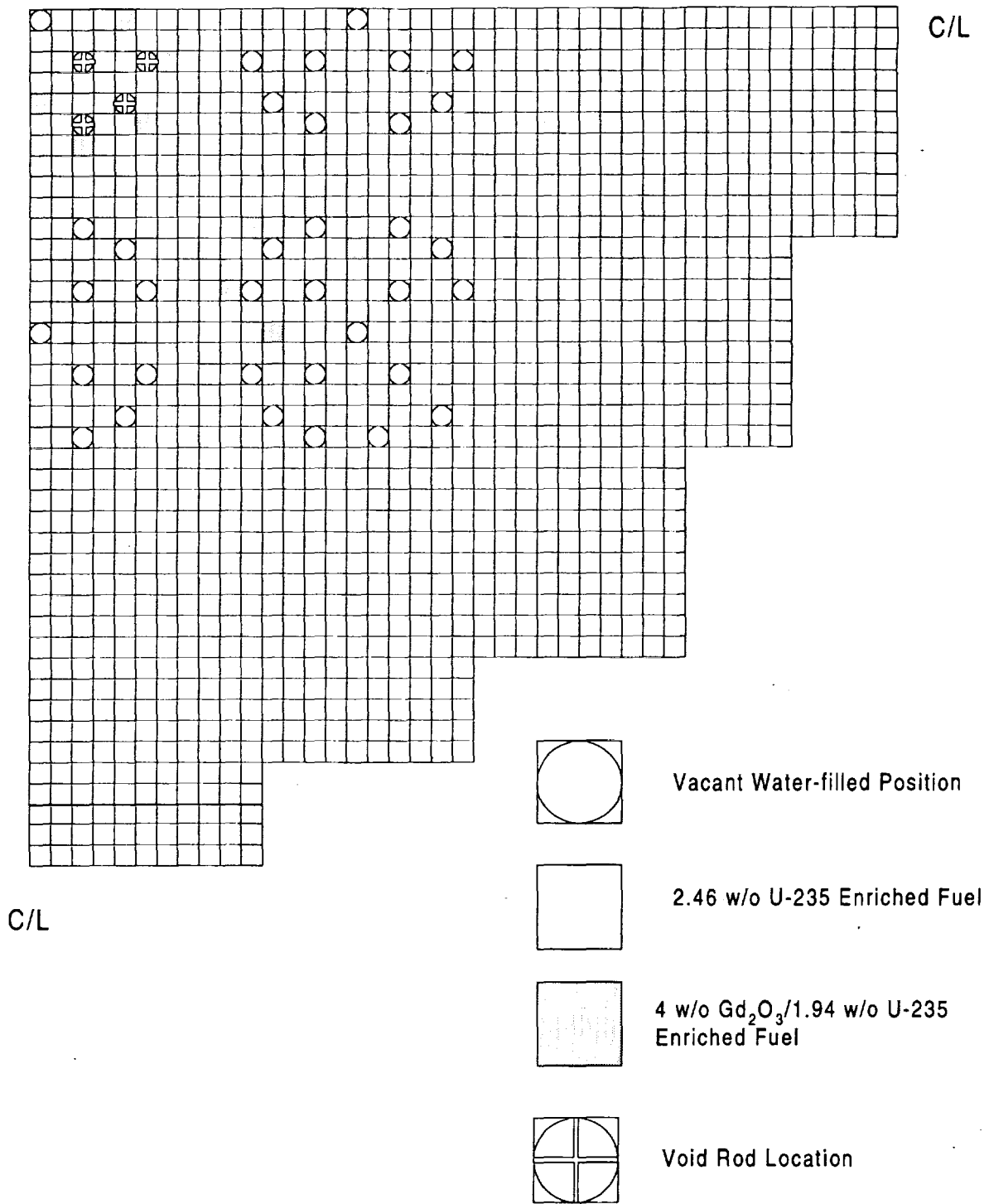


Figure 7.2.6-10. Core Loading Description for "ugd10" Experiment of the Urania-Gadolinia Critical Benchmark Set

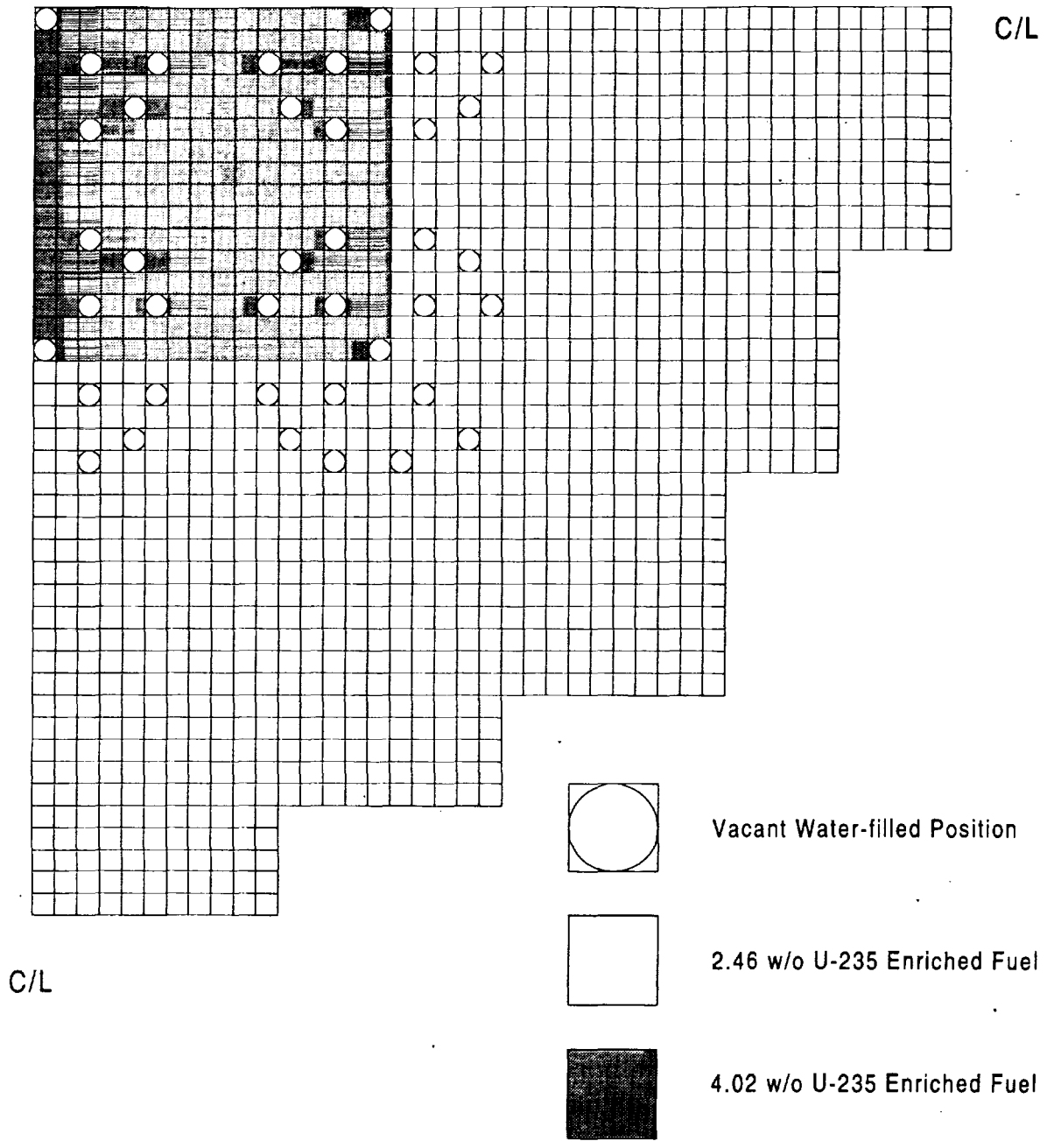


Figure 7.2.6-11. Core Loading Description for "ugd12" Experiment of the Urania-Gadolinia Critical Benchmark Set

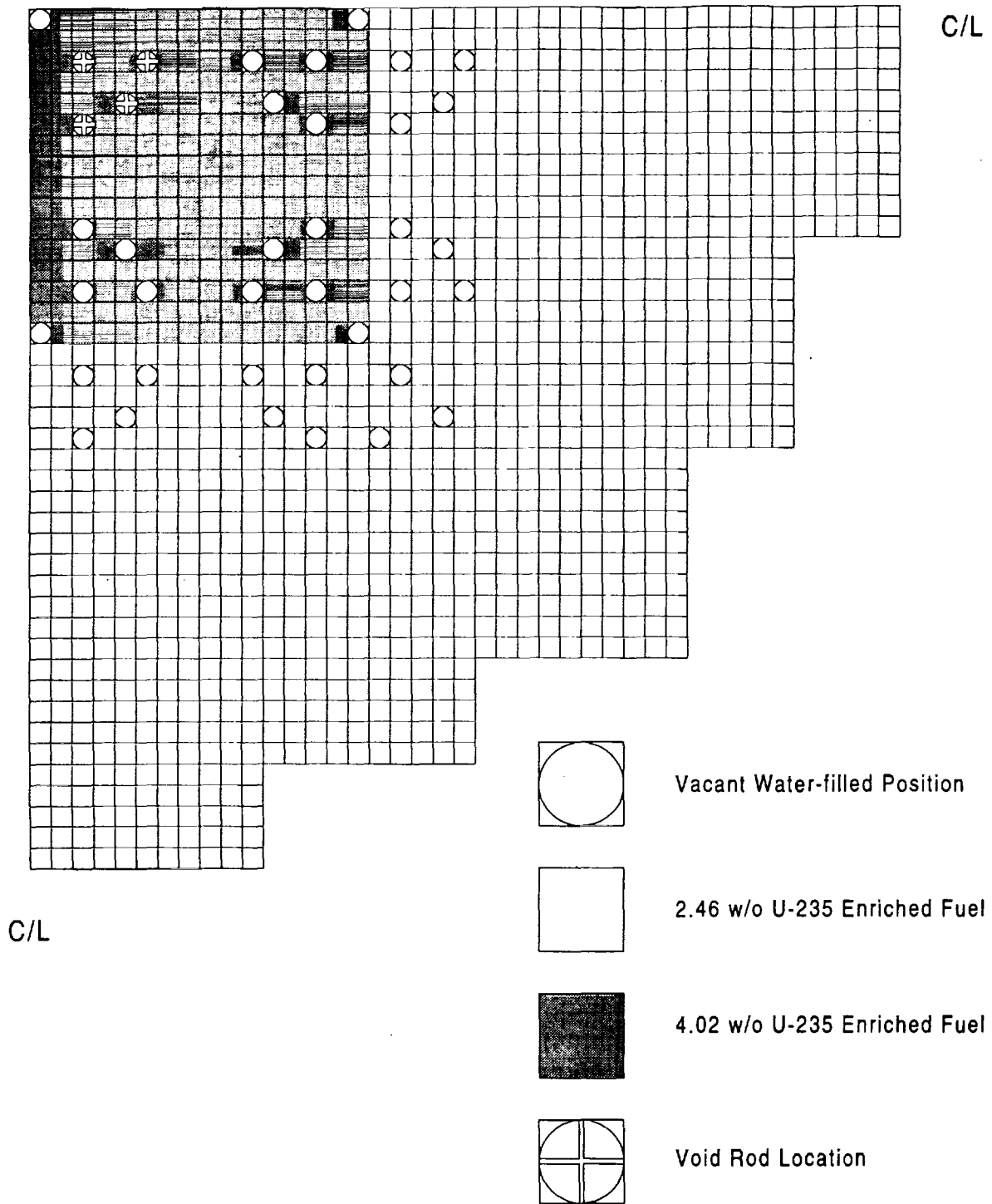


Figure 7.2.6-12.

Core Loading Description for "ugd13" Experiment of the Urania-Gadolinia Critical Benchmark Set

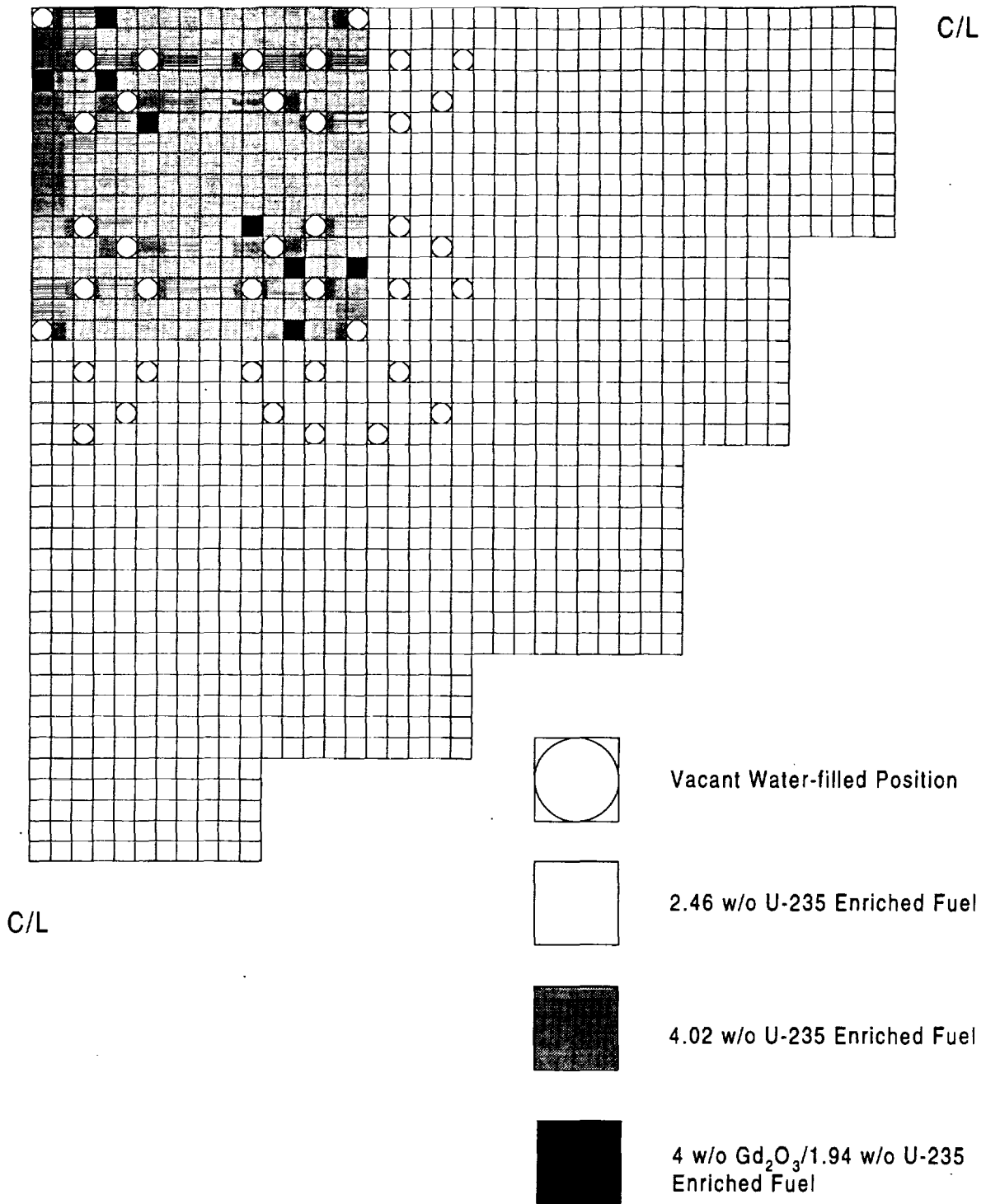


Figure 7.2.6-13. Core Loading Description for "ugd14" Experiment of the Urania-Gadolinia Critical Benchmark Set

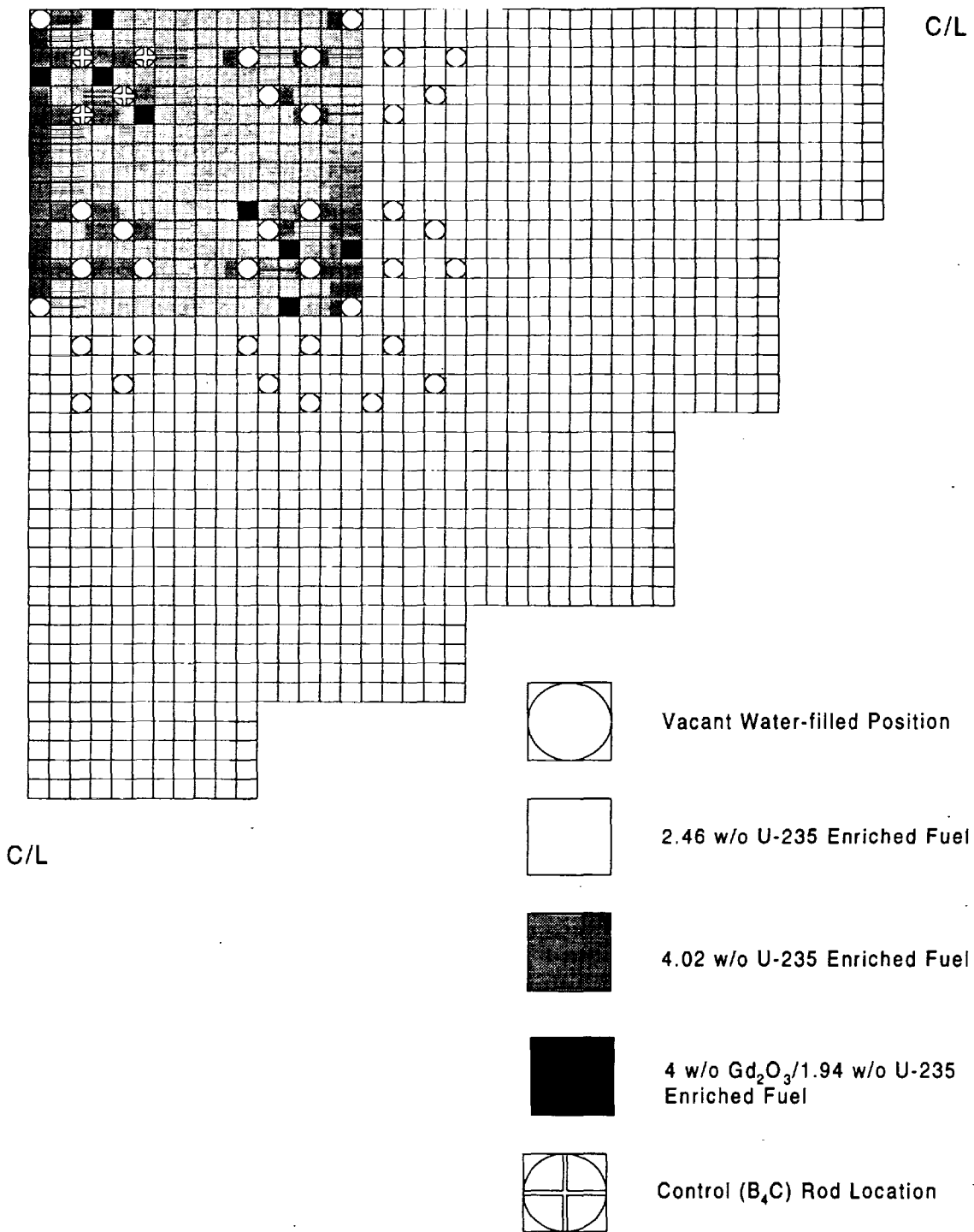


Figure 7.2.6-14. Core Loading Description for "ugd15" Experiment of the Urania-Gadolinia Critical Benchmark Set

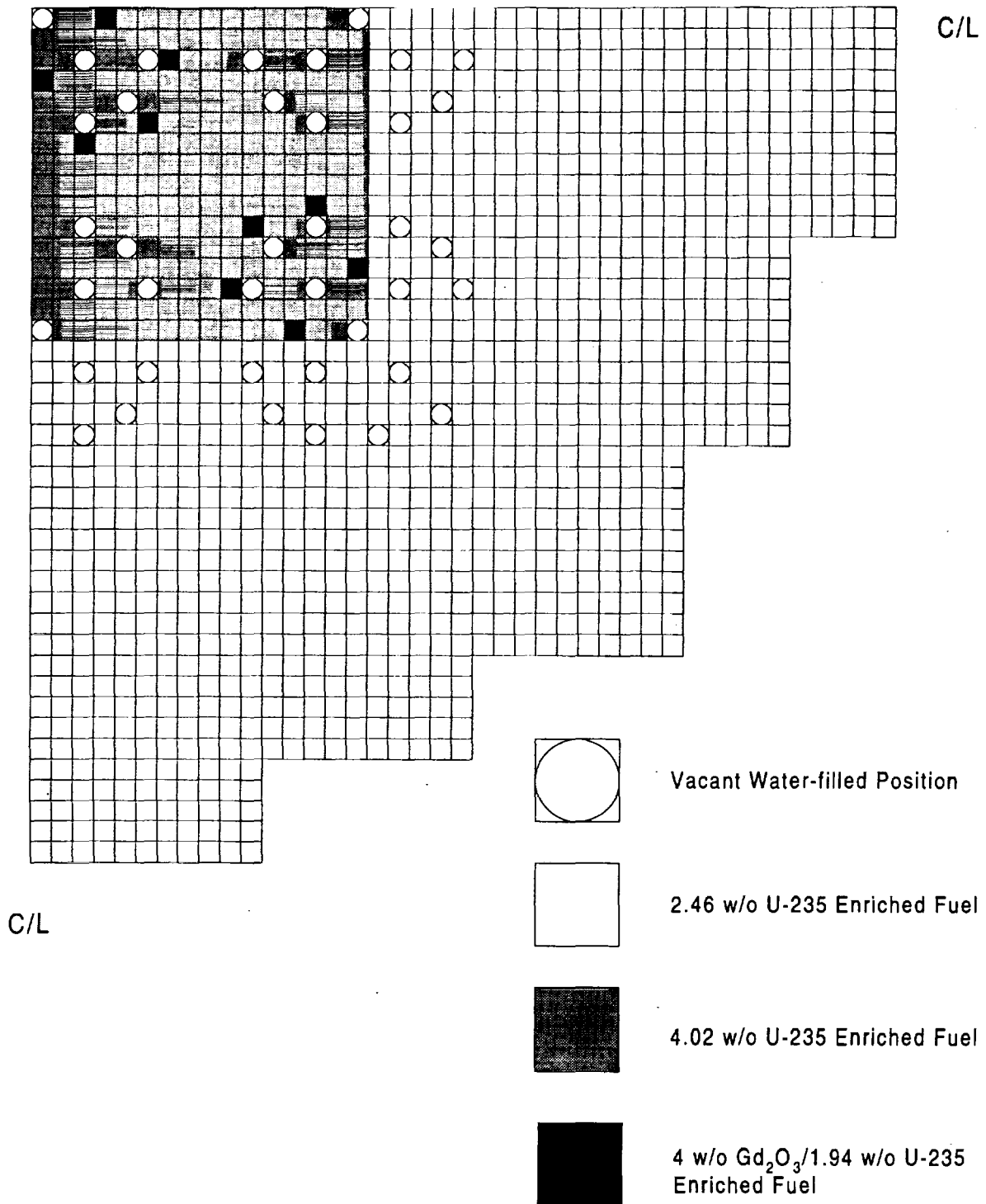


Figure 7.2.6-15. Core Loading Description for "ugd16" Experiment of the Urania-Gadolinia Critical Benchmark Set

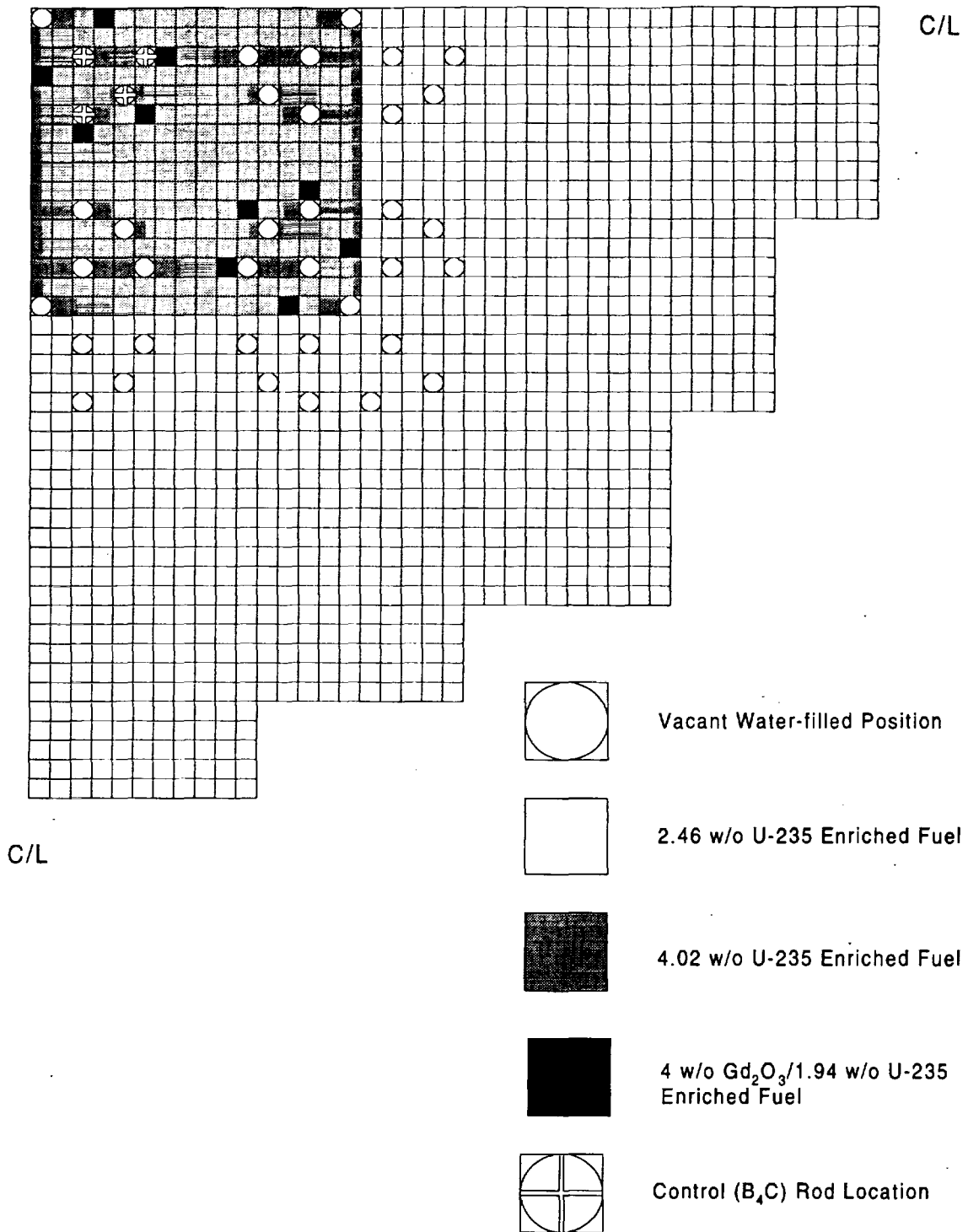


Figure 7.2.6-16. Core Loading Description for "ugd17" Experiment of the Urania-Gadolinia Critical Benchmark Set

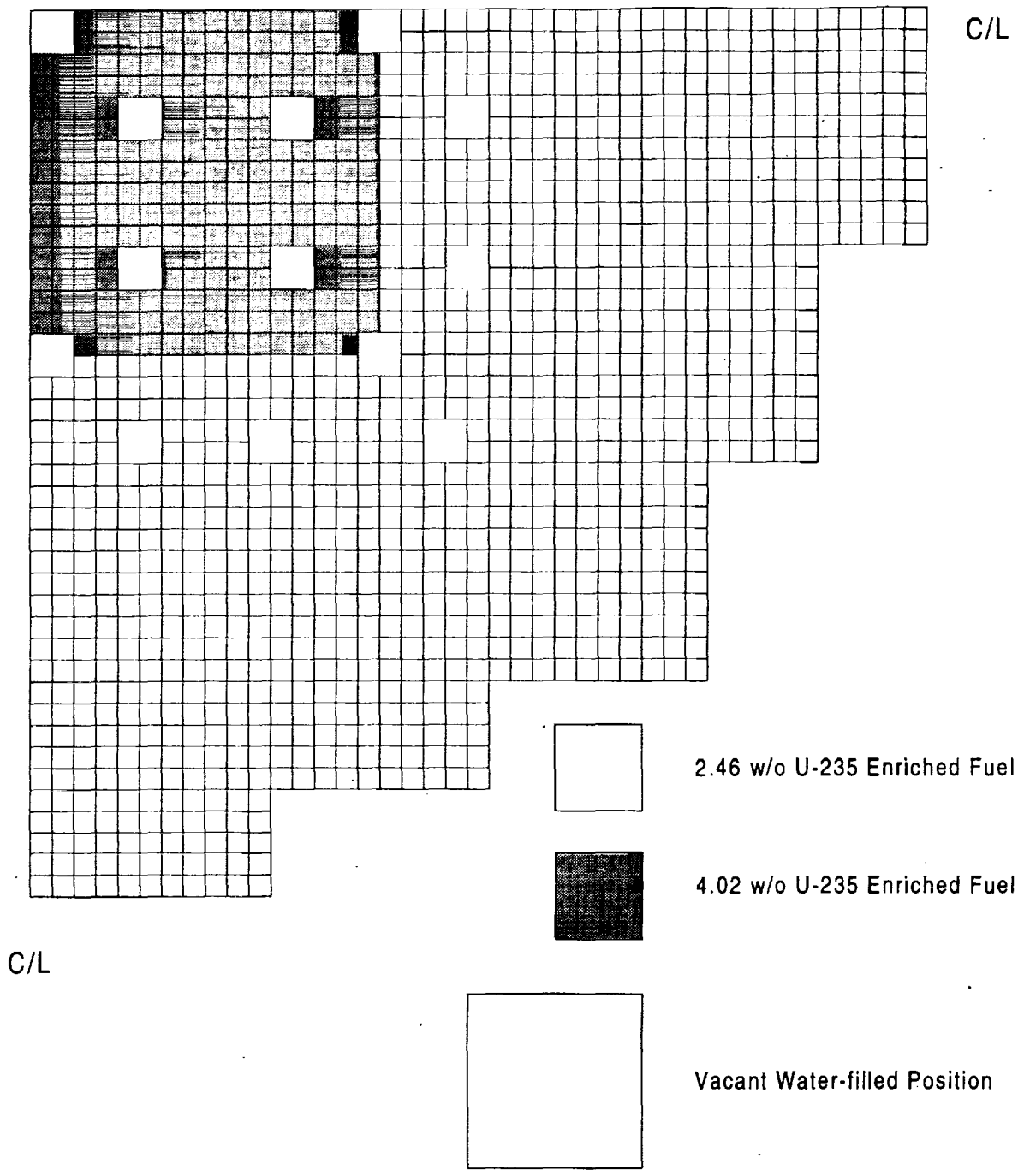


Figure 7.2.6-17. Core Loading Description for "ugd18" Experiment of the Urania-Gadolinia Critical Benchmark Set

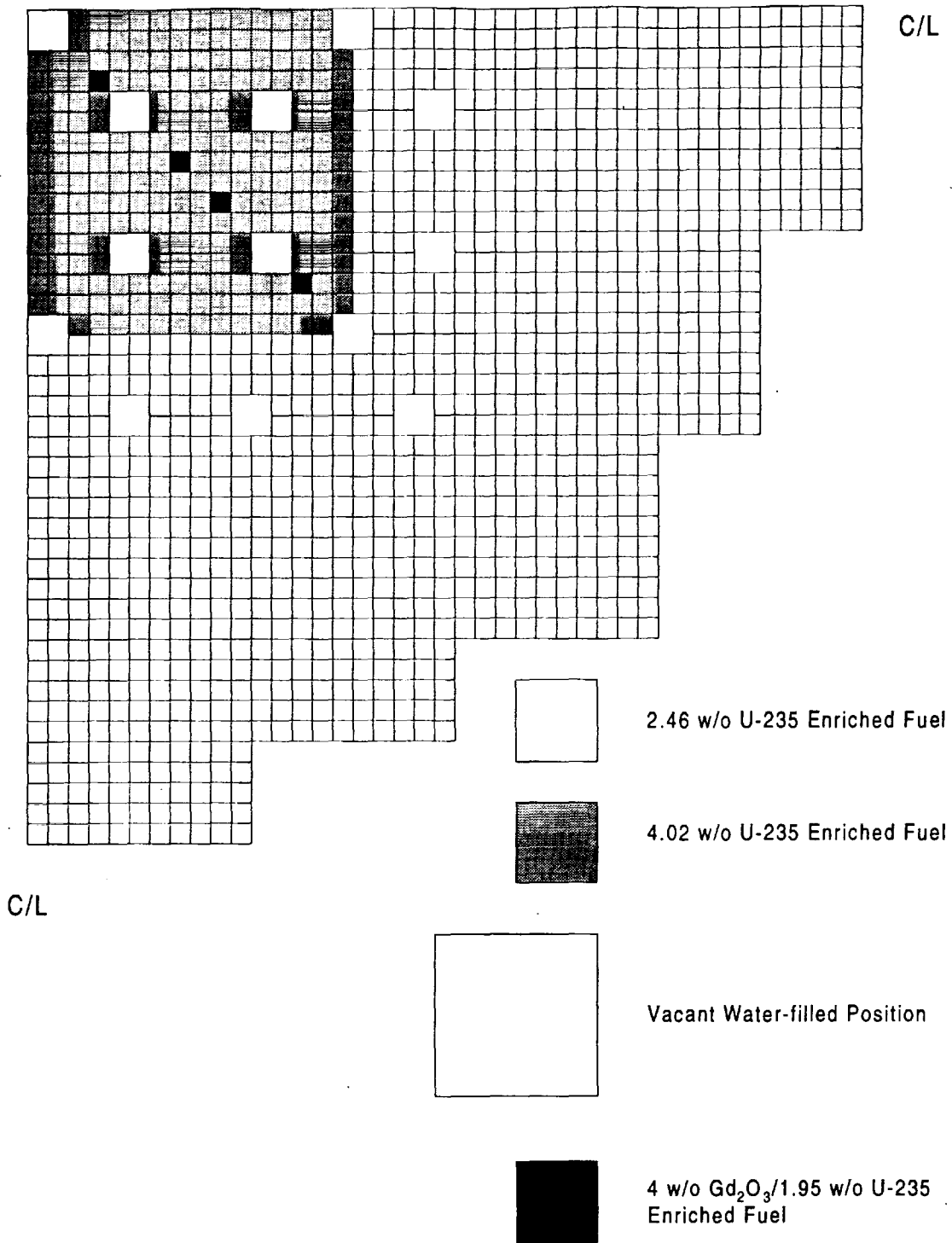


Figure 7.2.6-18. Core Loading Description for "ugd19" Experiment of the Urania-Gadolinia Critical Benchmark Set

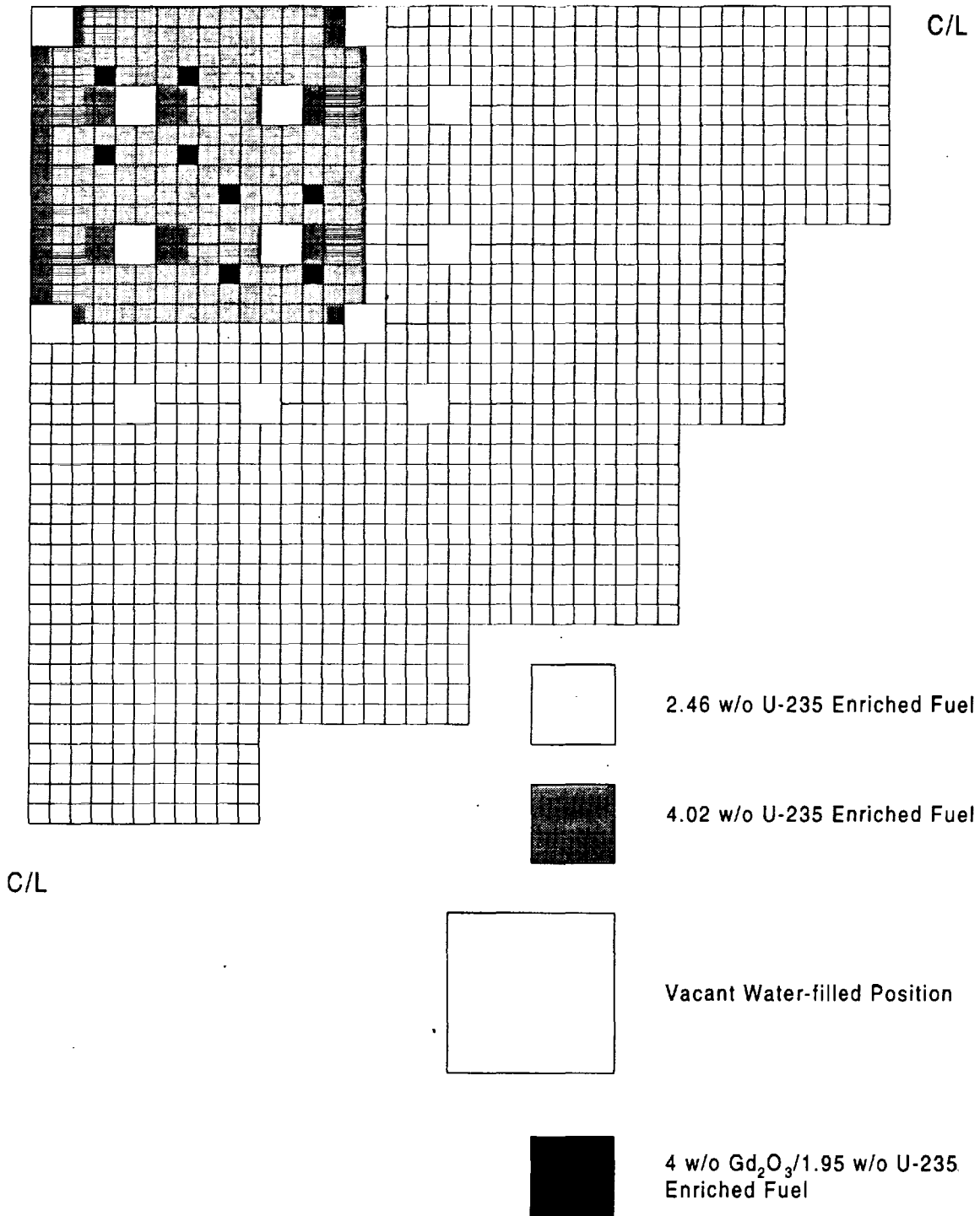


Figure 7.2.6-19. Core Loading Description for "ugd20" Experiment of the Urania-Gadolinia Critical Benchmark Set

7.2.7 Saxton UO₂ and PuO₂-UO₂ Critical Configurations

Westinghouse Electric Corporation performed small-core criticals for urania and mixed oxide fuel in the Saxton test reactor. This work was documented by Taylor (Reference 5.13) and subsequently described by Bowman (Reference 5.10). This section includes eight LCE configurations containing 5.74 wt% U-235 enriched UO₂ fuel rods and six LCE configurations containing 6.6 wt% PuO₂ (8 wt% Pu-240)/UO₂ fuel rods. An axial view of the general experimental configuration is shown in Figure 7.2.7-1. The fuel rods were loaded into a single rectangular array for each critical experiment. The fuel rods were supported by three aluminum grid plates with 1.008 cm diameter holes for rod emplacement. The UO₂ fuel rod description is shown in Table 7.2.7-1. The PuO₂/UO₂ fuel rod description is shown in Table 7.2.7-2. The fuel rod type, pitch, array size, moderator height, and boron concentration were adjusted in each LCE. Table 7.2.7-3 shows the various LCE configuration parameters.

Table 7.2.7-1. 5.74 wt% U-235 Enriched UO₂ Fuel Rod Description

Parameter	Value
Pellet Diameter	0.907 cm
Clad Outer Diameter	0.993 cm
Clad Inner Diameter	0.917 cm
Clad Material	Type 304 Stainless Steel
Percent of Theoretical Density	93 %
Fuel Length	92.96 cm
Enrichment	5.74 wt% U-235 in U
UO ₂ Theoretical Density	10.96 g/cc

Table 7.2.7-2. 6.6 wt% PuO₂ (9 wt% Pu-240)/UO₂ Fuel Rod Description

Parameter	Value
Pellet Diameter	0.857 cm
Clad Outer Diameter	0.993 cm
Clad Inner Diameter	0.875 cm
Clad Material	Zircaloy-4
Percent of Theoretical Density	94 %
Fuel Length	92.96 cm
Enrichment	6.6 wt% PuO ₂
PuO ₂ Theoretical Density	11.46 g/cc
Weight Percent of Oxygen	11.8469
Weight Percent of U-238	81.7474
Weight Percent of Pu-239	5.2676
Weight Percent of Pu-240	0.4989
Weight Percent of Pu-241	0.0518
Weight Percent of Pu-242	0.0023

Table 7.2.7-3. Saxton Critical Configuration Parameters

Experiment Identifier	Fuel Type	Pitch (cm)	Water/Fuel Volume Ratio	Critical H ₂ O Height (cm) [a]	Critical Number of Rods	Boron Conc. (ppm)
exp17	UO ₂	1.422	1.933	83.71	361 (19x19)	0
exp18	UO ₂	2.012	5.067	90.60	182 (13x14)	0
exp28	PuO ₂ -UO ₂	1.321	1.681	84.56	506 (22x23)	0
exp29	PuO ₂ -UO ₂	1.422	2.165	82.96	361 (19x19)	0
exp30	PuO ₂ -UO ₂	1.422	2.165	89.70	441 (21x21)	337
exp31	PuO ₂ -UO ₂	1.867	4.699	70.11	169 (13x13)	0
exp32	PuO ₂ -UO ₂	2.012	5.673	78.43	144 (12x12)	0
exp33	PuO ₂ -UO ₂	2.642	10.754	81.17	121 (11x11)	0

[a]. Measured from the bottom of the fuel.

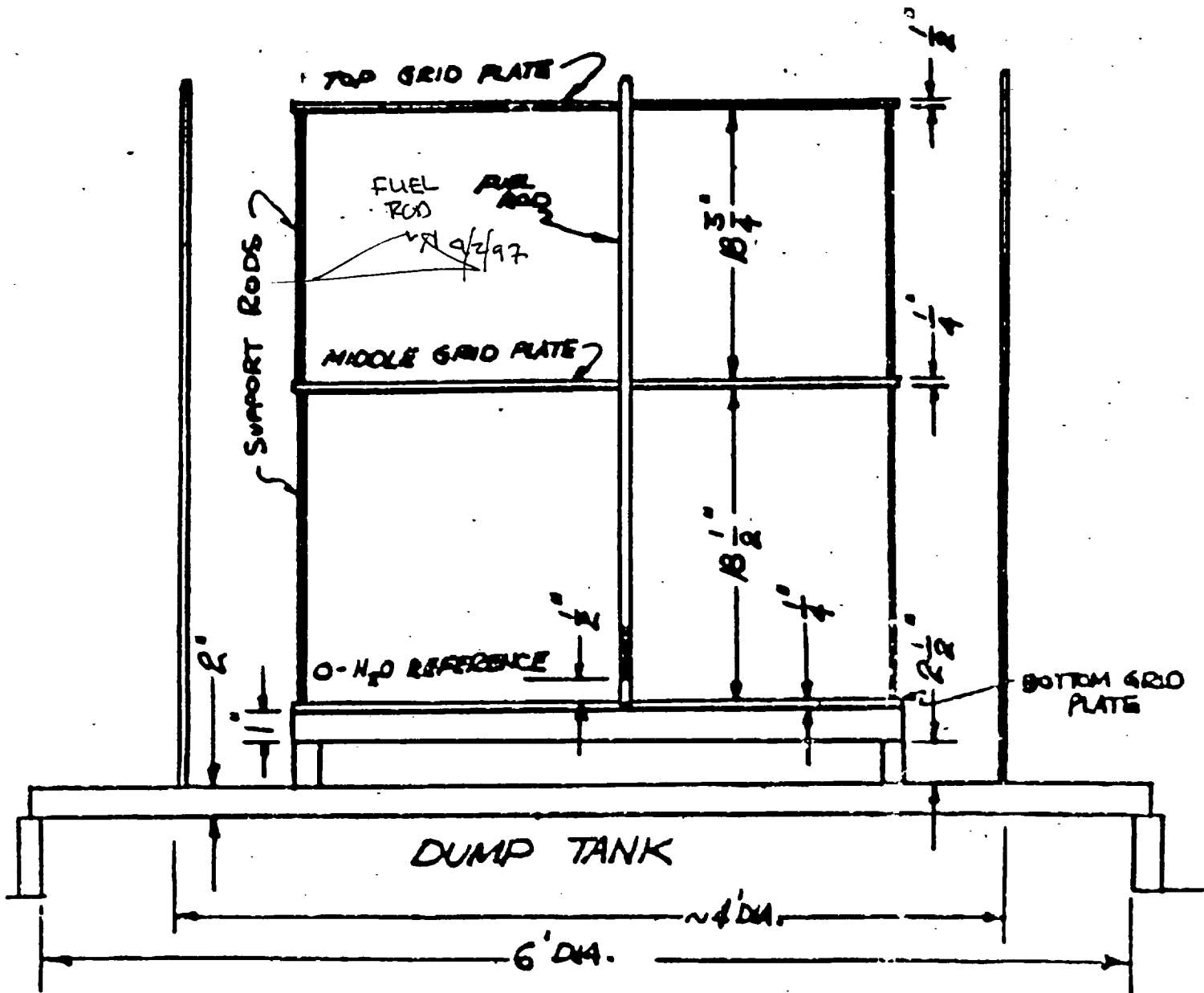


Figure 7.2.7-1. Axial View of General Saxton Critical Experiment Configuration

7.2.8 Critical Configurations Simulating Light Water Reactor Fuel in Close Proximity Water Storage

Babcock and Wilcox performed experiments simulating neutron multiplication in pool storage racks. These were documented by Baldwin (Reference 5.14). Twenty such critical configurations, each containing a 3 x 3 array of 14 x 14 fuel rod assemblies, were modeled with MCNP. Two different methods were utilized to support the fuel assemblies in the critical experiment core. The first support method utilizes top and bottom grid plates to hold the fuel rods in place (configurations one through nine). The second support method utilized a bottom grid plate and vertical alignment system consisting of locating bars and fastening plates (all other configurations). The two support methods are illustrated in Figures 7.2.8-1 and 7.2.8-2, respectively. The gaps between assemblies may have contained a number B₄C rods and water, stainless steel sheets and water, borated aluminum sheets and water, or only water.

The critical experiment arrays were assembled in an aluminum core tank of 152.4 cm diameter with 1.27 cm thick walls. The fuel rods are composed of 2.46 wt% U-235 enriched UO₂ clad in 0.081 cm thick Type 6061 aluminum. Table 7.2.8-1 shows the properties of the fuel rods. The fuel rod description is shown graphically in Figure 7.2.8-3. The aluminum composition used in the MCNP model is shown in Table 7.2.4-2. The B₄C rods are 0.089 cm thick aluminum tubes with an outside diameter of 1.113 cm filled with B₄C powder. The stainless steel sheets were 91.6 cm wide by 156 cm high with a thickness of 0.462 cm and were composed of Type 304 stainless steel. The borated aluminum sheets are 91.6 cm wide by 156 cm high with a thickness of 0.645 cm. Six sets of borated aluminum sheets were used utilized in the critical experiments. Two sets contained a nominal boron loading of about 1.62 wt%. The boron loading in the other four sets varied between 0.10 and 1.25 wt%. Table 7.2.8-2 contains the composition of the borated aluminum sheets. The soluble boron concentration and moderator heights were adjusted to obtain a critical configuration. The key parameters which distinguish the twenty critical configurations are shown in Table 7.2.8-3. Core loading diagrams of the twenty LCE configurations are shown in Figures 7.2.8-4 through 7.2.8-15.

**Table 7.2.8-1. 2.46 wt% U-235 Enriched UO₂ Fuel Rod Properties
for Close Proximity Criticals**

Parameter	Value
Outside Diameter	1.206 cm
Wall Thickness	0.081 cm
Wall Material	Aluminum
Pellet Diameter	1.030 cm
Total Length	156.44 cm
Active Fuel Length	153.34 cm
Enrichment	2.459 wt% U-235 in U
Density	10.218 g/cc

Table 7.2.8-2. Composition of Borated Aluminum Sheets in Close Proximity Criticals

Boron Content, wt% B		Starter Material, all sets	
Set Number	Avg. Boron Content	Material (wt%)	Boron (atom%)
1	0.100 ± 2.1	B: 0.001	B-10: 19.86
2	0.242 ± 1.4	Fe: 0.16	B-11: 80.14
3	0.401 ± 4.0	Si: 0.06	
4	1.257 ± 1.2	Zn: 0.02	
5	1.614 ± 1.3	Others: <0.02 each	
5a	1.620 ± 1.4	Al: Remainder (99.7)	
Density of all sheets = 2.7 g/cc			

Table 7.2.8-3. Close Proximity Critical Benchmark Characterization Parameters

Critical Exp. Ident.	Core Loading Figure	Assy Spacing, Pin Pitch	Number of B ₄ C Pins	Metal Between Unit Assys	Mod. Temp. (°C)	Mod. Boron (ppm ± 3)	Critical Mod. Height (cm ± 0.2)
core2	4.2.8-5	0	0	n/a	18.5	1037	144.29
core3	4.2.8-6	1	0	n/a	18	769	148.63
core4	4.2.8-7	1	84	n/a	17	0	145.68
core5	4.2.8-8	2	64	n/a	17.5	0	144.75
core6	4.2.8-9	2	64	n/a	17.5	0	107.67
core7	4.2.8-10	3	34	n/a	17.5	0	146.15
core8	4.2.8-11	3	34	n/a	17.5	0	111.49
core9	4.2.8-12	4	0	n/a	17.5	0	129.65
core10	4.2.8-13	3	n/a	none	24.5	143	149.12
core11	4.2.8-14	1	n/a	SS	25.5	510	145.86
core12	4.2.8-15	2	n/a	SS	26	217	150.17
core13	4.2.8-14	1	n/a	B/Al set 5	20	15	150.27
core14	4.2.8-14	1	n/a	B/Al set 4	18	92	149.12
core15	4.2.8-14	1	n/a	B/Al set 3	18	395	151.45
core16	4.2.8-15	2	n/a	B/Al set 3	17.5	121	149.16
core17	4.2.8-14	1	n/a	B/Al set 2	17.5	487	149.88
core18	4.2.8-15	2	n/a	B/Al set 2	18	197	149.02
core19	4.2.8-14	1	n/a	B/Al set 1	17.5	634	149.00
core20	4.2.8-15	2	n/a	B/Al set 1	17.5	320	148.10
core21	4.2.8-16	3	n/a	B/Al set 1	16.5	72	151.69

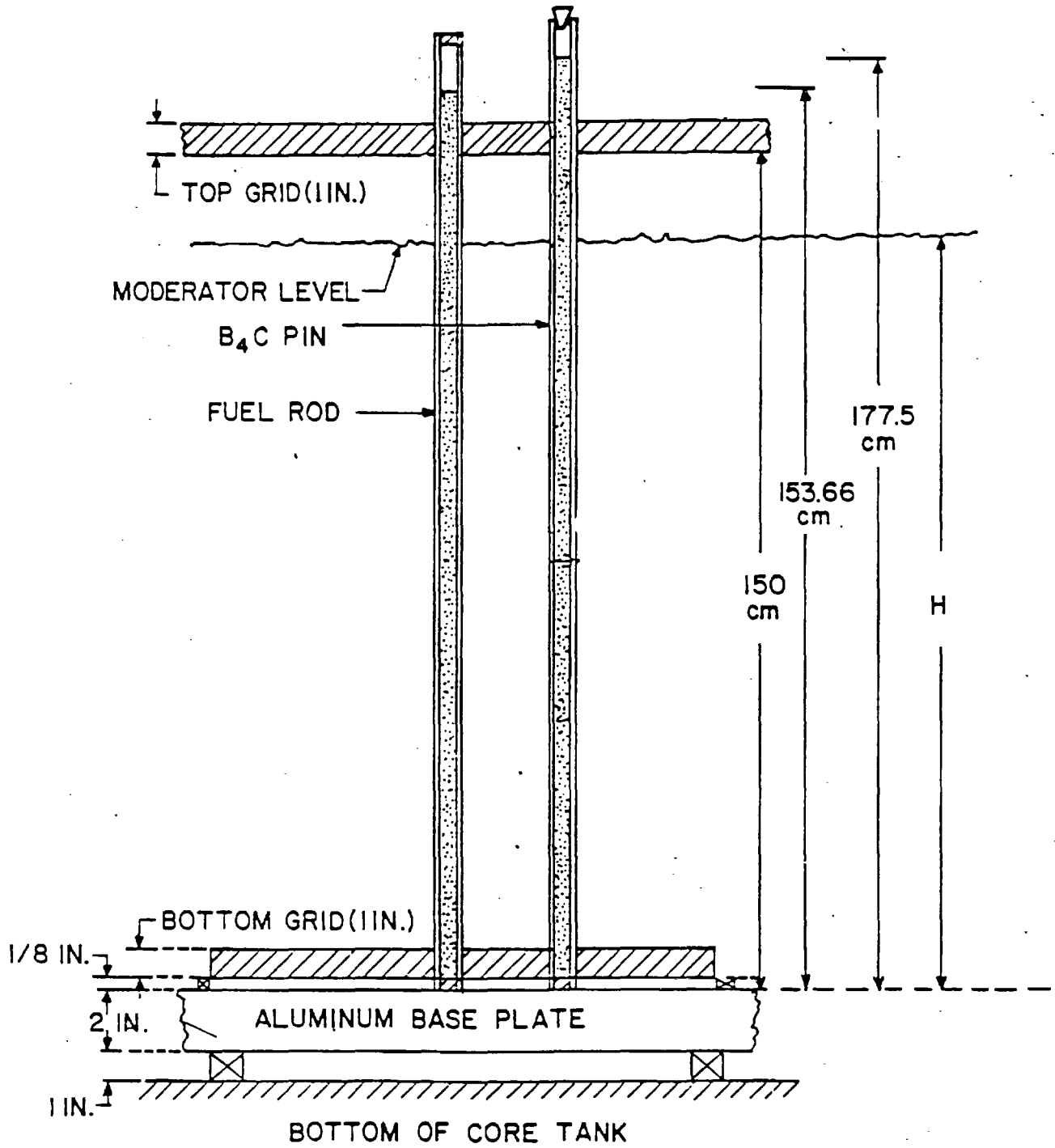
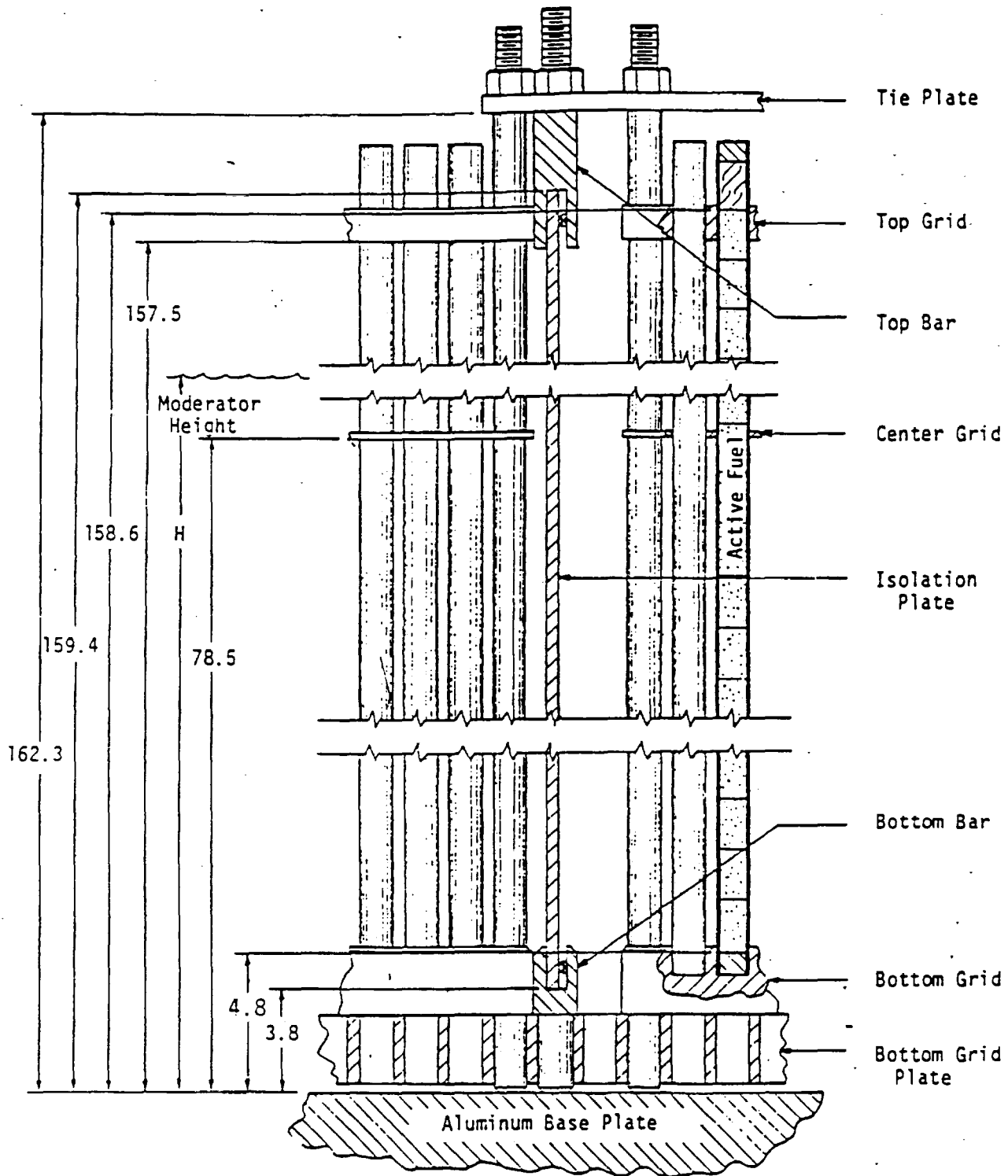
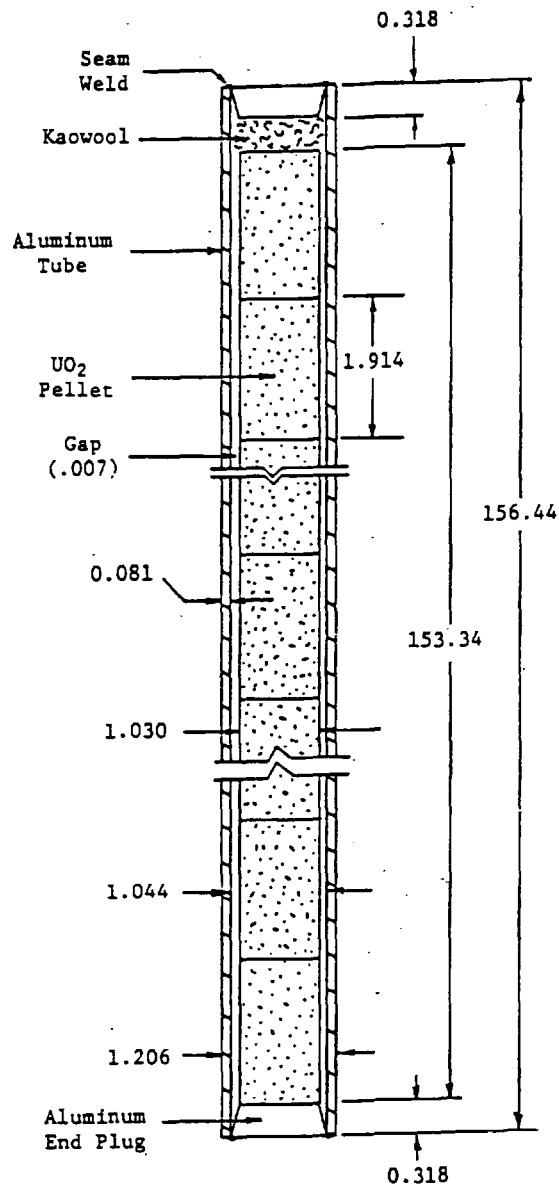


Figure 7.2.8-1. Top and Bottom Grid Plate Support Method of Close Proximity Critical Benchmark Experiments



Note: Dimensions given in centimeters.

Figure 7.2.8-2. Bottom Grid Plate and Vertical Alignment Support Method of Close Proximity Critical Benchmark Experiments



Note: All dimensions in centimeters.

Figure 7.2.8-3.

2.46 wt% Enriched UO₂ Fuel Rod Description for the Close Proximity Critical Benchmark Experiments

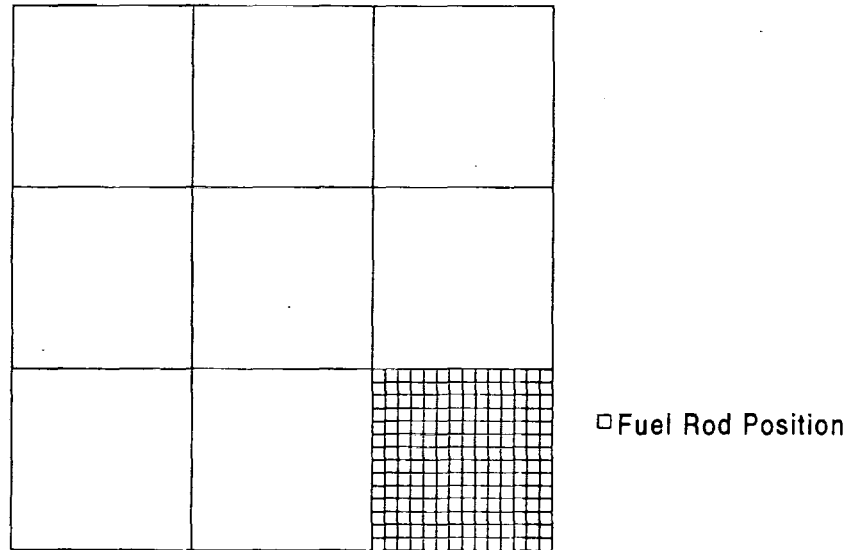


Figure 7.2.8-4. Core 2 Loading Diagram of Close Proximity Critical Benchmark Experiments

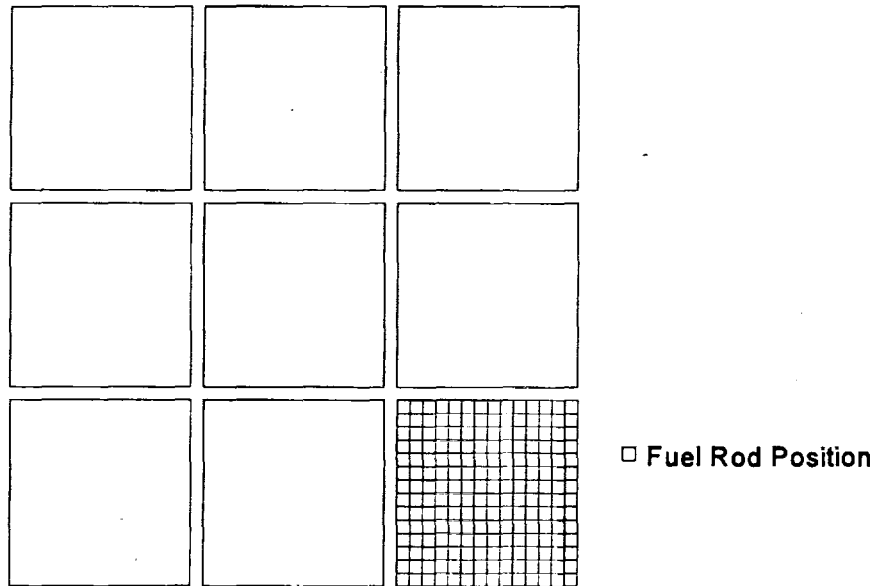


Figure 7.2.8-5. Core 3 Loading Diagram of Close Proximity Critical Benchmark Experiments

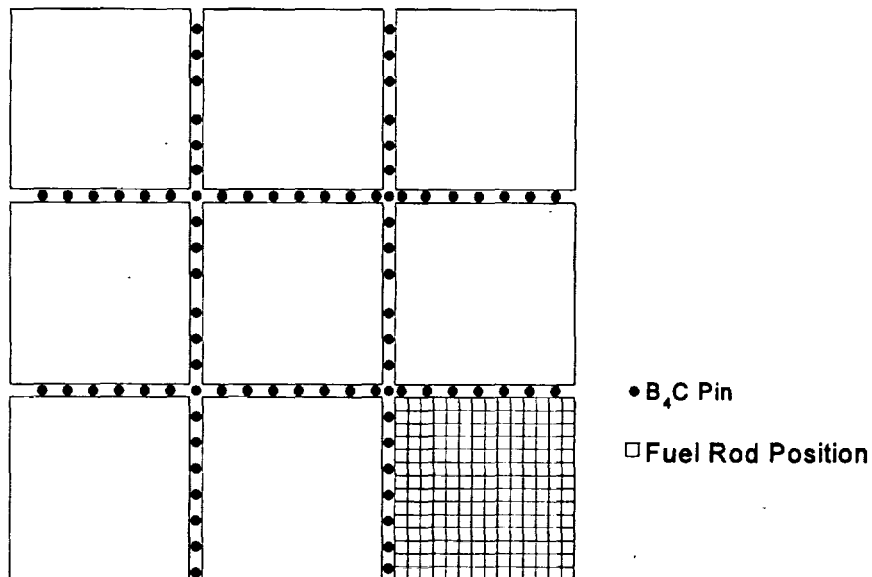


Figure 7.2.8-6. Core 4 Loading Diagram of Close Proximity Critical Benchmark Experiments

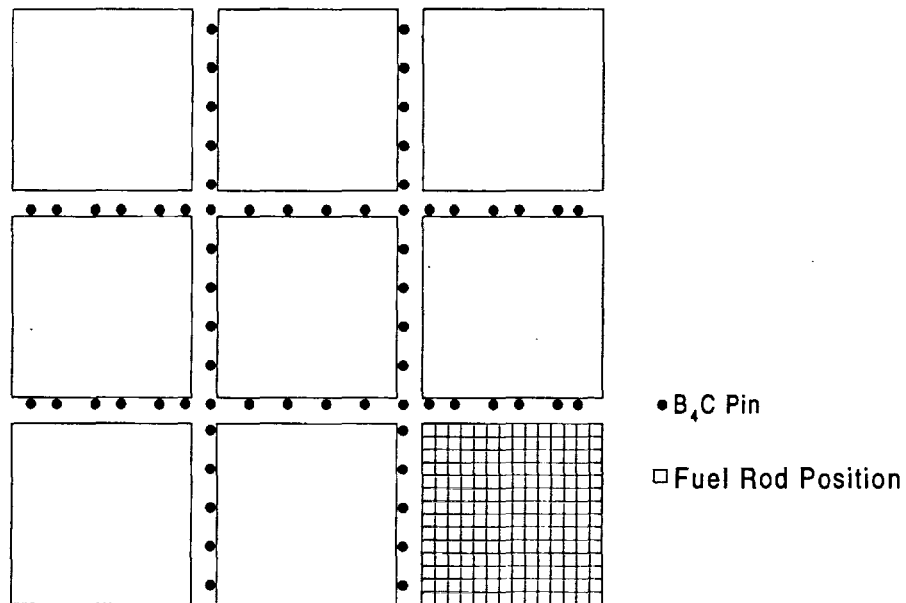


Figure 7.2.8-7. Core 5 Loading Diagram of Close Proximity Critical Benchmark Experiments

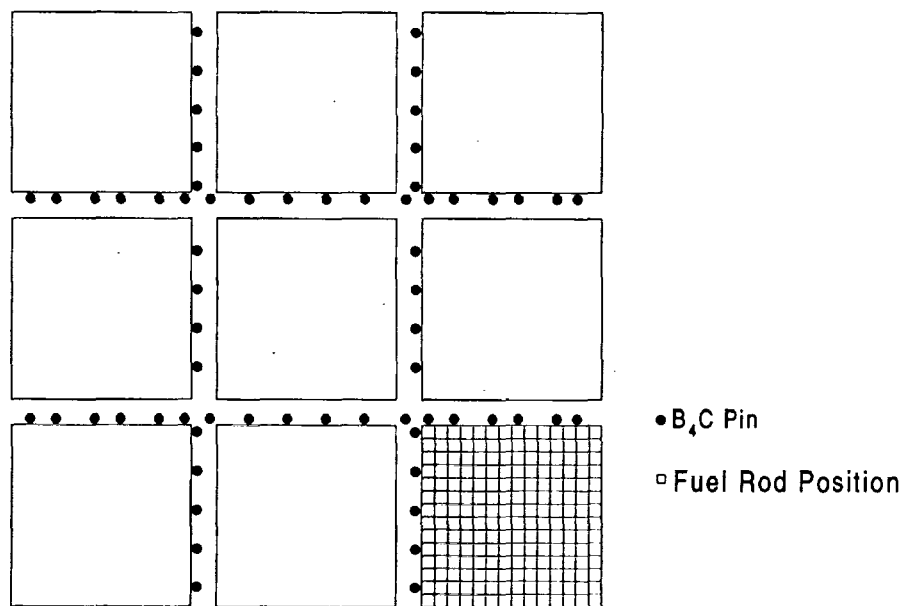


Figure 7.2.8-8. Core 6 Loading Diagram of Close Proximity Critical Benchmark Experiments

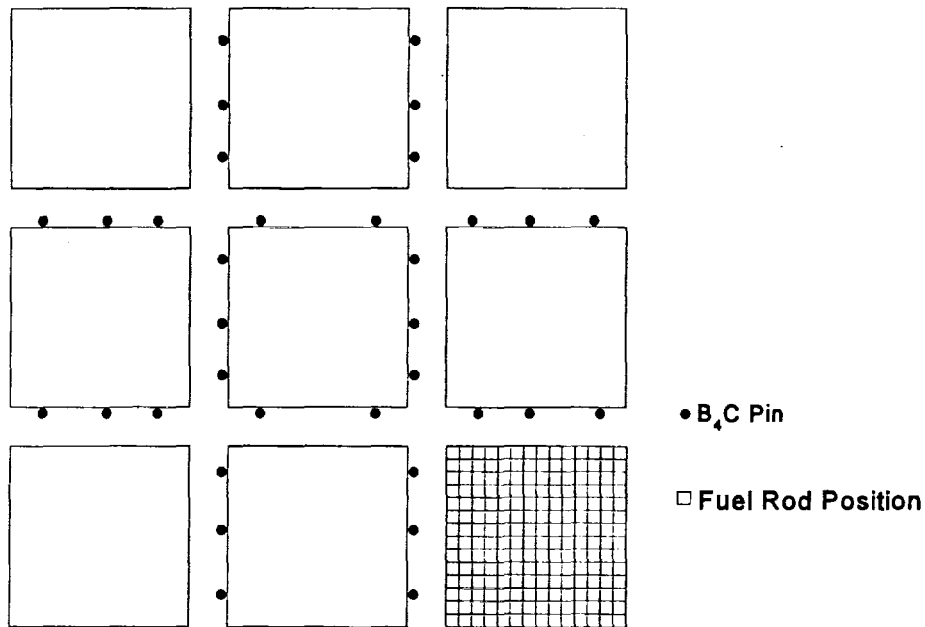


Figure 7.2.8-9. Core 7 Loading Diagram of Close Proximity Critical Benchmark Experiments

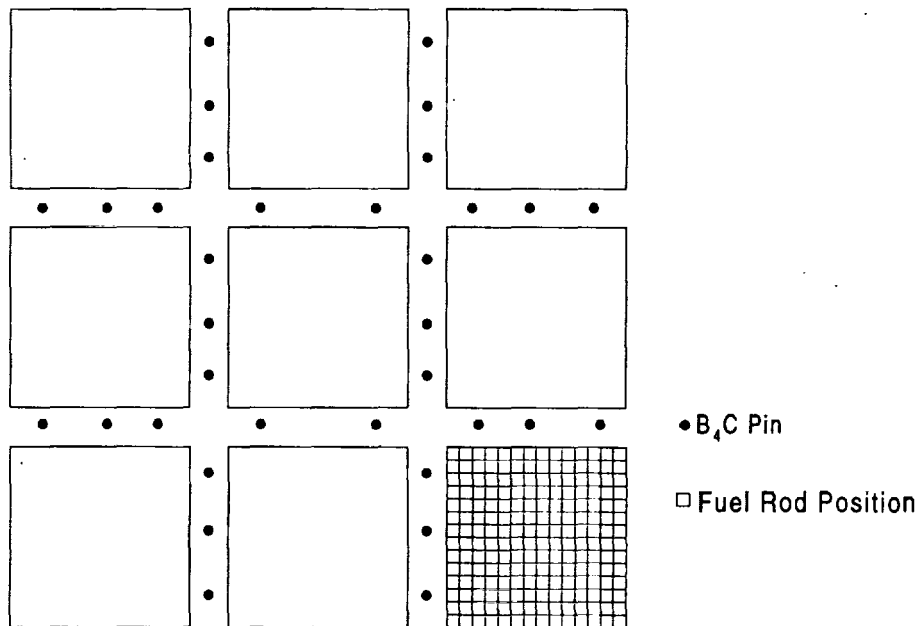


Figure 7.2.8-10. Core 8 Loading Diagram of Close Proximity Critical Benchmark Experiments

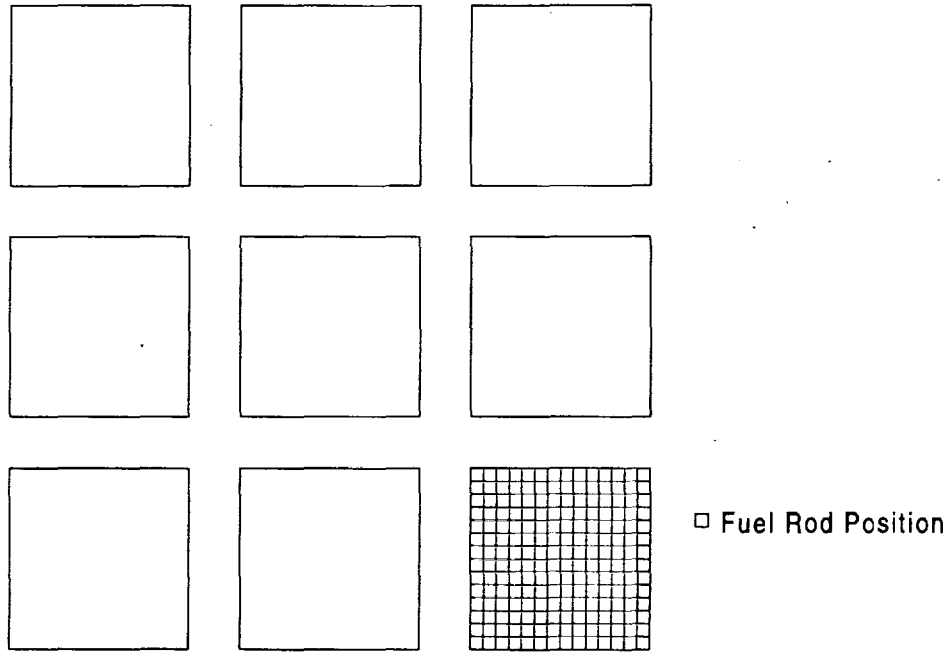


Figure 7.2.8-11. Core 9 Loading Diagram of Close Proximity Critical Benchmark Experiments

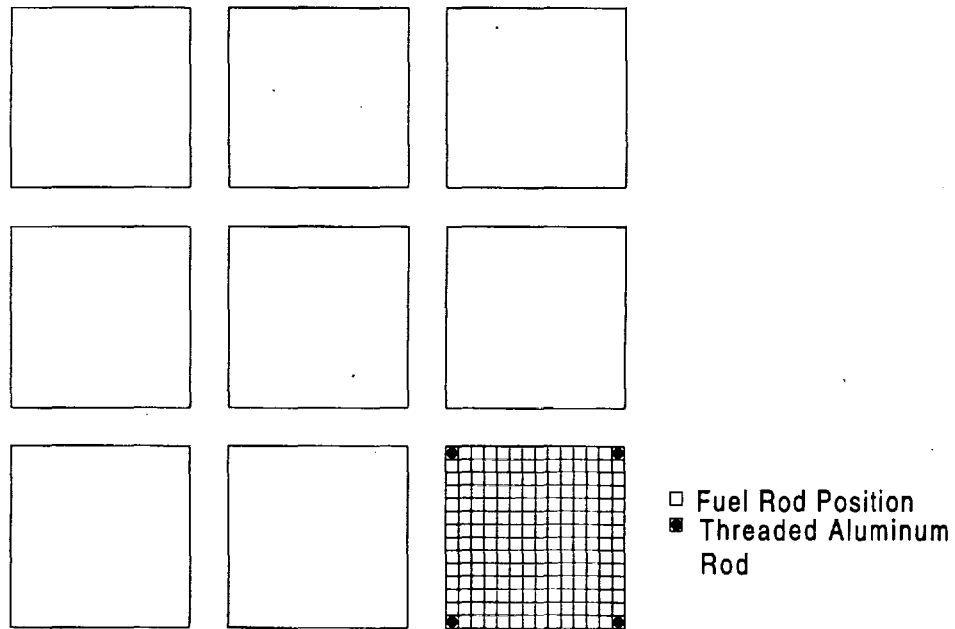


Figure 7.2.8-12. Core 10 Loading Diagram of Close Proximity Critical Benchmark Experiments

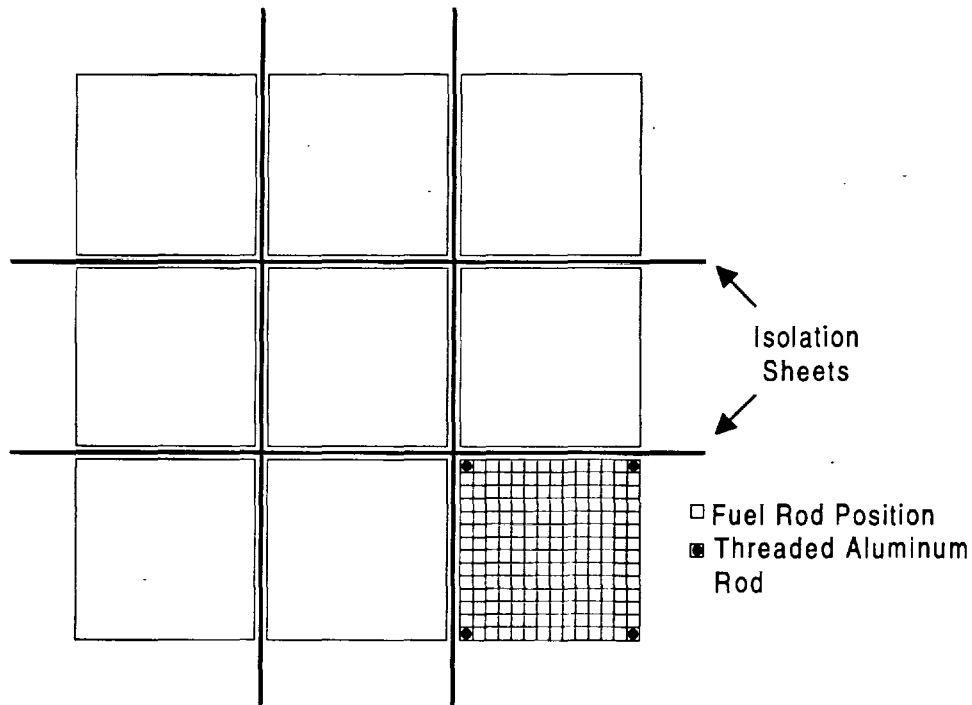


Figure 7.2.8-13. Core 11, 13, 14, 15, 17, and 19 Loading Diagrams of Close Proximity Critical Benchmark Experiments

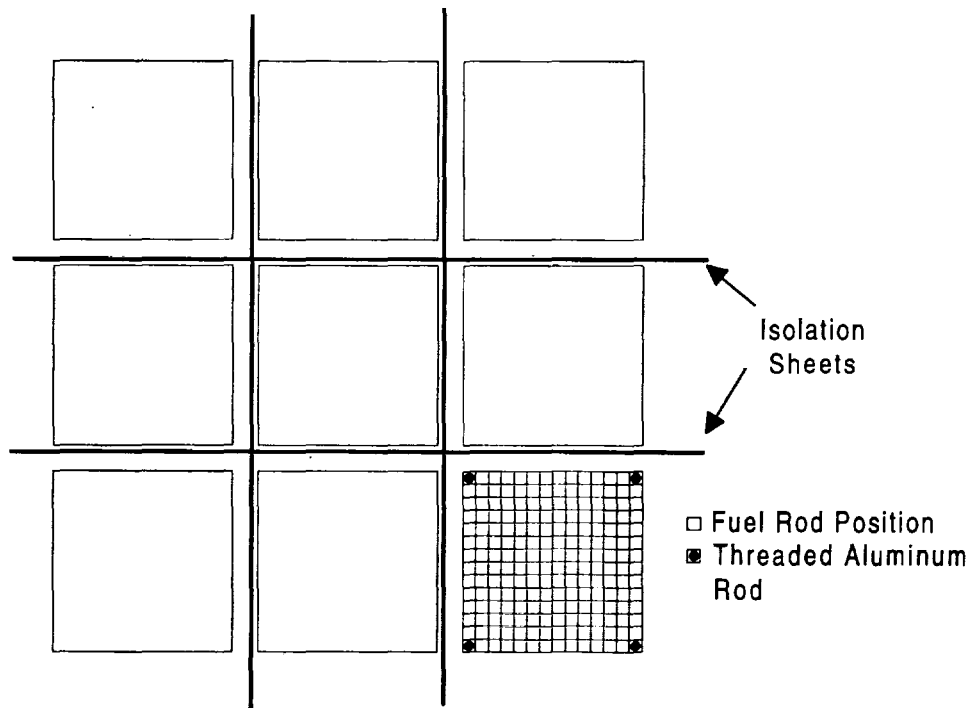


Figure 7.2.8-14. Core 12, 16, 18, and 20 Loading Diagrams of Close Proximity Critical Benchmark Experiments

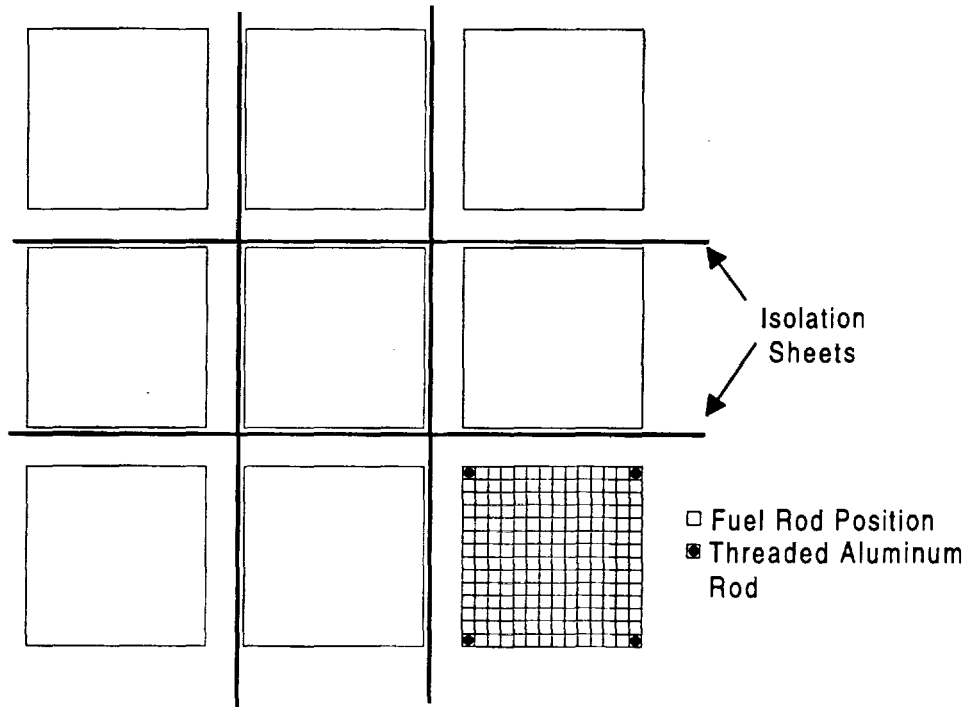


Figure 7.2.8-15. Core 21 Loading Diagram of Close Proximity Critical Benchmark Experiments

7.2.9 Electric Power Research Institute Mixed Oxide Critical Configurations

Smith (Reference 5.11) documents criticality tests with mixed oxide fuel performed for the Electric Power Research Institute. These same experiments were subsequently described by Bowman (Reference 5.10). Six critical experiment configurations composed of unborated and borated water moderated lattices of 2 wt% PuO₂ (8 wt% Pu-240)/98 wt% UO₂ (natural) fuel rods were modeled with MCNP. The PuO₂/UO₂ fuel rod description is shown in Figure 7.2.9-1. The PuO₂/UO₂ composition used in the MCNP models is shown in Table 7.2.9-1. The fuel rods are supported in a core structure composed of "eggcrate" type lattice plates with an upper lead shield. The axial view of the general core configuration is shown in Figure 7.2.9-2. The eggcrate lattice description is shown in Figure 7.2.9-3. The aluminum compositions used in the MCNP models are shown in Table 7.2.1-3. The configurations were closely reflected with at least 30 cm of water laterally and below the aluminum base plate.

Table 7.2.9-1. 2 wt% PuO₂ (8 wt% Pu-240)/98 wt% UO₂ (natural) Fuel Composition (9.54 g/cc) for EPRI Mixed Oxide Critical Benchmark Experiments

Element/Isotope	Atom Density (atoms/b·cm)
U-234	1.2462E-6
U-235	1.4891E-4
U-236	2.0943E-9
U-238	2.0619E-2
Pu-238	3.8850E-8
Pu-239	3.9477E-4
Pu-240	3.3218E-5
Pu-241	1.5634E-6
Pu-242	1.1887E-7
Am-241	1.5024E-6
Oxygen	4.3763E-2

The first experiment, designated "exp22," is a square lattice on a 1.778 cm pitch and contains 469 fuel rods. The core loading diagram is shown in Figure 7.2.9-4. The water-to-fuel volume ratio is 1.195 and the water moderator is unborated (contained residual boron of 1.7 ppm).

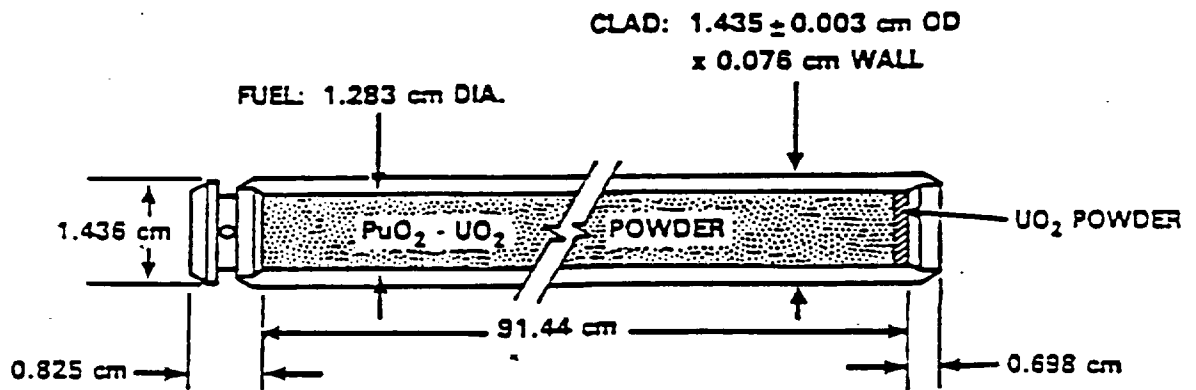
The second experiment, designated "exp23," is a square lattice on a 1.778 cm pitch and contains 761 fuel rods. The core loading diagram is shown in Figure 7.2.9-5. The water-to-fuel volume ratio is 1.195 and the water moderator contains 680.9 ppm of boron.

The third experiment, designated "exp24," is a square lattice on a 2.210 cm pitch and contains 197 fuel rods. The core loading diagram is shown in Figure 7.2.9-6. The 1.562 cm pitch eggcrate lattice plate is used in this experiment. The fuel rods are loaded into every other lattice location to obtain the 2.210 cm pitch. The water-to-fuel volume ratio is 2.527 and the water moderator is unborated (contained residual boron of 0.9 ppm).

The fourth experiment, designated "exp25," is a square lattice on a 2.210 cm pitch and contains 761 fuel rods. The core loading diagram is shown in Figure 7.2.9-7. The 1.562 cm pitch eggcrate lattice plate is used in this experiment. The fuel rods are loaded into every other lattice location to obtain the 2.210 cm pitch. The water-to-fuel volume ratio is 2.527 and the water moderator contains 1090.4 ppm of boron.

The fifth experiment, designated "exp26," is a square lattice on a 2.515 cm pitch and contains 160 fuel rods. The core loading diagram is shown in Figure 7.2.9-8. The 1.778 cm pitch eggcrate lattice plate is used in this experiment. The fuel rods are loaded into every other lattice location to obtain the 2.515 cm pitch. The water-to-fuel volume ratio is 3.641 and the water moderator is unborated (contained residual boron of 1.6 ppm).

The sixth experiment, designated "exp27," is a square lattice on a 2.515 cm pitch and contains 689 fuel rods. The core loading diagram is shown in Figure 7.2.9-9. The 1.778 cm pitch eggcrate lattice plate is used in this experiment. The fuel rods are loaded into every other lattice location to obtain the 2.515 cm pitch. The water-to-fuel volume ratio is 3.641 and the water moderator contains 767.2 ppm of boron.



CLADDING: ZIRCALOY-2 TUBING WITH PLUGS SEAL WELDED AT BOTH ENDS

LOADING:

ENRICHMENT - 2.00 WT% PuO₂ IN NATURAL UO₂
 OXIDE DENSITY - 9.54 g/cm³
 PuO₂ + UO₂ - 1128g/ROD
 Pu - 20.169 ± 0.004 g/ROD
 U - 970.306 ± 0.225 g/ROD
 UO₂ POWDER - NATURAL URANIUM ABOUT 0.2 cm THICK

Figure 7.2.9-1. PuO₂/UO₂ Fuel Rod Description for the EPRI Mixed Oxide Critical Benchmark Experiments

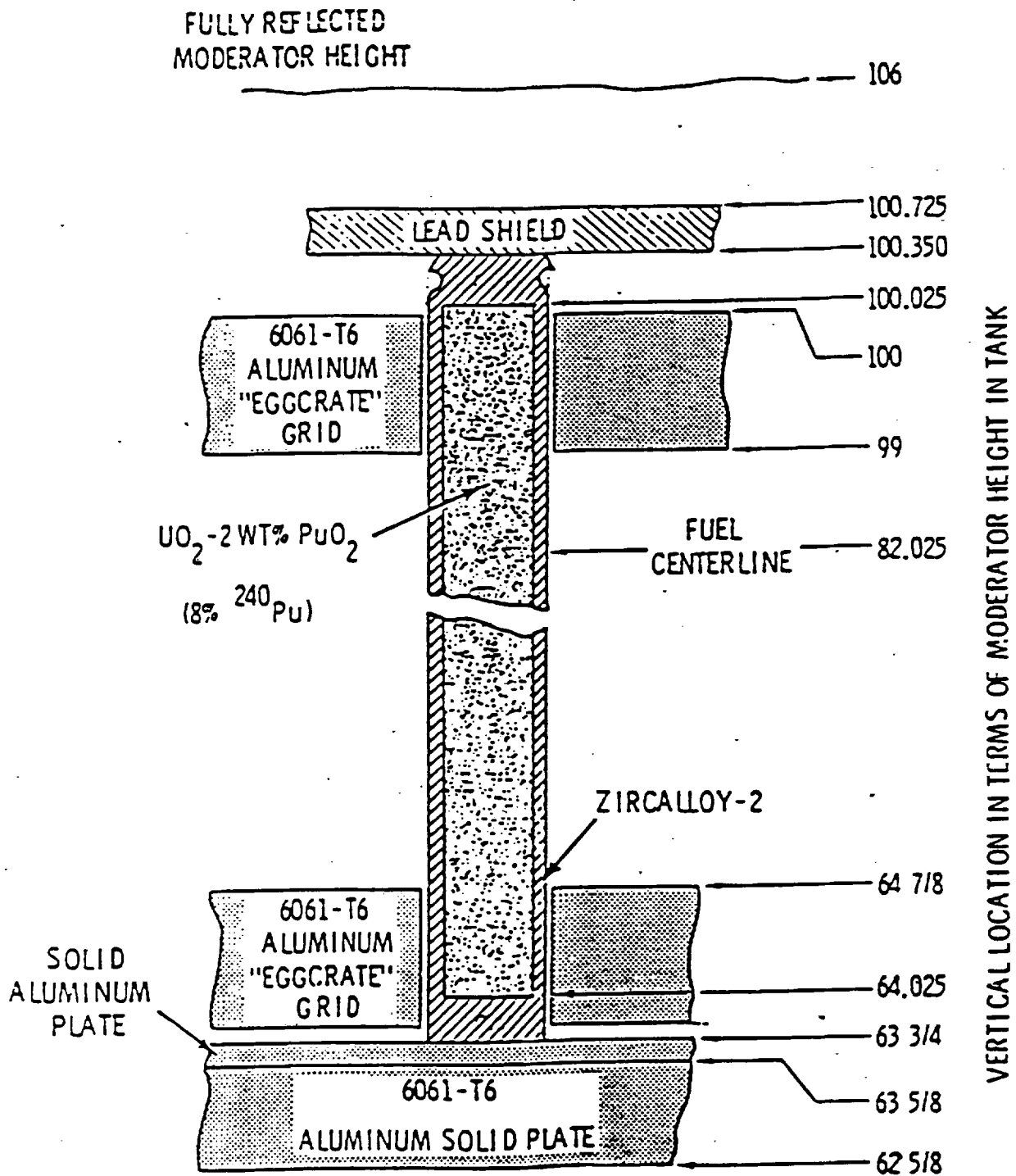
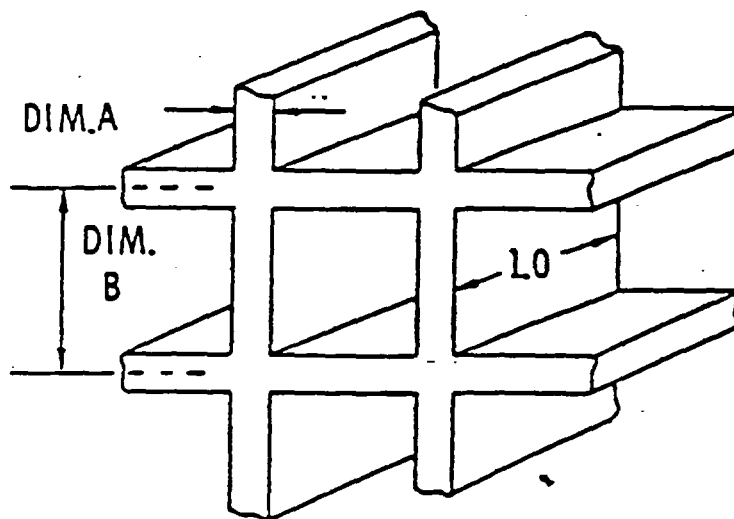


Figure 7.2.9-2.

Axial View of the General Core Configuration for the EPRI Mixed Oxide Critical Benchmark Experiments



FUEL TYPE	PITCH	GRID	DIM.A	DIM B
UO ₂ -2.35% ²³⁵ U	0.615 0.87	UPPER LOWER	0.032 0.090	0.615
UO ₂ -2 WT% PuO ₂ (8% ²⁴⁰ Pu)	0.87	UPPER LOWER	0.032 0.032	0.615
UO ₂ -2 WT% PuO ₂ (8% ²⁴⁰ Pu)	0.70 0.99	UPPER LOWER	0.125 0.125	0.70

Figure 7.2.9-3. Eggcrate Lattice Description for the EPRI Mixed Oxide Critical Benchmark Experiments

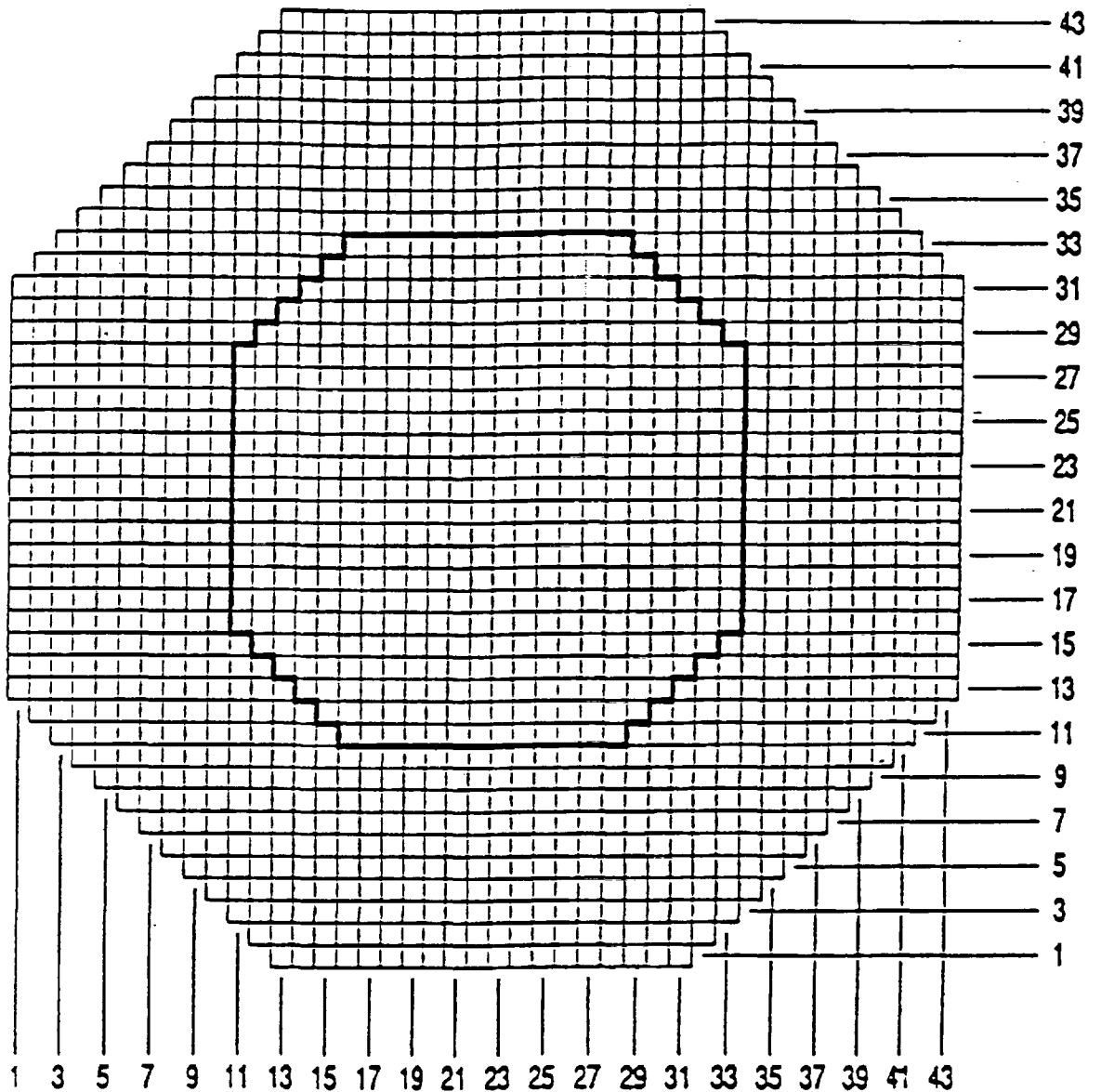


Figure 7.2.9-4. Core Loading Diagram for "exp22" of the EPRI Mixed Oxide Critical Benchmark Experiments

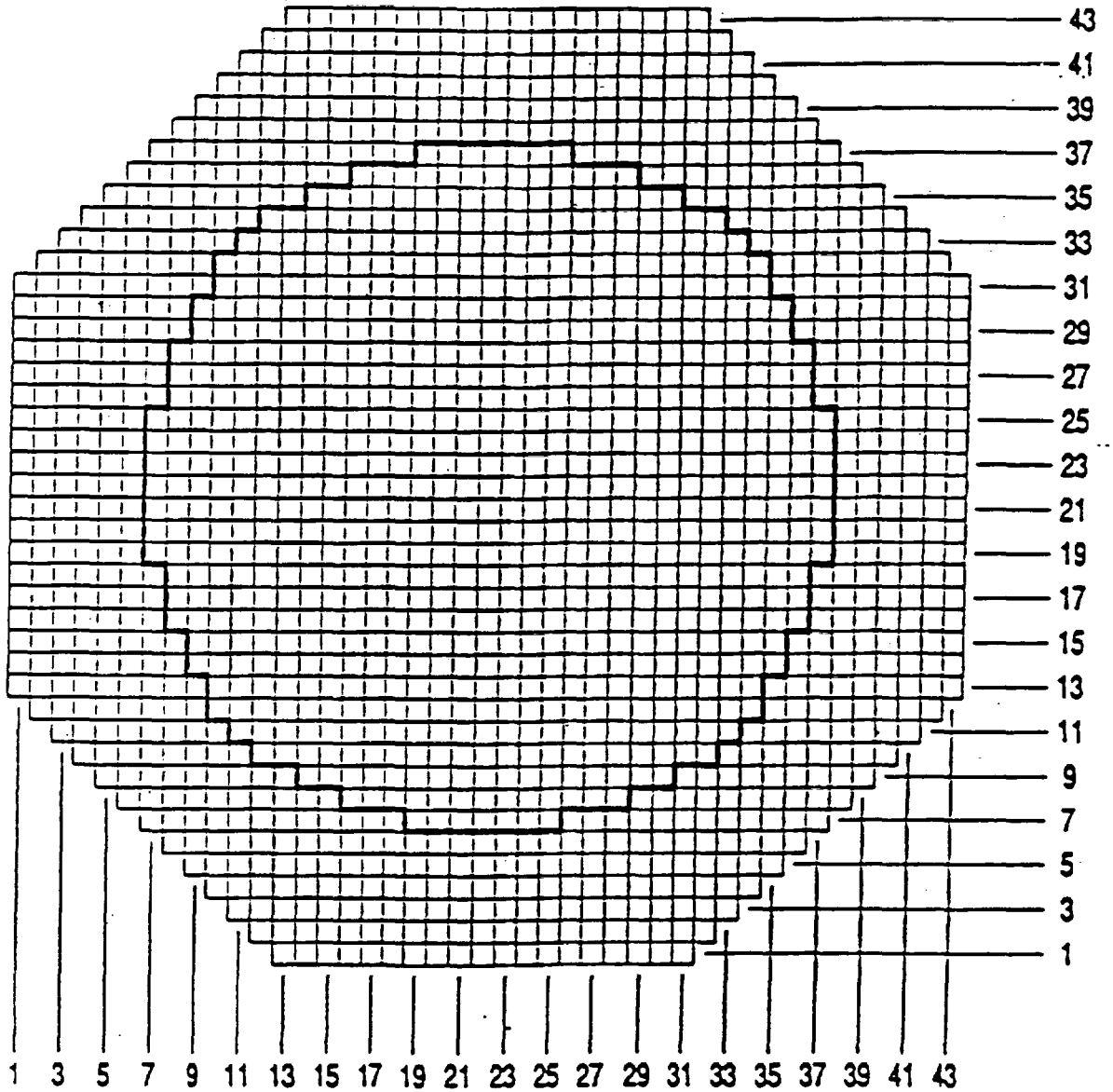


Figure 7.2.9-5. Core Loading Diagram for "exp23" of the EPRI Mixed Oxide Critical Benchmark Experiments

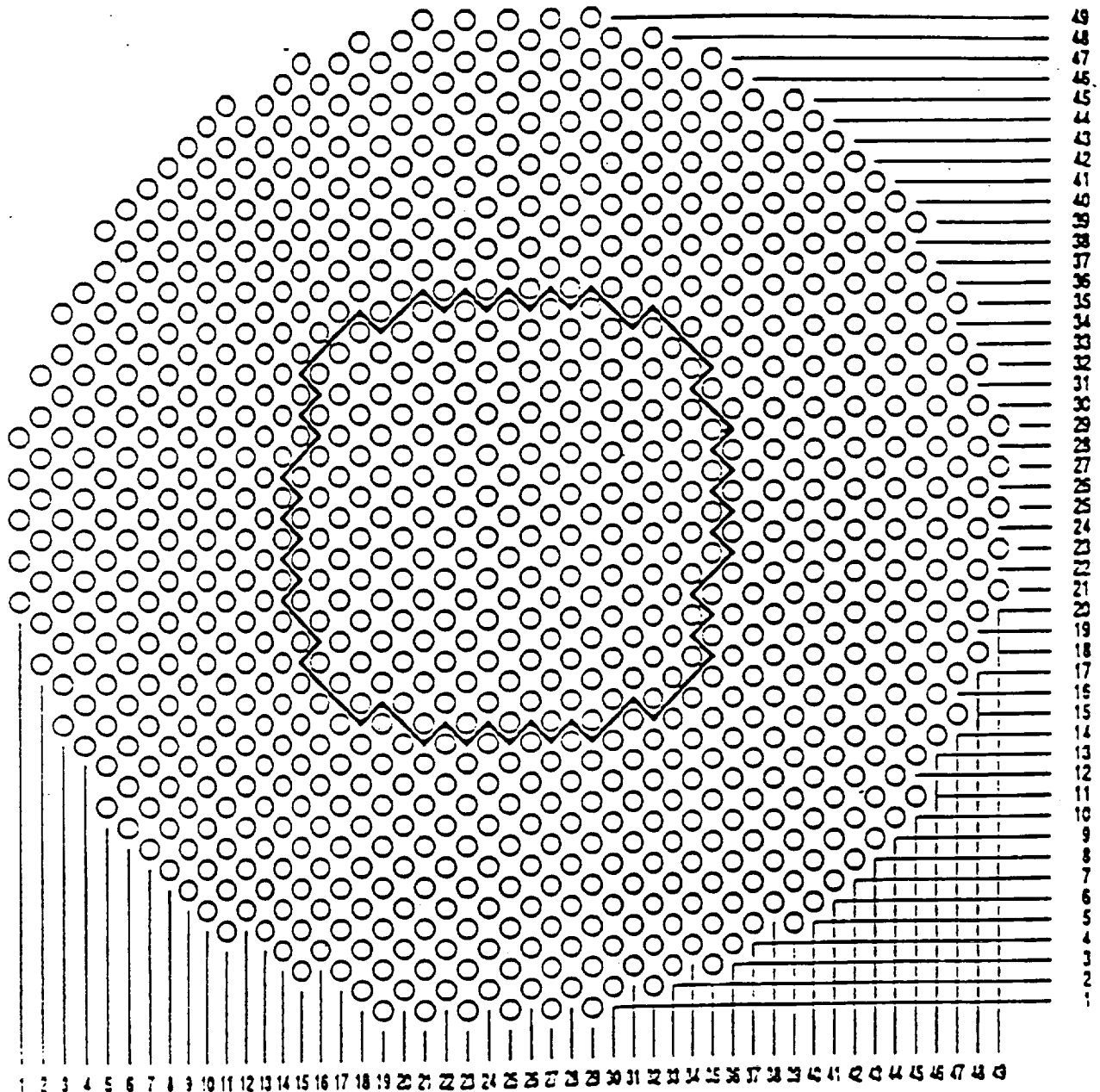


Figure 7.2.9-6. Core Loading Diagram for "exp24" of the EPRI Mixed Oxide Critical Benchmark Experiments

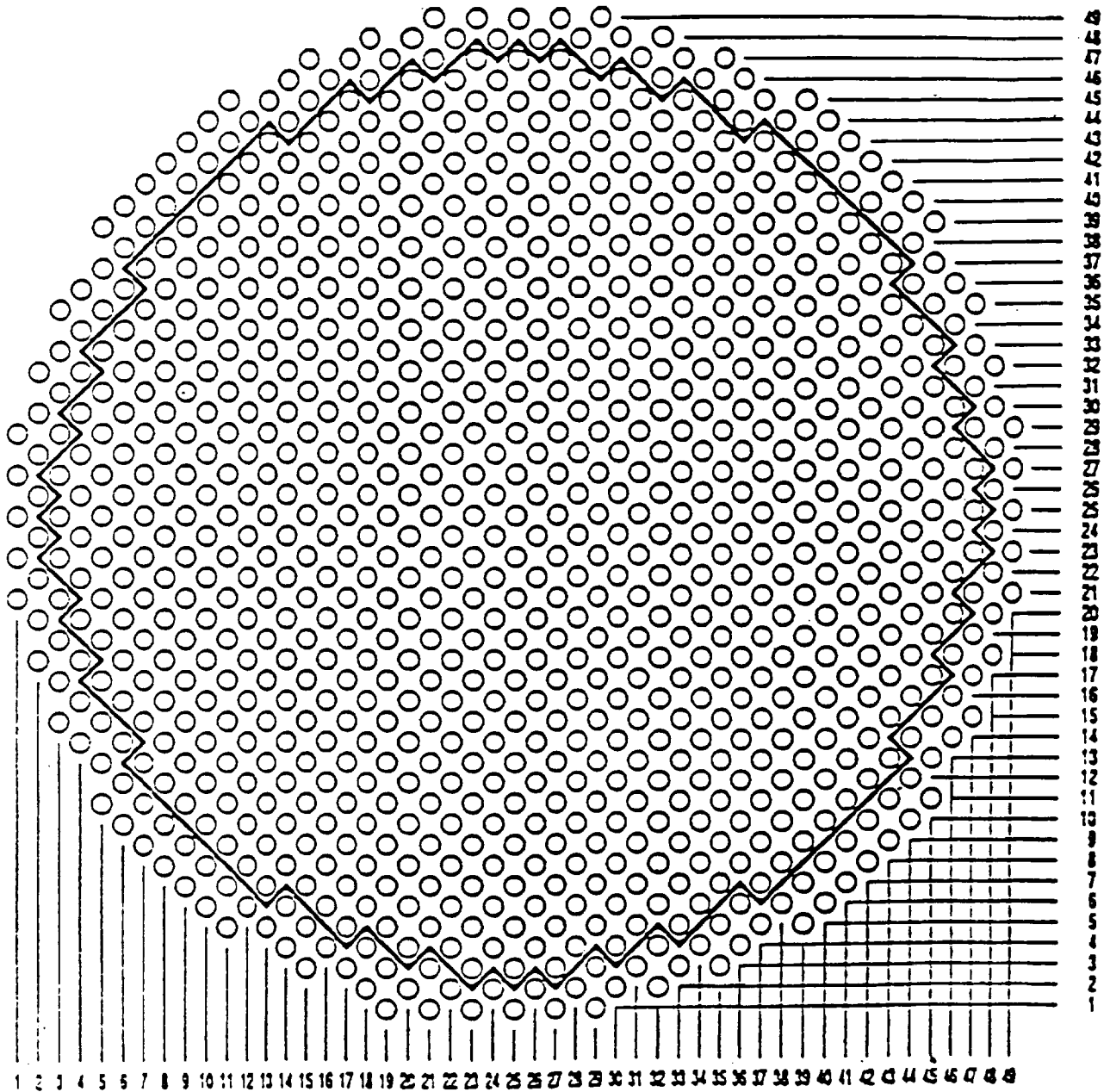


Figure 7.2.9-7. Core Loading Diagram for "exp25" of the EPRI Mixed Oxide Critical Benchmark Experiments

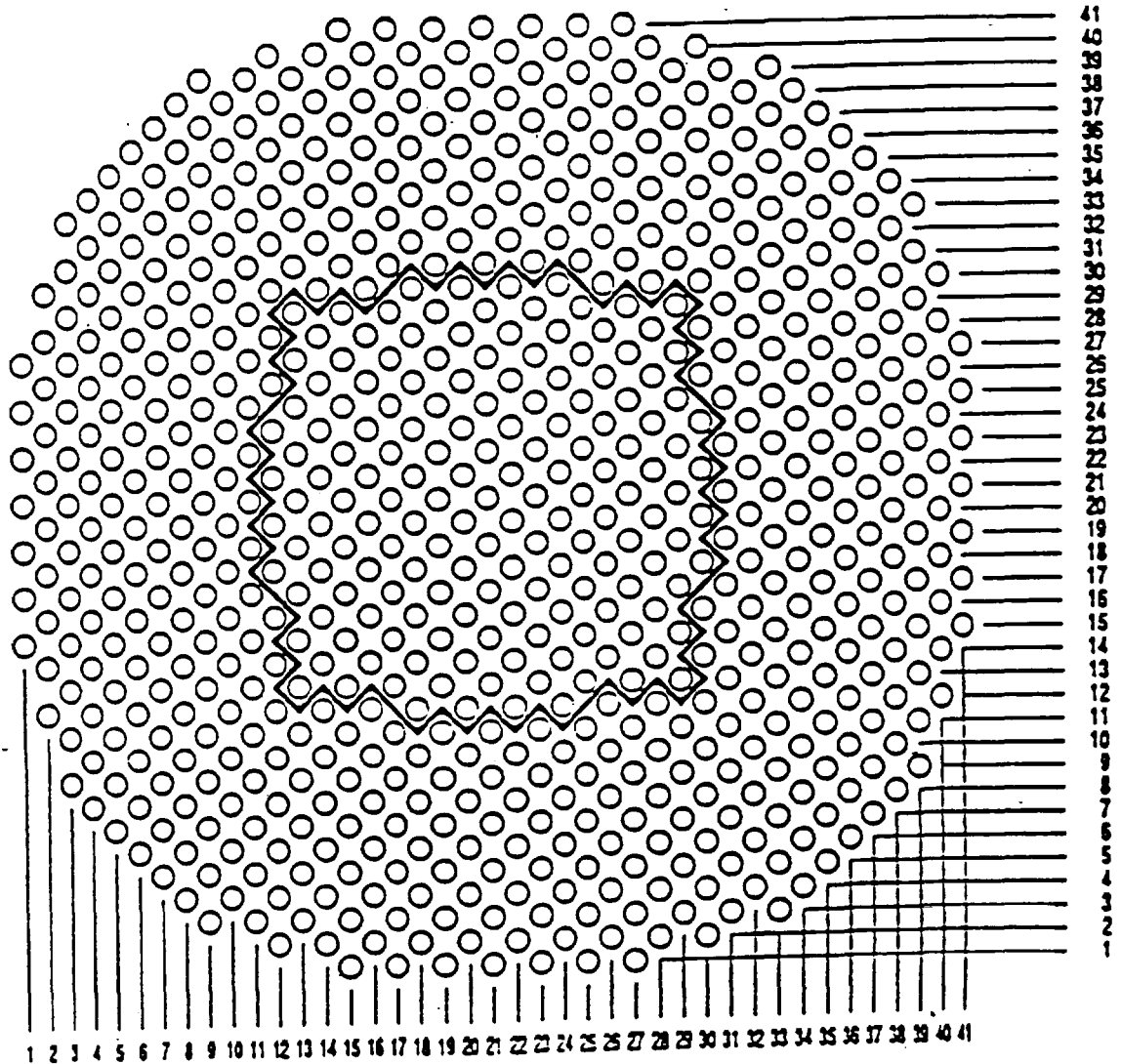


Figure 7.2.9-8. Core Loading Diagram for "exp26" of the EPRI Mixed Oxide Critical Benchmark Experiments

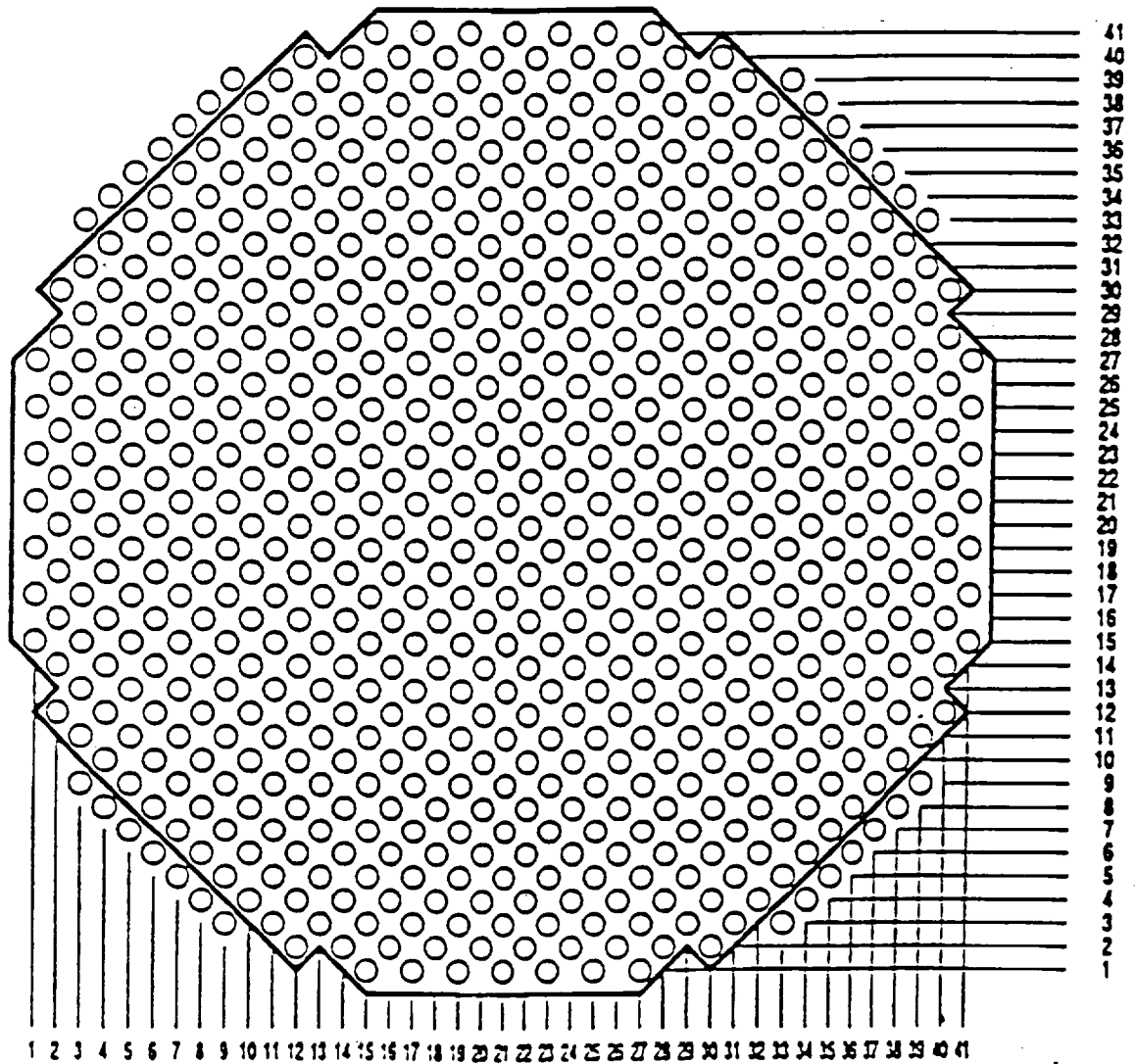


Figure 7.2.9-9.

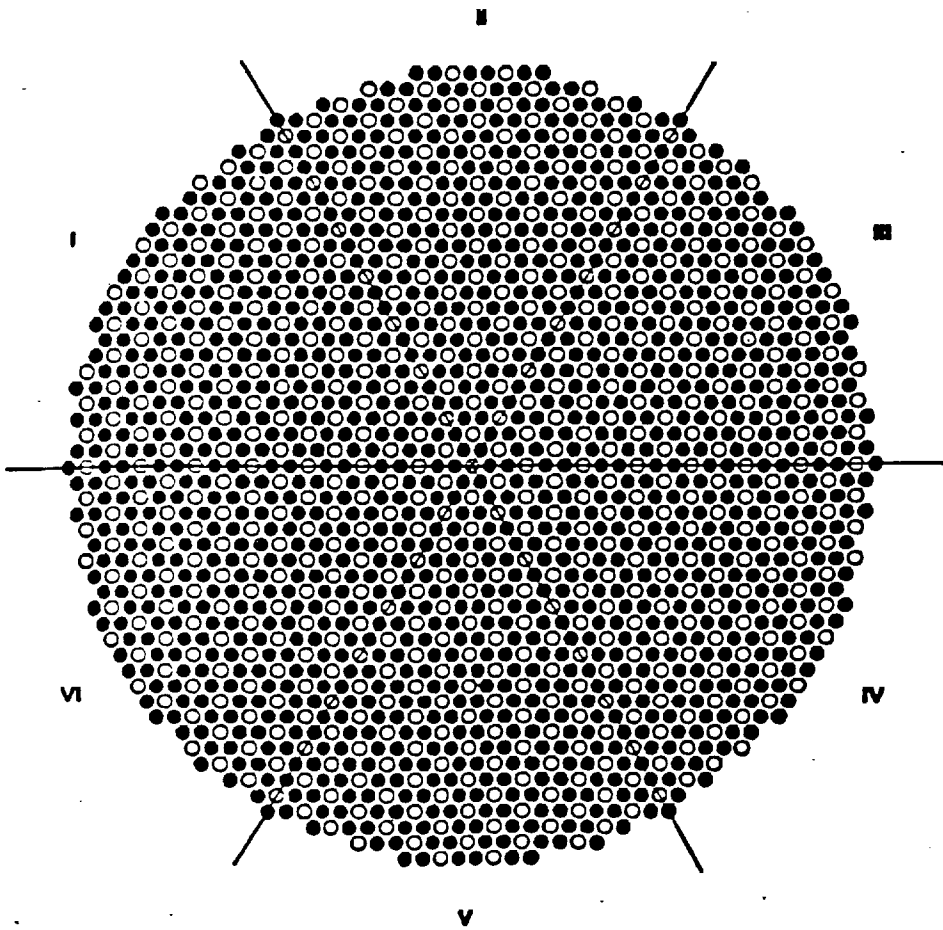
Core Loading Diagram for "exp27" of the EPRI Mixed Oxide Critical Benchmark Experiments

7.2.10 Critical Triangular Lattice of MOX & UO₂ Fuel Rods

Bierman (Reference 5.15) documented critical experiments performed at Pacific Northwest Laboratories incorporating both urania and mixed-oxide fuel rods in a triangular lattice. One such experiment, designated "exp34," contained a triangular lattice of uniformly distributed PuO₂-UO₂ and UO₂ fuel rods. The fuel rods were placed in a uniform distribution with a Pu/U-235 ratio approximating that of a 20,000 MWd/MTU burnup. Each PuO₂-UO₂ fuel rod was surrounded by six UO₂ fuel rods with a triangular lattice pitch of 1.598 cm. A planar view of the general experimental configuration is shown in Figure 7.2.10-1. The fuel rods were supported by three 1.35 cm thick polypropylene lattice plates. The axial view of the general configuration is shown in Figure 7.2.10-2. The critical configuration contained 583 mixed oxide fuel rods composed of 2 wt% PuO₂ and 98 wt% natural UO₂. The PuO₂ fuel composition is shown in Table 7.2.10-1. The description of the PuO₂/UO₂ fuel rod is shown in Figure 7.2.10-3. The critical configuration also contained 1174 uranium dioxide fuel rods composed of 4.31 wt% U-235 enriched UO₂. The description of the UO₂ fuel rod is shown in Figure 7.2.10-4.

Table 7.2.10-1. "exp34" MOX Fuel Rod PuO₂ Composition

Parameter	Value
Isotopic wt% of Pu-238	0.10 ± 0.001
Isotopic wt% of Pu-239	91.806 ± 0.551
Isotopic wt% of Pu-240	7.876 ± 0.394
Isotopic wt% of Pu-241	0.277 ± 0.008
Isotopic wt% of Pu-242	0.031
Concentration (ppm) Am-241	76



FUEL: 4.31 wt% ²³⁵U ENRICHED UO₂ AND PuO₂.
 NATURAL UO₂ CONTAINING 2.0 wt% PuO₂

EXPERIMENT: 4.3-002-196

LATTICE: 32

PITCH: 1.598 ± 0.005 cm

GADOLINIUM: SEE COMMENTS

CONTROL ROD: NONE

SAFETY ROD: NONE

REACTION RATES: NONE

RODS: 583 MO₂ RODS AT ○ PLUS 1174 UO₂ RODS AT ●

k_{eff}: SEE COMMENTS

COMMENTS: PERIPHERIAL UNUSED LATTICE LOCATIONS NOT SHOWN

k_{eff} = 1.0 AT ZERO g Gd/liter

k_{eff} = 0.957 AT 0.194 ± 0.001 g Gd/liter

k_{eff} = 0.931 AT 0.408 ± 0.006 g Gd/liter

k_{eff} = 0.914 AT 0.626 ± 0.008 g Gd/liter

k_{eff} = 0.891 AT 0.918 ± 0.015 g Gd/liter

Figure 7.2.10-1. General Planar View of the "exp34" Critical Benchmark Experimental Configuration

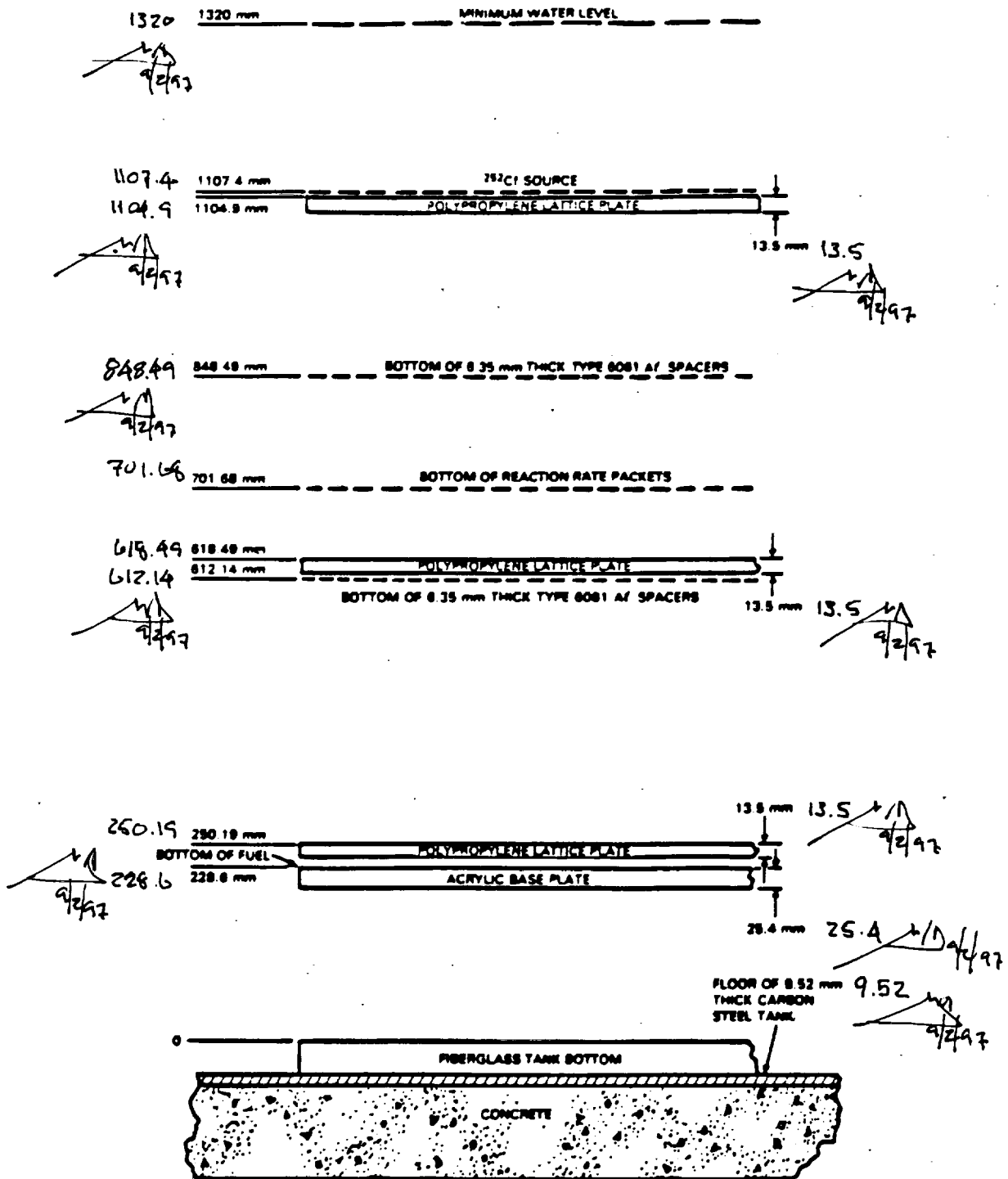
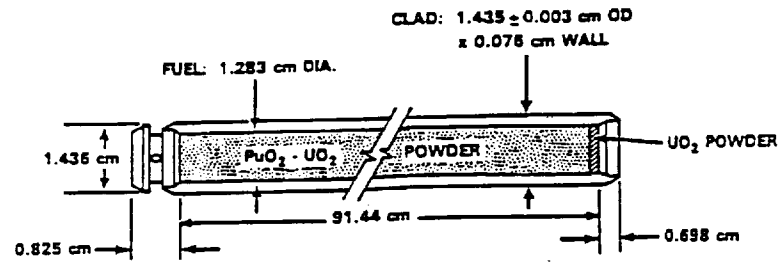


Figure 7.2.10-2. General Axial View of the "exp34" Critical Benchmark Experimental Configuration



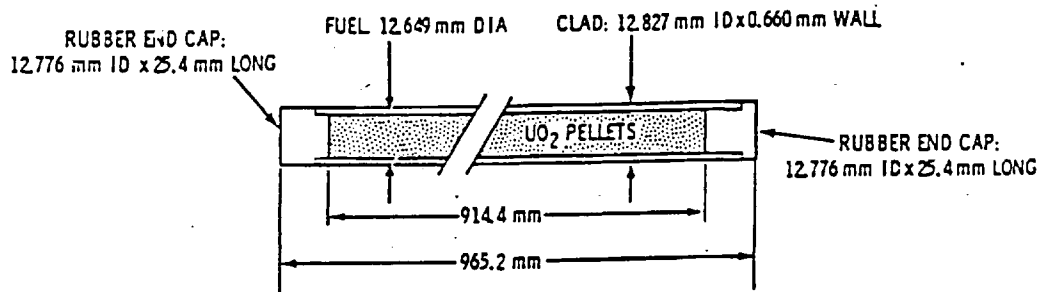
CLADDING: ZIRCALOY-2 TUBING WITH PLUGS SEAL WELDED AT BOTH ENDS

LOADING:

- ENRICHMENT - 2.00 WT% PuO₂ IN NATURAL UO₂
- OXIDE DENSITY - 9.54 g/cm³
- PuO₂ + UO₂ - 1128g/ROD
- Pu - 20.169 ± 0.004 g/ROD
- U - 970.306 ± 0.225 g/ROD
- UO₂ POWDER - NATURAL URANIUM ABOUT 0.2 cm THICK

Figure 7.2.10-3. Description of the PuO₂/UO₂ Fuel Rod for the "exp34" Critical Benchmark Experiment

4.31 wt% ²³⁵U ENRICHED UO₂ RODS



CLADDING: 6061 ALUMINUM TUBING

LOADING:

- ENRICHMENT - 4.31 ± 0.01 wt% ²³⁵U
- FUEL DENSITY - 94.9 ± 0.55% OF THEORETICAL DENSITY
- URANIUM ASSAY - 88.055 ± 0.261 wt% OF TOTAL FUEL COMPOSITION
- UO₂ - 1203.38 ± 4.12 g/ROD

END CAP:

- DENSITY - 1.321 g/cm³
- COMPOSITION- C - 58 ± 1 wt%
- H - 6.5 ± 0.3 wt%
- Ca - 11.4 ± 1.8 wt%
- S - 1.7 ± 0.2 wt%
- O - 22.1 wt% (BALANCE)
- Si - 0.3 ± 0.1 wt%

Figure 7.2.10-4. Description of the UO₂ Fuel Rod for the "exp34" Critical Benchmark Experiment

7.3 Laboratory Critical Experiment k_{eff} Results

This section tabulates the MCNP k_{eff} results for the LCEs according to experimental similarities. Tables 7.3-1 through 7.3-4 present the results for the LCEs according to the following distinct experimental classifications:

Table 7.3-1	Moderated Lattices Containing UO_2 Fuel
Table 7.3-2	Moderated Lattices Containing UO_2 Fuel and Gadolinia
Table 7.3-3	Moderated Lattices Containing UO_2 Fuel and Absorber Plates
Table 7.3-4	Moderated Lattices Containing Mixed Oxide Fuel

The same results are exhibited graphically in Figures 7-3.1 through 7-3.4.

**Table 7.3-1. Moderated Lattices Containing UO₂ Fuel
(ENDF/B-V Libraries)**

Case Name	k _{eff}	σ	k _{eff} - 1	Reference
<i>Urania Fuel</i>				
exp1	0.99943	0.00091	-0.057%	5.7, 5.12
core9	0.99178	0.00141	-0.822%	5.16
exp8	1.0073	0.00103	0.730%	5.10, 5.12
exp10	1.00693	0.00167	0.693%	5.10, 5.12
exp11	1.00175	0.00165	0.175%	5.10, 5.12
exp14	0.99687	0.00099	-0.313%	5.12, 5.13
exp15	1.00072	0.00090	0.072%	5.12, 5.13
exp17	0.99888	0.00172	-0.112%	5.15
exp18	1.00024	0.00162	0.024%	5.15
<i>Urania Fuel with Boron Soluble Poison</i>				
ugd1	0.99871	0.00154	-0.129%	5.14
ugd12	1.00047	0.00142	0.047%	5.14
ugd18	0.99706	0.00152	-0.294%	5.14
exp9	1.0073	0.00107	0.730%	5.10, 5.12
core2	0.99804	0.00154	-0.196%	5.16
core3	0.99863	0.00156	-0.137%	5.16
core10	0.99896	0.00146	-0.104%	5.16
<i>Urania Fuel with Boron Soluble Poison and Ag-In-Cd Control Rods</i>				
ugd2	0.99870	0.00144	-0.130%	5.14
<i>Urania Fuel with Boron Soluble Poison and B₄C Control Rods</i>				
ugd13	0.99714	0.00148	-0.286%	5.14
<i>Urania Fuel with Reflectors</i>				
exp5	0.99696	0.00102	-0.304%	5.8, 5.9, 5.12
exp6	0.99999	0.00112	-0.001%	5.8, 5.9, 5.12
exp7	0.99809	0.00109	-0.191%	5.8, 5.9, 5.12
<i>Urania Fuel with Flux Traps</i>				
exp12	1.00538	0.00111	0.538%	5.11, 5.12
exp13	1.00226	0.00112	0.226%	5.11, 5.12
<i>Urania Fuel with Intermediate B₄C Pins</i>				
core4	0.99434	0.00156	-0.566%	5.16
core5	0.99126	0.00158	-0.874%	5.16
core6	0.99415	0.00148	-0.585%	5.16
core7	0.99581	0.00145	-0.419%	5.16
core8	0.99081	0.00152	-0.919%	5.16

Uncertainty =

0.00138	-0.00114
---------	----------

 = Average

**Table 7-3.1. (cont'd) Moderated Lattices Containing UO₂ Fuel
(ENDF/B-VI Libraries)**

Case Name	k _{eff}	σ	k _{eff} - 1	Reference
<i>Urania Fuel</i>				
exp1	0.99164	0.00087	-0.836%	5.7, 5.12
core9	0.98780	0.00141	-1.220%	5.16
exp8	1.00501	0.00112	0.501%	5.10, 5.12
exp10	1.00301	0.00169	0.301%	5.10, 5.12
exp11	0.99761	0.00167	-0.239%	5.10, 5.12
exp14	0.99075	0.00102	-0.925%	5.12, 5.13
exp15	0.99664	0.00090	-0.336%	5.12, 5.13
exp17	0.99888	0.00172	-0.112%	5.15
exp18	1.00024	0.00162	0.024%	5.15
<i>Urania Fuel with Boron Soluble Poison</i>				
ugd1	0.99934	0.00144	-0.066%	5.14
ugd12	0.99959	0.00148	-0.041%	5.14
ugd18	0.99803	0.00150	-0.197%	5.14
exp9	1.00648	0.00107	0.648%	5.10, 5.12
core2	0.99631	0.00150	-0.369%	5.16
core3	0.99616	0.00150	-0.384%	5.16
core10	0.98979	0.00144	-1.021%	5.16
<i>Urania Fuel with Boron Soluble Poison and Ag-In-Cd Control Rods</i>				
ugd2	0.99501	0.00144	-0.499%	5.14
<i>Urania Fuel with Boron Soluble Poison and B₄C Control Rods</i>				
ugd13	1.00166	0.00148	0.166%	5.14
<i>Urania Fuel with Reflectors</i>				
exp5	0.99607	0.00107	-0.393%	5.8, 5.9, 5.12
exp6	0.99514	0.00110	-0.486%	5.8, 5.9, 5.12
exp7	0.99499	0.00106	-0.501%	5.8, 5.9, 5.12
<i>Urania Fuel with Flux Traps</i>				
exp12	0.99873	0.00110	-0.127%	5.11, 5.12
exp13	0.99859	0.00109	-0.141%	5.11, 5.12
<i>Urania Fuel with Intermediate B₄C Pins</i>				
core4	0.99197	0.00163	-0.803%	5.16
core5	0.98994	0.00156	-1.006%	5.16
core6	0.99273	0.00159	-0.727%	5.16
core7	0.98566	0.00149	-1.434%	5.16
core8	0.98866	0.00148	-1.134%	5.16

Uncertainty =

0.00138	-0.00406
---------	----------

 = Average

Table 7.3-2. Moderated Lattices Containing UO₂ Fuel and Gadolinia

(ENDF/B-V Libraries)

Case Name	k _{eff}	σ	k _{eff} - 1	Reference
<i>Urania/Gadolinia Fuel with Boron Soluble Poison</i>				
ugd3	1.00171	0.00147	0.171%	5.14
ugd5	0.99721	0.00146	-0.279%	5.14
ugd7	1.00083	0.00154	0.083%	5.14
ugd8	0.99784	0.00152	-0.216%	5.14
ugd14	1.00204	0.00147	0.204%	5.14
ugd16	0.99871	0.00148	-0.129%	5.14
ugd19	1.00000	0.00153	0.000%	5.14
ugd20	1.00035	0.00148	0.035%	5.14
<i>Urania/Gadolinia Fuel with Boron Soluble Poison and Ag-In-Cd Control Rods</i>				
ugd4	1.00034	0.00150	0.034%	5.14
ugd6	1.00048	0.00136	0.048%	5.14
ugd9	1.00014	0.00144	0.014%	5.14
<i>Urania/Gadolinia Fuel with Boron Soluble Poison and B₄C Control Rods</i>				
ugd15	1.00126	0.00145	0.126%	5.14
ugd17	1.00156	0.00150	0.156%	5.14
<i>Urania/Gadolinia Fuel with Boron Soluble Poison and Void Locations</i>				
ugd10	0.99722	0.00142	-0.278%	5.14

Uncertainty =

0.00147	-0.00002
---------	----------

 = Average

(ENDF/B-VI Libraries)

Case Name	k _{eff}	σ	k _{eff} - 1	Reference
<i>Urania/Gadolinia Fuel with Boron Soluble Poison</i>				
ugd3	0.99764	0.00146	-0.236%	5.14
ugd5	0.99672	0.00146	-0.328%	5.14
ugd7	0.99716	0.00152	-0.284%	5.14
ugd8	0.99862	0.00149	-0.138%	5.14
ugd14	0.99831	0.00144	-0.169%	5.14
ugd16	0.99799	0.00158	-0.201%	5.14
ugd19	0.99855	0.00155	-0.145%	5.14
ugd20	1.00044	0.00153	0.044%	5.14
<i>Urania/Gadolinia Fuel with Boron Soluble Poison and Ag-In-Cd Control Rods</i>				
ugd4	0.99970	0.00143	-0.030%	5.14
ugd6	0.99728	0.00146	-0.272%	5.14
ugd9	1.00041	0.00153	0.041%	5.14
<i>Urania/Gadolinia Fuel with Boron Soluble Poison and B₄C Control Rods</i>				
ugd15	0.99675	0.00151	-0.325%	5.14
ugd17	0.99722	0.00156	-0.278%	5.14
<i>Urania/Gadolinia Fuel with Boron Soluble Poison and Void Locations</i>				
ugd10	0.99872	0.00147	-0.128%	5.14

Uncertainty =

0.00150	-0.00175
---------	----------

 = Average

Table 7.3-3. Moderated Lattices Containing UO₂ Fuel and Absorber Plates

(ENDF/B-V Libraries)

Case Name	k _{eff}	σ	k _{eff} - 1	Reference
<i>Urania Fuel with Absorber Plates</i>				
exp2	0.99808	0.00091	-0.192%	5.7, 5.12
exp3	1.00047	0.00089	0.047%	5.7, 5.12
exp4	1.00008	0.00089	0.008%	5.8, 5.9, 5.12
<i>Urania Fuel with Absorber Plates and Boron Soluble Poison</i>				
core11	0.99660	0.00147	-0.340%	5.16
core12	0.99347	0.00155	-0.653%	5.16
core13	0.99705	0.00165	-0.295%	5.16
core15	0.98776	0.00160	-1.224%	5.16
core16	0.98911	0.00155	-1.089%	5.16
core17	0.99223	0.00286	-0.777%	5.16
core18	0.99173	0.00157	-0.827%	5.16
core19	0.99477	0.00158	-0.523%	5.16
core20	0.99086	0.00159	-0.914%	5.16
core21	0.99071	0.00148	-0.929%	5.16

Uncertainty =

0.00158	-0.00593
---------	----------

 = Average

(ENDF/B-VI Libraries)

Case Name	k _{eff}	σ	k _{eff} - 1	Reference
<i>Urania Fuel with Absorber Plates</i>				
exp2	0.98994	0.00093	-1.006%	5.7, 5.12
exp3	0.99040	0.00088	-0.960%	5.7, 5.12
exp4	0.99167	0.00090	-0.833%	5.8, 5.9, 5.12
<i>Urania Fuel with Absorber Plates and Boron Soluble Poison</i>				
core11	0.99726	0.00148	-0.274%	5.16
core12	0.99234	0.00150	-0.766%	5.16
core13	0.99514	0.00563	-0.486%	5.16
core14	0.98804	0.00145	-1.196%	5.16
core15	0.98912	0.00201	-1.088%	5.16
core16	0.98289	0.00143	-1.711%	5.16
core17	0.98963	0.00160	-1.037%	5.16
core18	0.98473	0.00187	-1.527%	5.16
core19	0.98901	0.00156	-1.099%	5.16
core20	0.98566	0.00150	-1.434%	5.16
core21	0.98867	0.00151	-1.133%	5.16

Uncertainty =

0.00207	-0.01039
---------	----------

 = Average

Table 7.3-4. Moderated Lattices Containing Mixed Oxide Fuel

(ENDF/B-V Libraries)

Case Name	k_{eff}	σ	k_{eff-1}	Reference
<i>Mixed-oxide Fuel</i>				
exp28	1.00424	0.00175	0.424%	5.15
exp29	1.00541	0.00176	0.541%	5.15
exp31	1.00597	0.00180	0.597%	5.15
exp32	1.00634	0.00166	0.634%	5.15
exp33	1.00882	0.00168	0.882%	5.15
exp22	0.99676	0.00157	-0.324%	5.12, 5.13
exp24	1.00362	0.00167	0.362%	5.12, 5.13
exp26	1.00872	0.00154	0.872%	5.12, 5.13
<i>Mixed-oxide Fuel in Triangular Lattice</i>				
exp34	0.99133	0.00156	-0.867%	5.12, 5.17
<i>Mixed-oxide Fuel with Boron Soluble Poison</i>				
exp30	1.00019	0.00193	0.019%	5.15
exp23	1.00262	0.00167	0.262%	5.12, 5.13
exp25	1.00580	0.00173	0.580%	5.12, 5.13
exp27	1.01048	0.00166	1.048%	5.12, 5.13

Uncertainty =

0.00169

0.00387

 = Average

(ENDF/B-VI Libraries)

Case Name	k_{eff}	σ	k_{eff-1}	Reference
<i>Mixed-oxide Fuel</i>				
exp28	0.99245	0.00188	-0.755%	5.15
exp29	0.99385	0.00182	-0.615%	5.15
exp31	0.99825	0.00185	-0.175%	5.15
exp32	0.99786	0.00185	-0.214%	5.15
exp33	1.00014	0.00164	0.014%	5.15
exp22	0.99168	0.00170	-0.832%	5.12, 5.13
exp24	0.99591	0.00172	-0.409%	5.12, 5.13
exp26	1.00003	0.00165	0.003%	5.12, 5.13
<i>Mixed-oxide Fuel in Triangular Lattice</i>				
exp34	0.98936	0.00150	-1.064%	5.12, 5.17
<i>Mixed-oxide Fuel with Boron Soluble Poison</i>				
exp30	0.99596	0.00182	-0.404%	5.15
exp23	0.99222	0.00171	-0.778%	5.12, 5.13
exp25	0.99954	0.00164	-0.046%	5.12, 5.13
exp27	0.99922	0.00157	-0.078%	5.12, 5.13

Uncertainty =

0.00172

-0.00412

 = Average

Figure 7.3-1. Moderated Lattices with Urania Fuel

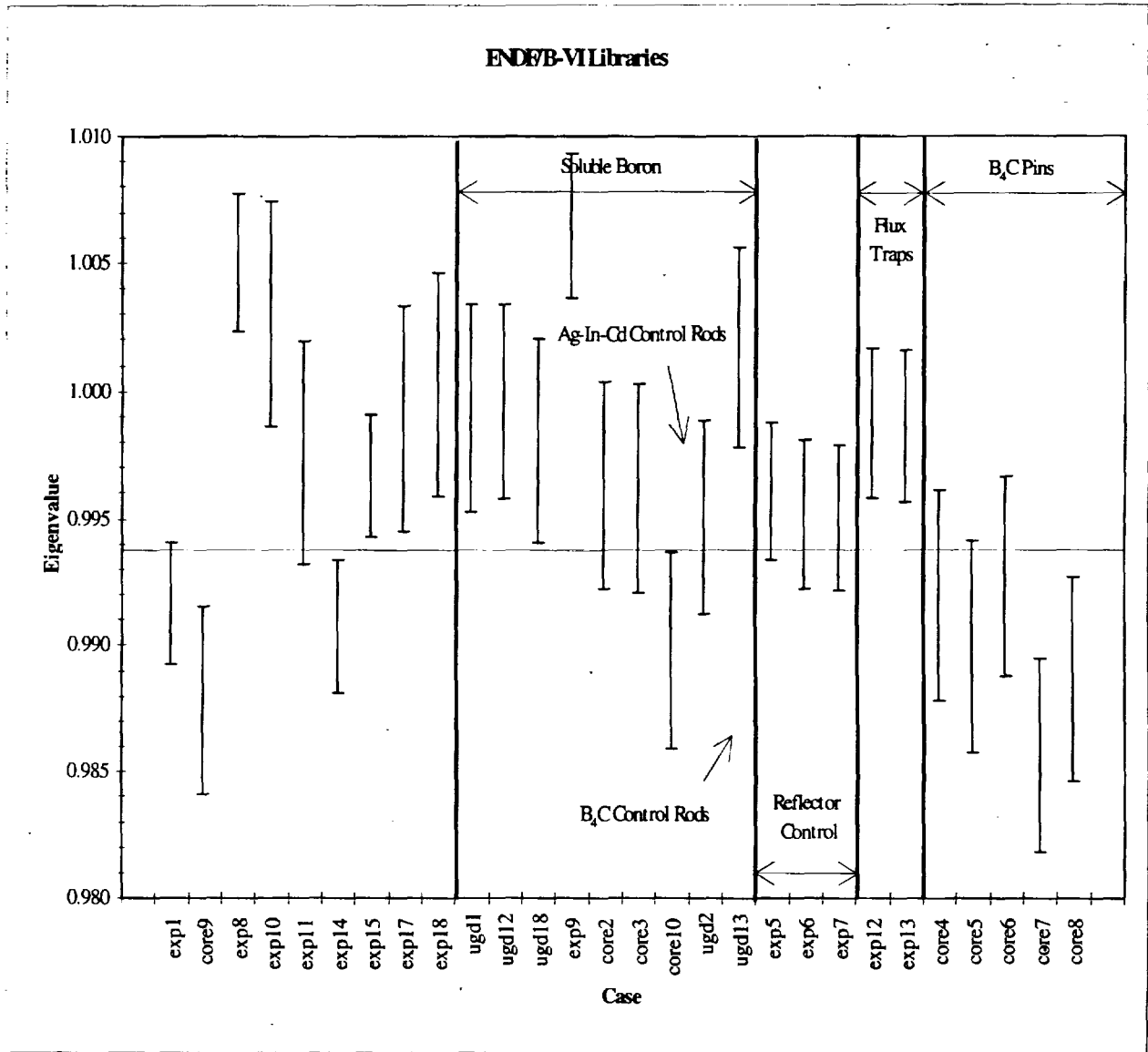


Figure 7.3-1. (cont'd)

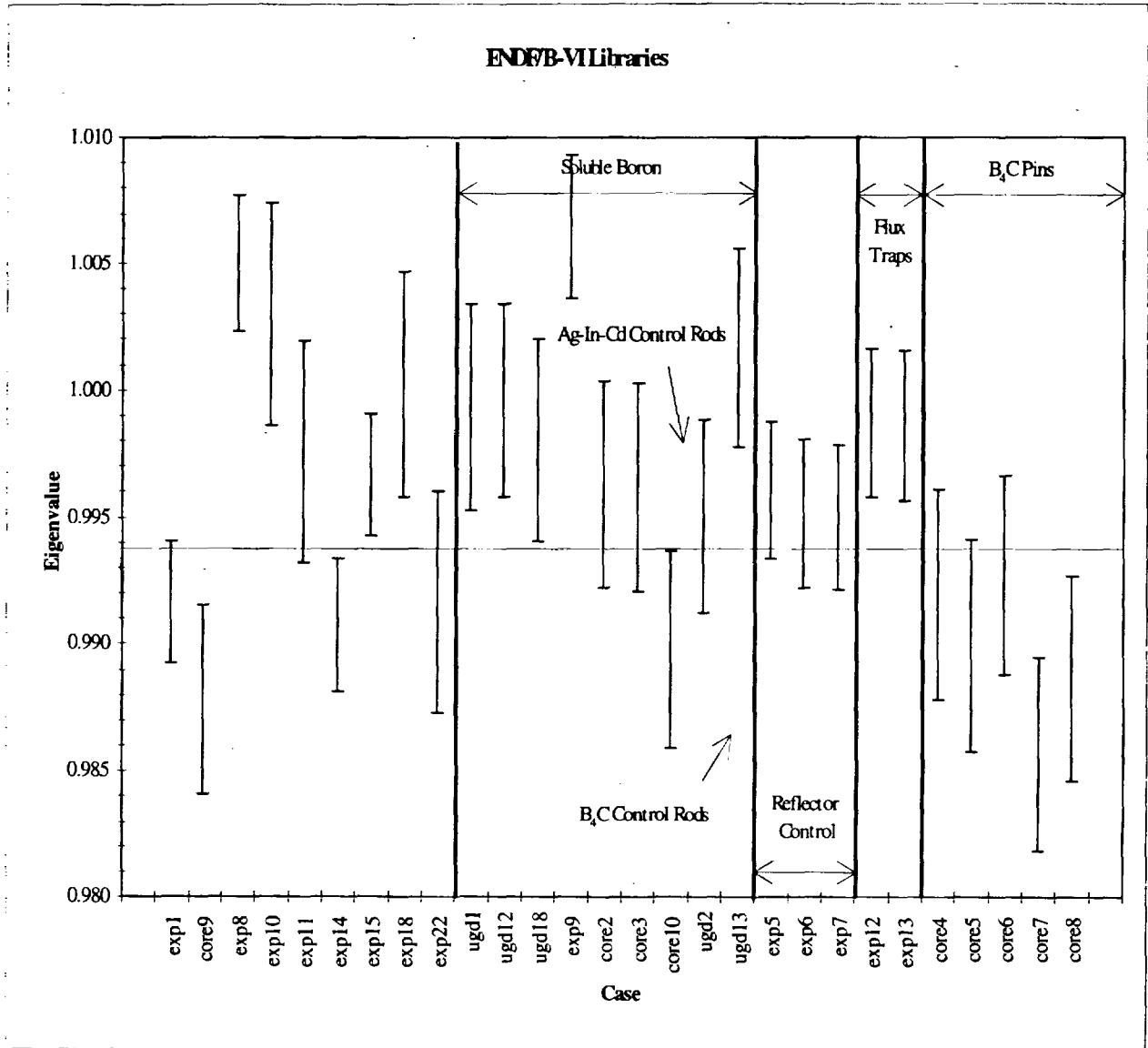


Figure 7-3.2. Moderated Urania Fuel with Gadolinia

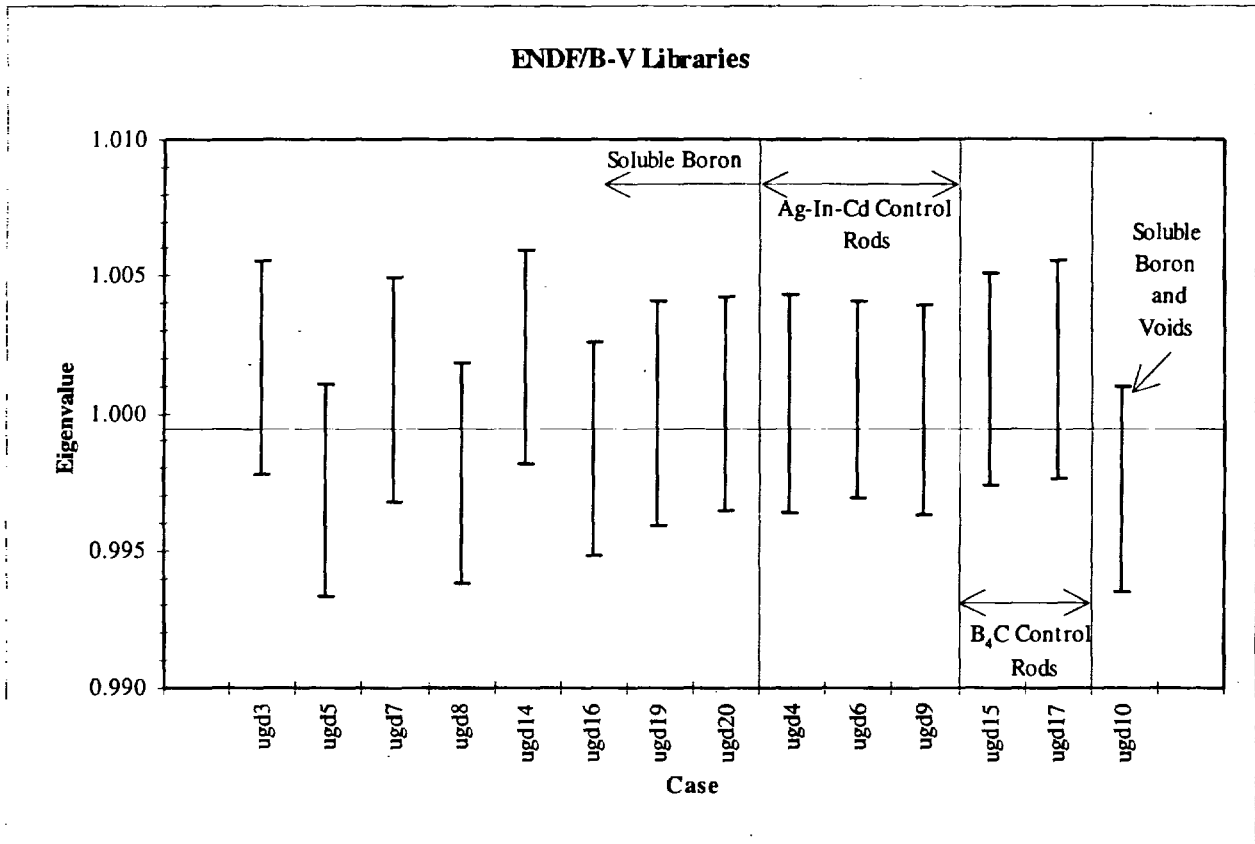


Figure 7-3.2. (cont'd)

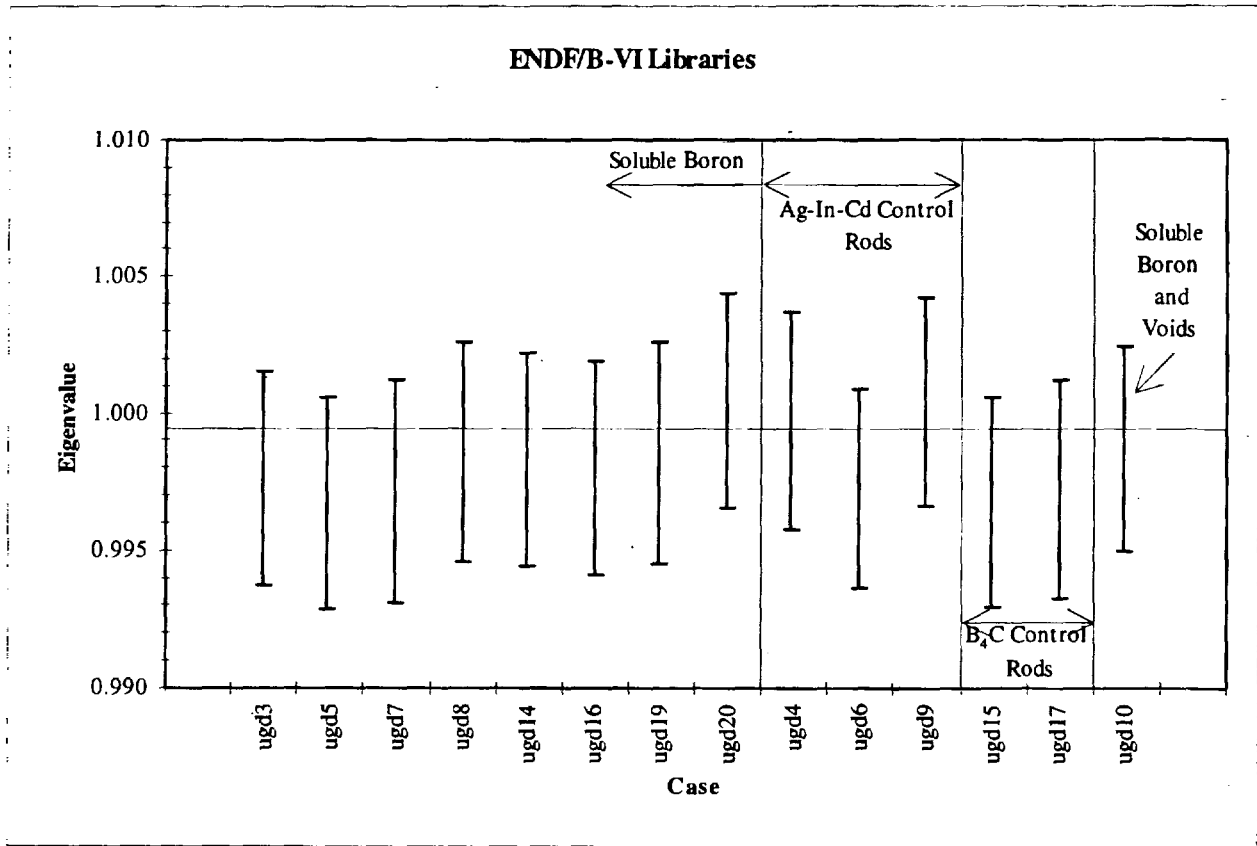


Figure 7.3-3. Moderated Lattices Containing Urania Fuel with Absorber Plates

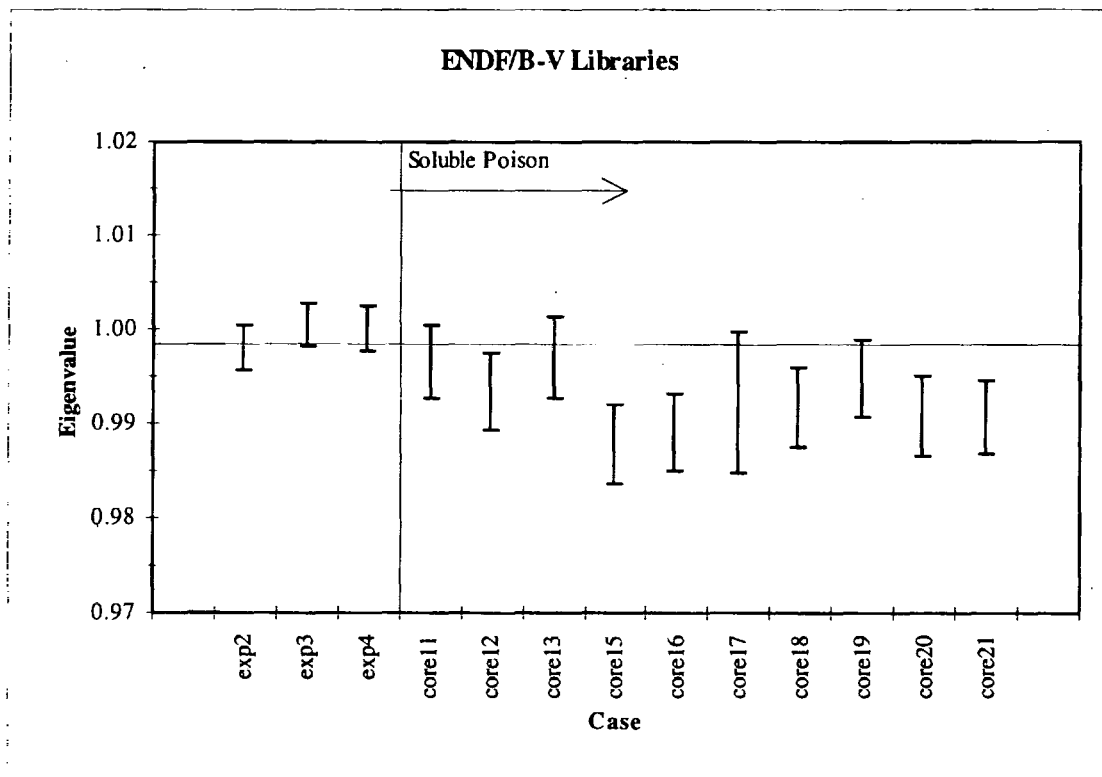


Figure 7-3.3. (cont'd)

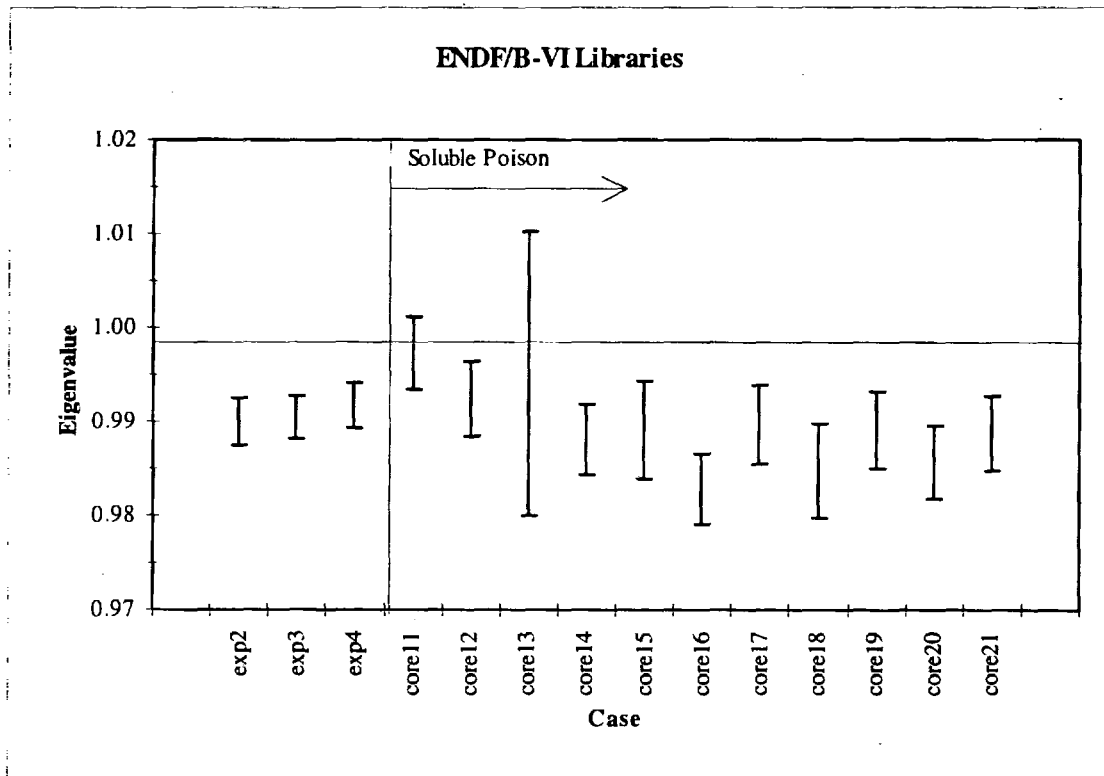


Figure 7.3-4. Moderated Lattices containing Mixed Oxide Fuel

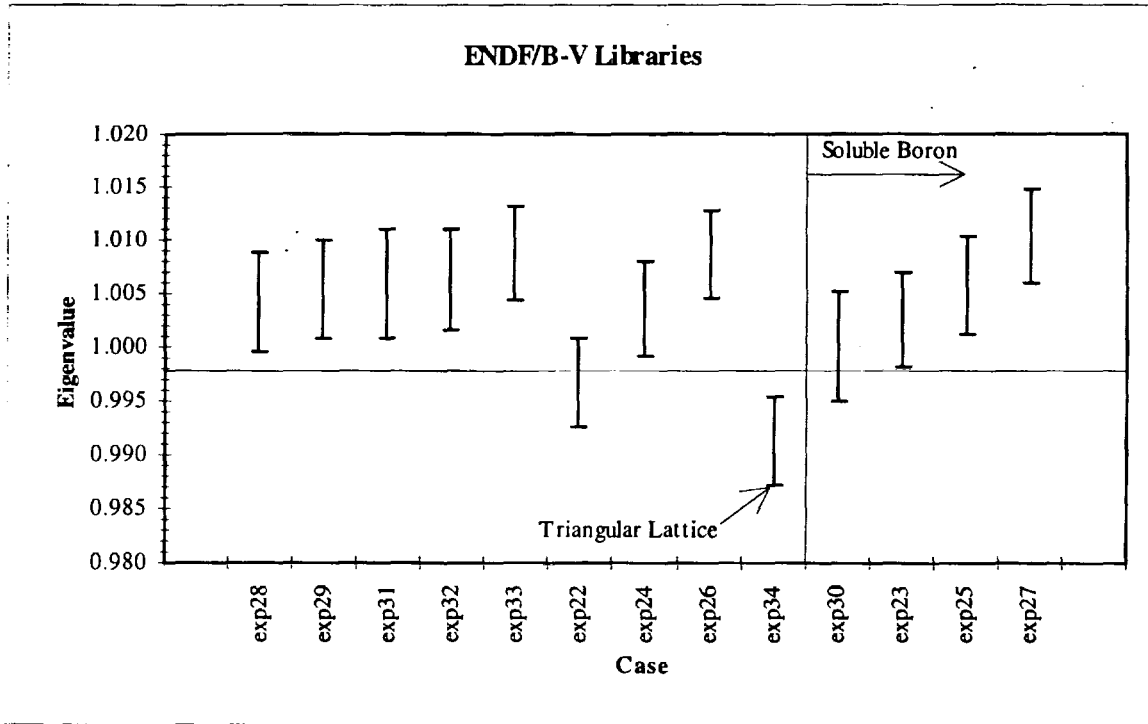
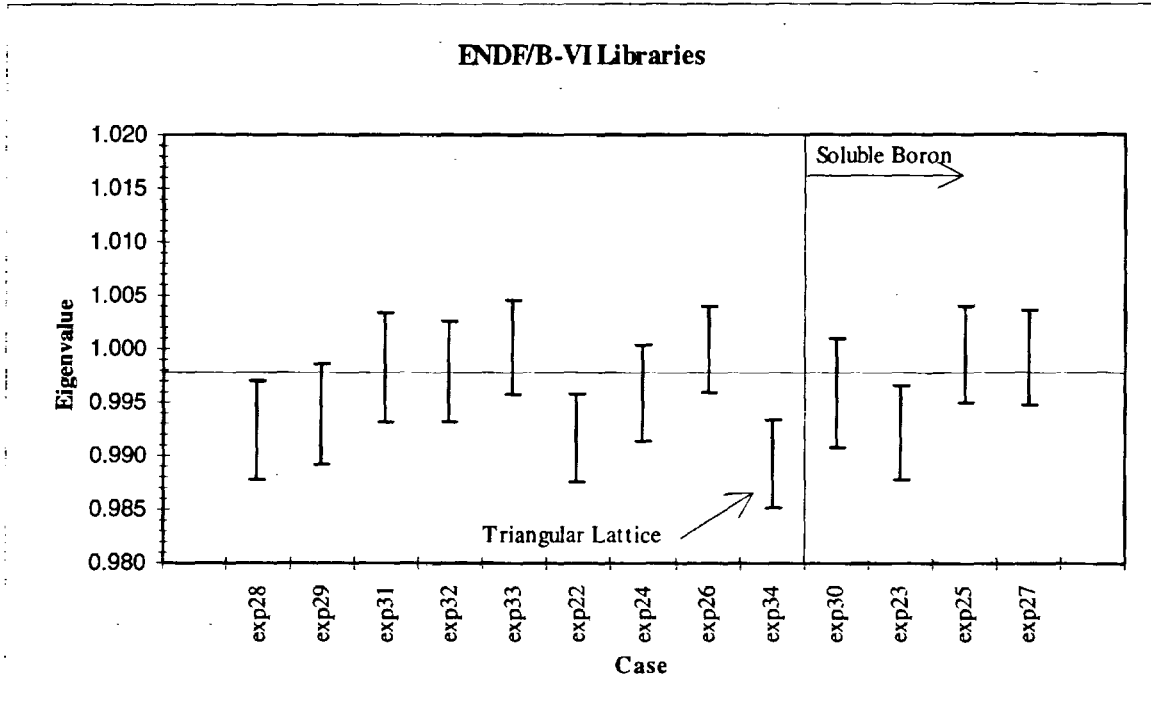


Figure 7.3-4. (cont'd)



7.4 MCNP Results

The average k_{eff} values and uncertainty values for each of the classes of cases are summarized in Table 7.4-1 for both the ENDF/B-V and ENDF/B-VI libraries. For this constellation of Laboratory Critical Experiments, somewhat surprisingly, the ENDF/B-V libraries resulted in a smaller difference from experiment than the ENDF/B-VI libraries; however, the uncertainties are sufficiently close to be statistically indistinguishable. The differences in the results obtained for each library may be summarized as:

1. For lattices containing only urania fuel, the ENDF/B-V libraries are superior by almost a factor of four to the ENDF/B-VI libraries.
2. For urania lattices incorporating gadolinia as an integral burnable absorber, the eigenvalue difference for the ENDF/B-V libraries was statistically indistinguishable from zero. The results for the ENDF/B-VI libraries were substantially better than for such fuel without gadolinia and comparable to the ENDF/B-V results for undoped urania fuel.
3. Results for configurations incorporating absorber plates as a neutron multiplication control mechanism, the eigenvalue difference is substantially larger for both cross section sets, with the ENDF/B-VI bias being about a factor of two higher than the corresponding ENDF/B-V bias.
4. Substantial improvement in the ENDF/B-VI eigenvalue difference was observed for mixed oxide fuel loadings, with the eigenvalue differences from both ENDF/B-V and ENDF/B-VI being statistically indistinguishable.
5. Uncertainties in the average eigenvalues for each library set were essentially the same, with the ENDF/B-VI uncertainties being marginally worse.

It is important to note that the average eigenvalues and uncertainty values shown in Table 7-4.1 are not those intended for use in repository calculations, but are only factors in determining the bias function to use in such applications.

Table 7.4-1. MCNP Average Eigenvalues and Uncertainties

ENDF/B-V Libraries

Description	$k_{eff}-1$	Uncertainty	Number
Moderated Lattices containing UO ₂ Fuel	-0.00114	0.00138	28
Moderated Lattices containing UO ₂ Fuel and Gadolinia	-0.00002	0.00147	14
Moderated Lattices containing UO ₂ Fuel and Absorber Plates	-0.00593	0.00158	13
Moderated Lattices containing Mixed Oxide Fuel	0.00387	0.00169	13
	Average	Average	Total
	-0.00081	0.00150	68

ENDF/B-VI Libraries

Description	$k_{eff}-1$	Uncertainty	Number
Moderated Lattices containing UO ₂ Fuel	-0.00406	0.00138	28
Moderated Lattices containing UO ₂ Fuel and Gadolinia	-0.00175	0.00150	14
Moderated Lattices containing UO ₂ Fuel and Absorber Plates	-0.01039	0.00207	14
Moderated Lattices containing Mixed Oxide Fuel	-0.00412	0.00172	13
	Average	Average	Total
	-0.00508	0.00163	69

8. Conclusions

The ability of the M&O controlled version of MCNP 4A to predict critical experiment results for urania and mixed oxide fuel was determined for a large constellation of Laboratory Critical Experiments using both ENDF/B-V and ENDF/B-VI cross section libraries. While only rudimentary comparisons were made, a tentative conclusion is that the ENDF/B-V libraries are superior for predicting the eigenvalues for such configurations.

In order to better understand the sensitivity of the results to the libraries used and to clearly quantify the range of parameters important to criticality embodied in each experiment, additional studies should be performed. Sensitivity studies might include investigations of the specific cross section treatments for the fissionable nuclides to improve agreement with libraries tuned to the specific problem set. Range-of-applicability studies would be used to study the variation in the eigenvalue and might include the following parameters:

- H/U ratio,
- leakage from the critical configuration,
- ratio of fissile plutonium to fissile uranium,
- integral burnable absorber loading,
- soluble boron concentration, and
- lattice geometry, including dimensionality and arrangement.

Further, these results should be compared with those obtained in the Organization for Economic Cooperation and Development compilation (Reference 5.21), which was the source of the MCNP input representations for the vast majority of the configurations studied.

The purpose of this analysis was to evaluate MCNP's ability to predict the neutron multiplication of criticality safety benchmark experiments involving lattices of urania and mixed oxide fuel.

9. Attachments

List of Attachments

Attachment	Description	Number of Pages
I	List of MCNP Output Files on Enclosed Magnetic Tape [a].	1

[a]. The magnetic tape has been logged to the Document Records as Reference 5.22.

Waste Package Development Design Analysis (Attachment)

Title: MCNP Evaluation of Laboratory Critical Experiments: Lattice Criticals

Document Identifier: BBA000000-01717-0200-00009 REV 00

Attachment I

Page 1 of 1

Contents of Tape Containing Output Files

File Name	Size (KB)	File Name	Size (KB)	File Name	Size (KB)
CORE10E5.OUT	646	EXP18E5.OUT	613	UGD14E6.OUT	785
CORE10E6.OUT	657	EXP18E6.OUT	626	UGD15E5.OUT	759
CORE11E5.OUT	723	EXP1E5.OUT	624	UGD15E6.OUT	784
CORE11E6.OUT	751	EXP1E6.OUT	630	UGD16E5.OUT	759
CORE12E5.OUT	722	EXP22E5.OUT	613	UGD16E6.OUT	785
CORE12E6.OUT	730	EXP22E6.OUT	625	UGD17E5.OUT	759
CORE13E5.OUT	707	EXP23E5.OUT	616	UGD17E6.OUT	784
CORE13E6.OUT	302	EXP23E6.OUT	628	UGD18E5.OUT	760
CORE20E6.OUT	748	EXP24E5.OUT	615	UGD18E6.OUT	785
CORE14E6.OUT	746	EXP24E6.OUT	627	UGD19E5.OUT	759
CORE15E5.OUT	698	EXP25E5.OUT	615	UGD19E6.OUT	784
CORE15E6.OUT	541	EXP25E6.OUT	627	UGD1E5.OUT	761
CORE16E5.OUT	698	EXP26E5.OUT	613	UGD1E6.OUT	786
CORE16E6.OUT	721	EXP26E6.OUT	624	UGD20E5.OUT	759
CORE17E5.OUT	398	EXP27E5.OUT	616	UGD20E6.OUT	784
CORE17E6.OUT	753	EXP27E6.OUT	628	UGD2E5.OUT	760
CORE18E5.OUT	734	EXP28E5.OUT	614	UGD2E6.OUT	786
CORE18E6.OUT	575	EXP28E6.OUT	623	UGD3E5.OUT	760
CORE19E5.OUT	698	EXP29E5.OUT	613	UGD3E6.OUT	785
CORE19E6.OUT	721	EXP29E6.OUT	622	UGD4E5.OUT	759
CORE21E6.OUT	720	EXP2E5.OUT	643	UGD4E6.OUT	785
EXP10E5.OUT	621	EXP2E6.OUT	659	UGD5E5.OUT	760
CORE20E5.OUT	698	EXP30E5.OUT	615	UGD5E6.OUT	786
CORE21E5.OUT	697	EXP30E6.OUT	624	UGD6E5.OUT	760
CORE2E5.OUT	625	EXP31E5.OUT	612	UGD6E6.OUT	785
CORE2E6.OUT	629	EXP31E6.OUT	621	UGD7E5.OUT	760
CORE3E5.OUT	624	EXP32E5.OUT	612	UGD7E6.OUT	785
CORE3E6.OUT	629	EXP32E6.OUT	621	UGD8E5.OUT	760
CORE4E5.OUT	626	EXP33E5.OUT	612	UGD8E6.OUT	785
CORE4E6.OUT	631	EXP33E6.OUT	621	UGD9E5.OUT	760
CORE5E5.OUT	626	EXP34E5.OUT	699	UGD9E6.OUT	785
CORE5E6.OUT	631	EXP34E6.OUT	730		
CORE6E5.OUT	626	EXP3E5.OUT	642		
CORE6E6.OUT	631	EXP3E6.OUT	650		
CORE7E5.OUT	626	EXP4E5.OUT	643		
CORE7E6.OUT	631	EXP4E6.OUT	655		
CORE8E5.OUT	626	EXP5E5.OUT	627		
CORE8E6.OUT	631	EXP5E6.OUT	630		
CORE9E5.OUT	627	EXP6E5.OUT	628		
CORE9E6.OUT	632	EXP6E6.OUT	631		
EXP10E6.OUT	624	EXP7E5.OUT	634		
EXP11E5.OUT	623	EXP7E6.OUT	644		
EXP11E6.OUT	627	EXP8E5.OUT	611		
EXP12E5.OUT	684	EXP8E6.OUT	614		
EXP12E6.OUT	703	EXP9E5.OUT	614		
EXP13E5.OUT	722	EXP9E6.OUT	616		
EXP13E6.OUT	750	UGD10E5.OUT	760		
EXP14E5.OUT	612	UGD10E6.OUT	785		
EXP14E6.OUT	617	UGD12E5.OUT	760		
EXP15E5.OUT	612	UGD12E6.OUT	785		
EXP15E6.OUT	616	UGD13E5.OUT	760		
EXP17E5.OUT	614	UGD13E6.OUT	785		
EXP17E6.OUT	627	UGD14E5.OUT	759		